SHORT-TERM TRENDS AND SPATIAL VARIABILITY IN PRECIPITATION CHEMISTRY IN THE SOUTH COAST AIR BASIN

Final Report

for

The California Air Resources Board

1800 15th. St.
Sacramento, California 95814

Eric Fujita, Project Manager

Contract Number: A4–142–32

Prof. Michael R. Hoffmann

Principal Investigator

Environmental Engineering Science
W. M. Keck Laboratories
California Institute of Technology
Pasadena, California 91125

28 February 1989

TABLE OF CONTENTS

Abstract

Automated sub–event sequential rain samplers were used to sample rain during the winter and spring of 1987 in the South Coast Air Basin. The five sites used in the study were located at West Los Angeles, Pasadena, Henninger Flats, Mount Wilson, and Riverside. These sites were specifically chosen to represent a "vertical" profile in the basin (Pasadena to Henninger Flats to Mt. Wilson) and an east–west profile (Riverside to Pasadena to West Los Angeles). Measurements of aerosol and gas phase species also were made at the five sites using filter pack methods and an automated sampler.

The highest rainwater concentrations of NO_3^- and SO_4^{2-} were observed at Pasadena; highest NH_4^+ levels were measured at Riverside; highest average levels of rainwater Na^+ and Cl^- were found at West Los Angeles. Rainwater pH levels varied from 4 to 6 at West Los Angeles and Henninger Flats, from 4 to 5.5 at Pasadena, from 4.3 to 5.7 at Mt. Wilson, and from 4.5 to 6.8 at Riverside. Rainwater concentrations at all five sites generally were dominated by NH_4^+, SO_4^{2-}, NO_3^-, and H^+. Na^+ and Cl^- were important contributors in some samples, particularly those collected near the coast. The highest deposition rates of some species were often observed at the site with the lowest rainwater concentrations, Mt. Wilson, due to heavier rainfall there.

Rainfall concentration data from the "vertical" profile indicate that much of of the ionic loading in the rain at Henninger Flats (elev. 700 m) was picked up between there and Mt. Wilson (1700 m), while much of the ionic loading in the rain at Pasadena (200 m) was picked up between there and Henninger Flats. Measurements of the atmospheric burdens of aerosol and gas phase species prior to a storm indicated that considerably more N(V) and S(VI) were deposited in rainfall than could be accounted for by pre–storm atmospheric burdens of these species. Pre–storm burdens of Ca^{2+}, Mg^{2+}, Na^+ , and N(–III) were closer to the measured deposition of these species in the rainfall. In–cloud production of SO_4^{2-} may account for at

least a portion of the additional SO_4^{2-} deposition; no evidence was seen for in–cloud production of NO_3^-.

The aerosol at elevated sites in the South Coast air basin is a mixture of sea salt and pollution–derived secondary aerosol. The influence of sea salt declines with increasing distance from the coast. Nitric acid appears to react with the NaCl in sea–salt aerosol to release $HCl_{(g)}$ and form $NaNO_3$ in the aerosol. At inland sites aerosol concentrations differ during onshore and offshore flow. The highest concentrations are observed during the day when the onshore flow transports pollutants to the sites, while lower concentrations were observed at night when drainage flows from nearby mountains influenced the sites. Variations in liquid water content are a major influence on cloudwater concentration.

Comparisons of the ionic concentrations in two size–segregated fractions collected during each sampling interval suggest that there is a large difference between the average composition of the smaller droplets and that of the larger droplets. For each time interval, the concentration of Na^+, Ca^{2+} and Mg^{2+} in the large droplet fraction was observed to be higher than in the small droplet fraction. The concentrations of SO_4^{2-}, NO_3^-, NH_4^+, and H^+ were higher in the small droplet fraction. Chloride concentrations were nearly equal in both fractions. Differences in the composition of size–fractionated cloudwater samples suggest that large droplets are formed from sea salt and soil dust, which are large aerosol, and small droplets are formed on small secondary aerosol composed of primarily ammonium sulfate and ammonium nitrate. The concentrations of several components that exist partly in the gas phase (e.g. Cl^-, HCOOH, and CH_3COOH) appear to be independent of droplet size.

Research Objectives

The principal objectives of this research project were to study the chemistry, physics, transport, and meteorology of selected wet deposition events that can be characterized phenomenologically as either Pacific cyclonic storms or as stratus rain events. The study involved the chemical characterization of wet deposition collected with automated fraction collectors, the chemical characterization of precursor and post–event fine aerosol samples, and the use of tracers for the characterization of large scale transport, mixing, and scavenging of water soluble gases characteristic of components of the polluted SCAB air mass.

At the request of the Air Resources Board Research Staff we revised the work to be performed under CARB Contract #A4–142–32. This modification was made in order to redirect resources and personnel to participate in the Southern California Air Quality Study (SCAQS). The scope of the precipitation chemistry measurements and related tracer studies were modified, while a program involving the measurement of fog and cloudwater composition during SCAQS sampling periods was added. The tracer studies originally scheduled for the winter period were shifted to the SCAQS sampling periods. These later studies were undertaken independently by Prof. Fredrick Shair.

In the area of precipitation chemistry, the principal objectives were modified to include a study of the chemistry and meteorology of selected wet deposition events. Temporal variation in solute concentrations during precipitation events were determined and compared to meteorological parameters and variations in emission fluxes. This data was used to determine the contributions of in–cloud and below–cloud scavenging to wet deposition in the South Coast Air Basin (SOCAB), and to identify chemical transformation mechanisms important during storm periods. Secondly, aerosol and gas–phase concentrations were measured preceding and following storm events in order to determine the scavenging efficiency of storms. The accumulation of secondary species such as NO_3^- and SO_4^{2-} aerosol, organic acids

and carbonyls following storms can be used to estimate the characteristic times for their formation.

The Suggested Program Plan for SCAQS (Blumenthal et al., 1986) identified the need to measure cloud and fog in the SOCAB in order to properly understand gas and aerosol processes. There is considerable evidence that the presence of fog or low cloud in the basin is associated with high SO_4^{2-} aerosol loadings and poor visibility in the SOCAB. Previous research sponsored by the CARB at Caltech has identified pre–existing aerosol as a major contributor to the acidity level in fog and cloud. Conversely, evaporated fog and cloud droplets are a major source of aerosol. The primary objectives of Caltech's participation in SCAQS are to assess the role that fog and cloud play in the formation of aerosol in the SOCAB (Objective 3, issue 1 of SCAQS) and to quantify the scavenging of precursor aerosol and gases during droplet formation. The extensive data available from SCAQS on meteorology, emissions, gas and aerosol concentrations will be used to evaluate cloud and fog droplet chemistry models.

Background

In Los Angeles, storm systems originate over the Pacific Ocean and have little or no contact with polluted air masses until they reach the South Coast Air Basin (SCAB). However once a storm system reaches the SCAB, rainwater will be have elevated concentrations of chemical species due to *in situ* chemical transformations, gas scavenging, and aerosol scavenging. Non–reactive gases and aerosols are scavenged by water droplets via impaction and diffusion according to the following equation:

$$\frac{dC_{Pi}}{dZ} = \frac{3\ E_i\ C_{ai}}{4\ D_P}$$

where C_{Pi} and C_{ai} are concentrations of component i in precipitation and air, respectively; D_P is the droplet diameter; Z is the height; and E_i is the scavenging efficiency, which is set at 1.0 for diffusion of soluble gases and varied according to particle size for impaction. Calculations of E_i based on aerosol impaction theory predict that particles with diameter > 3 mm will impact to some extent on the falling drops, but most of the SO_4^{2-} and NO_3^- aerosol in the SCAB is below this size range and will not be effectively scavenged by falling drops. Our previous results suggest that even low concentrations of gaseous pollutants could account for enhanced sulfate levels which have been attributed to below cloud scavenging. Sulfate aerosol was shown to be an unlikely contributor to the observed sulfate increase between Mt. Wilson and Pasadena because it is too small to be scavenged by impaction. Nitric acid and ammonia are very soluble over the pH range of 2 to 6 and as a consequence they will be rapidly scavenged by precipitation. In order to account for the observed nitrate and ammonium ion increases between Mt. Wilson and Pasadena gas phase concentrations of 1.0 ppb and 0.22 ppb are required for HNO_3 and NH_3, respectively.

The impact of below cloud scavenging should be most pronounced during the initial phases of the storm, when the atmosphere is most heavily laden with gases and aerosol. In most of the observed storms, the concentrations of Na^+ and Cl^-, which are derived from sea salt, were nearly equal at both sites or have a slight excess at Mt. Wilson.

In addition to the Pacific cyclonic storms, which provide the majority of precipitation in the SCAB, stratus clouds may thicken sufficiently to produce light drizzle. This drizzle exhibits very high concentrations of H^+, NH_4^+, NO_3^-, and SO_4^{2-}, but is only a minor contributor to the total precipitation budget in the basin. Stratus rain events occurred within a developed marine layer. The ionic concentrations of these rains were significantly higher than for the storm events.

Pacific storms are associated with weather systems which advect moist, unstable oceanic air with fairly intense convective activity at heights > 5000 m. On the other hand, light rains (drizzle or mist) usually occur within a developed marine layer constrained by a strong temperature inversion aloft. This limits the vertical extent of mixing, and as a consequence the stratus cloud droplets form and have longer lifetimes in the polluted atmosphere. The cloud >> drizzle hiearchy of solute concentration also reflects the relationship between droplet size and dilution. The growth of non–freezing cloud droplets to a size with appreciable sedimentation velocity occurs solely by condensation of water vapor for sizes below 50 μm diameter; subsequently both coalescence and condensation lead to drizzle (0.2 to 5.0 mm) and raindrop (> 0.5 mm) sizes depending upon the intensity of vertical motion.

Stratus rain events led to solute deposition which was clearly disproportinate to the water flux. Stratus rain accounted for only ~ 1 % of the measured rainfall at Henninger Flats while it accounted for nearly 20 % of the total deposition of H^+, NO_3^-, and SO_4^{2-} in less than 16 mm of precipitation. Na^+ and Cl^- were substantially less enhanced in stratus rain than winter storm events. The winter storms responsible for most of the precipitation form over the eastern Pacific Ocean. They are more effective at generating and transporting sea salt aerosol due to their greater convective activity. For stratus rain, the enhancement of H^+, and NO_3^-

was greatest, and for NH_4^+ and SO_4^{2-} it was somewhat less. The difference in nitrate/sulfate ratios for stratus (1.4) versus storm events if a further indication of the meteorological and seasonal variation in SO_2 and NO_x oxidation and transport.

Technical Approach

In order to achieve the objectives noted above, we operated five sampling sites in the SOCAB during the period December 1986 – March 1987. Three of the sites (West Los Angeles, Pasadena, and Riverside) determined a transect across the basin, while the remaining two sites (Henninger Flats and Mt. Wilson) made up a vertical transect above Pasadena. Precipitation was sampled with automated fractionating precipitation collectors capable of segmenting an event into as many as 20 sequential samples. Aerosol and gasphase species were collected with an automated filter pack. Aerosol was retained on Teflon filters; nylon, oxalic acid–impregnated glass, and base–impregnated quartz filters behind the teflon filters retain HNO_3, NH_3, and organic acids respectively. Filter cassettes for three sampling periods can be loaded and run by a programmable timer. Aerosol sampling was initiated the day before a storm was forecast and continued long enough after the end of the storm to monitor the aerosol buildup.

Since the cloud base during storms normally intersects the mountains below Mt. Wilson, the contributions of in–cloud and below–cloud scavenging were determined from precipitation chemistry along the vertical transect above Pasadena. Variations in chemistry along the West Los Angeles – Riverside transect were used to indicate transport and transformation processes during the storm. Additional information about transport and transformation rates were obtained by comparing temporal variations in precipitation and aerosol chemistry to temporal changes in emission strength.

· ***SCAQS Participation***

Previous experience indicated that low–lying stratus cloud were likely to be a common event during the early summer sampling period. During the summer study period four cloud sampling sites were operated at elevated locations along a rough transect across the SoCAB. When possible these sites were located near SCAQS sites. The sites were located in Palos Verdes, in the Verdugo Mountains near Pasadena, in the San Gabriel Mountains at Henniger

Flats, and in the San Jose Hills located in San Dimas.

Each sampling site included an Active Strand Cloudwater Collector with an automatic fraction collector and a cloudwater sensor, and an automated filter pack. The CASC collects droplets by inertial impaction in 510 μm Teflon strands. The 50% collection efficiency cutoff predicted from impaction theory is 3.5 μm diameter. The cloudwater sensor is a scaled–down version of the CASC that is run continuously. Water collected on the sensor is detected by a resistance grid. When the sensor detects the presence of cloud the main collector is turned on.

The role of fog and cloud in producing aerosol in the SoCAB was assessed using measurements of aerosol before and after fog/cloud events and comparisons of fog/cloud chemistry to aerosol and gas concentrations upwind and downwind of the fog or cloud. Scavenging efficiencies by droplets for various gas and aerosol species were determined by simultaneous collection of droplets, gas and interstitial aerosol, and by comparisons of droplet chemistry to precursor aerosol and gas at the fog/cloud sampling sites and along upwind transects. The extensive data collected during SCAQS provided a rare opportunity to evaluate models of droplet–phase chemistry and assess the importance of aqueous–phase reaction mechanisms in pollutant transformations. Previous observations of droplet chemistry agree qualitatively with model predictions, but the available data have been insufficient to make a quantitative comparison.

Major Findings

1. An automated sub–event sequential precipitation sampler was designed and built. The sampler features a rain sensor, a collection surface that is covered between periods of rain, and a refrigerated compartment for storing collected rain samples. The sampler is capable of collecting up to 20 separate fractions of a rain event. A U. S. Patent was granted for this device (Patent Number: 4,732,037, Granted: March 22, 1988)

2. Rain samples were collected during the winter of 1987 at five sites throughout the Los Angeles Basin. These sites formed a "horizontal" transect from West L.A. to Pasadena to Riverside and a "vertical" transect from Pasadena to Henninger Flats to Mt. Wilson. Collection of these samples was done automatically using the Caltech fractionating rain collector. This collector permitted us to collect sequential samples with a time resolution as fine as five minutes.

3. The fine time resolution of the sampling allowed us to demonstrate the rapid scavenging of solutes at the beginning of a rain event. Pauses in the rain allowed solutes to be replenished.

4. Data from the vertical profile indicated that much of the solute loading in rainwater samples was being accumulated in the rain as it fell through the lowest few hundred meters of the atmosphere. Samples obtained at Pasadena were much more concentrated in all major ions than were samples at Henninger Flats. The samples at Henninger Flats were likewise considerably more concentrated than those at Mt. Wilson.

5. pH values of the sampled rain ranged from 4 to 6 with Pasadena and Henninger Flats being the most acidic. Riverside, which is near a large concentrations of feedlots, and West L.A., which is upwind of most major sources during a storm, have lower levels of acidity. In the "vertical" transect pH traces of the events were similar for all three events with Mt. Wilson rain samples being only slightly less acidic than those at Pasadena and Henninger flats. This similarity in pH was seen despite the fact that samples generally became more dilute with increasing elevation.

6. SO_4^{2-} was generally the dominant anion in rain samples collected at the West L.A. site. It was also found in slight excess over NO_3^- in the Riverside rain samples, in sharp contrast to fogwater we had previously sampled at Riverside, which was strongly dominated by NO_3^-. Nitrate was more often found to be the dominant anion in rain samples obtained at Pasadena, Henninger Flats, and Mt. Wilson, although, once again, not to the extent that it typically is in fogwater at the same sites.

7. Ratios of NO_3^- to SO_4^{2-} in collected rainwater were observed to change considerably between rain storms, and even during the course of a single storm, at a given site.

8. Deposition of SO_4^{2-} and NO_3^-, during an extended basin–wide rain event, was observed to be higher than what could be accounted for by washout of the pre–storm atmospheric burden of these species over the South Coast Air Basin. Deposition of Na^+, Ca^{2+}, and Mg^{2+} was comparable to the pre–storm atmospheric burden of these species.

9. Evidence was seen for in–cloud production of SO_4^{2-} during an extended rain storm. The calculated production rate was of the same order of magnitude as that for the aqueous phase oxidation of S(IV) to S(VI) by ozone at the pH observed in the rainfall. No evidence was seen for in–cloud production of NO_3^-.

10. An automated aerosol sampler was designed and constructed. This instrument can be programmed to collect aerosol samples during up to three independent time periods before operator attendance is required. The sampler was used in both the rain sampling study and the SCAQS cloudwater study.

11. A fog sensor and automatic sampling system was built and used with the CASC. Over 330 cloudwater samples from San Pedro Hill, Henninger Flats, and Long Beach have been obtained with the automated sampling system.

12. Cloudwater samples obtained at San Pedro Hill, Henninger Flats, and Long Beach were consistently acidic. pH values of the samples ranged from 2.4 to 5.0 at San Pedro Hill, from 2.6 to 4.8 at Henninger Flats, and from 2.6 to 5.6 at Long Beach.

13. Variations in cloudwater chemical composition were observed over time intervals as short as 10 minutes indicating that the automatic collection system is capable of observing the effects of pollutant puffs on cloudwater chemistry. Other intervals gave very consistent result for consecutive samples.

14. A fractionating inlet was designed and constructed for use with the CASC. Droplets larger than $\simeq$ 15 μm are collected on teflon rods at the mouth of the inlet. The remaining droplets pass through to the teflon strands and are collected there.

15. The size–fractionating inlet was used to collect intercepted stratus on San Pedro Hill. Ions associated with soil dust and sea salt (Ca^{2+}, Mg^{2+}, and Na^{+}) were enriched in the large droplet fraction. The secondary aerosol ions (NH_4^+ , SO_4^{2-}, NO_3^-, and H^+) were enriched in the small droplet fraction. Cl^-, which may have been introduced to the

droplets primarily as HCl, showed mixed behavior.

Conclusions

The chemical composition of precipitation collected during several events in the South Coast Air Basin (SoCAB) was dominated by inputs from basin emissions of SO_2, NO_x, and NH_3. These inputs typically are introduced in the form of aerosol containing NO_3^-, SO_4^{2-}, and NH_4^+, as well as gas phase inputs of HNO_3 and NH_3. Na^+ and Cl^- often contribute significantly to the composition of samples collected near the coast, reflecting their origin in marine aerosol. The strong dominance of NO_3^- over SO_4^{2-} normally observed in fog and cloudwater samples collected in the SoCAB generally was not observed in the precipitation samples. Higher precipitation amounts at elevated sites in the basin appear to lead frequently to greater wet deposition fluxes of pollutants there than are observed at sites on the basin floor, despite the fact that precipitation pollutant concentrations normally are much higher near the basin floor.

Both in–cloud and below–cloud scavenging of aerosol and gases were shown to play an important role in determining precipitation composition. In–cloud production of SO_4^{2-} was indicated by the results of a mass balance completed around the precipitating clouds in one event. The SO_2 oxidation rate required to complete the mass balance was consistent with the expected rate of oxidation by O_3 for the conditions observed. No evidence was observed for in–cloud production of NO_3^-.

Comparisons of the ionic concentrations in two size–segregated fractions collected during each sampling interval suggest that there is a large difference between the average composition of the smaller droplets and that of the larger droplets. For each time interval, the concentration of Na^+, Ca^{2+} and Mg^{2+} in the large droplet fraction was observed to be higher than in the small droplet fraction. The concentrations of SO_4^{2-}, NO_3^-, NH_4^+, and H^+ were higher in the small droplet fraction. Chloride concentrations were nearly equal in both fractions. Differences in the composition of size–fractionated cloudwater samples suggest that large

droplets are formed from sea salt and soil dust, which are large aerosol, and small droplets are formed on small secondary aerosol composed of primarily ammonium sulfate and ammonium nitrate. The concentrations of several components that exist partly in the gas phase (e.g. Cl^-, HCOOH, and CH_3COOH) appear to be independent of droplet size.

The differences in concentration between the size fractions are consistent with the suggestion that large nuclei produce large droplets and small nuclei produce small droplets. For the size–dependent aerosol composition to be preserved in the droplets requires nucleation scavenging to be the dominant scavenging process. Because Na^+, Ca^{2+} and Mg^{2+} are associated with sea salt and soil dust they are found predominantly in the large droplets; while NH_4^+, SO_4^{2-}, and to some extent NO_3^-, which are mostly found in secondary aerosol, would be in the small droplets. However, NO_3^-, which can exist in the gas phase or on large aerosol by exchange with Cl^-, would also be found to a substantial extent in large droplets. However, the cloudwater concentrations of these ions may be altered by absorption of precursor gas phase species followed by chemical reaction. For example, $NH_{3(g)}$ can be absorbed by the droplets and protonated to form NH_4^+; $HNO_{3(g)}$ can be absorbed, followed by deprotonation to yield NO_3^-; $SO_{2(g)}$ can be absorbed and oxidized to SO_4^{2-}. The first two processes are extremely rapid, while the oxidation of S(IV) to S(VI) in cloudwater is also rapid in the presence H_2O_2 or a metal catalyst and O_2. Since S(IV) and H_2O_2 were not found concurrently in the time– and size–resolved samples, the rapid oxidation of S(IV) to S(VI) by H_2O_2 was likely to have taken place.

CHAPTER 1

Automated Fractionating Sampler Design

by

Bruce Daube, Jr., Jeff Collett, Jr., J. William Munger, and Michael R. Hoffmann

Environmental Engineering Science
W. M. Keck Laboratories, 138–78
California Institute of Technology
Pasadena, CA 91125

March 1988

Introduction

To facilitate the simultaneous collection of sub–event sequential rainwater samples at several sites, an automated fractionating sampling system was designed and ten units were constructed. The sampler is comprised of a rain sensor, a funnel with a covering mechanism, and an autosampler consisting of a refrigerated sample reservoir and carousel containing 20 sample bottles, controlling electronics, and a printer. The assembled system is illustrated in Figure 1.

The rain sensor consists of a stainless steel grid and heated plate separated by a small distance. When dry, the grid is maintained at an electrical potential of 24 volts above that of the plate. A rain droplet bridging the grid and plate changes this potential and turns on the main system. Upon activation of the main system, the funnel cover is removed and sample collection commences. Rain collected in the funnel enters the autosampler through a Teflon tube and accumulates in a polyethylene reservoir. When the collected water rises above a preset level in the reservoir, a liquid level sensor, located on a side tube connected to the reservoir, activates a drain valve at the bottom of the reservoir. The sample is dispensed through this valve into a 60 ml. polyethylene bottle. The carousel then rotates, placing a new bottle in position below the drain valve. A counter records the number of bottles that have been used and turns off the main system if all of the bottles are full. The funnel remains uncovered until the event ends.

When the precipitation ceases, the heater on the rain sensor evaporates any remaining water on the grid and the system is shut down. The funnel cover closes to prevent dry deposition from contaminating the funnel. The printer records the time and date of when the system came on, when each sample bottle was changed, and when the system shut down. The samples are stored at 4 C.

The automated fractionating system will collect sequential samples of precipitation for the duration of most events. Figure 2 shows a plot of the expected time required to fill the carousel as a function of rainfall intensity. For a typical rainfall rate of 5 mm/hr, the carousel will take about 8 hours to fill.

Rain Sensor Design

The rain sensing system is comprised of a sensing grid, a heating element, and a controlling electronic circuit board. The rain sensor grid and plate are illustrated in Figure 3. Both components are made of Type 304 stainless steel and both have been passivated to minimize oxidation. A heating element (TIP–33C npn power transistor) is mounted to the underside of the plate and has a maximum output of 55 W. It is typically operated at 12 W.

As previously described, the sensor activates the main system when a droplet of water bridges the 0.75 mm gap between the grid and the plate. The presence of water across the sensor provides a pathway for a small current to flow from the grid to the plate. The sensor circuitry, shown schematically in Figure 4, monitors the plate voltage with a voltage comparator. When the plate voltage rises above a preset threshold, a relay coil is energized, activating the heating element and the main system. The maximum resistance across the sensor that will still activate the system is approximately 15,000 ohms. At this setting, rainwater is always sufficiently conductive to initiate sampler operation. Light dew or human contact will generally not activate the sampler.

An additional electronic circuit monitors the ambient temperature using a thermistor. If the temperature drops below 2 C, the plate heating element is switched on. This permits the detection and collection of snow or ice.

At the end of a rain event, the wetted sensor gradually dries. Based on the geometry of the grid and plate, the maximum amount of accumulated water on the sensor

is approximately 0.35 ml. With the heater set at 12 W, the sensor completely evaporates this water in 10 to 15 minutes, causing the funnel cover to close and the main system to turn off.

Cover Mechanism Design

A funnel cover prevents dry deposition from entering the funnel during periods without rain. The position of this cover is controlled by the cover mechanism illustrated in Figure 5. This mechanism consists of an actuating arm, a 4 rpm bi–directional AC motor, and a notched cam with two limit switches.

The funnel cover mechanism was designed to minimize obstructions near the funnel and to protect the cover from potential damage due to high winds when the cover is open. This was achieved by rotating the actuating arm through an arc of 270 degrees, placing the opened cover well away from the funnel opening and supporting it against the mounting pole. The cover is positioned vertically when opened to prevent accumulation of rain on it during an event. This also helps to rinse off any dry deposition collected on the cover, reducing the potential for funnel contamination when the cover closes.

The torque required to operate the mechanism can be calculated by determining the weight and center of gravity of the cover and actuating arm as a function of cover position. At the half–open position, the torque required to operate the cover reaches a maximum value of 0.9 N m. Wind loads on the cover are also important. For a flat surface the size of the funnel cover positioned perpendicular to the wind, a 13.5 m/s wind will generate a force of 9.3 N on the cover. The torque required to overcome this wind load is 2.0 N m. The selected motor, which rotates at 4 rpm, has a maximum output of 4.5 N m, providing sufficient torque to operate the mechanism satisfactorily even under high wind conditions.

The open and closed positions of the cover are controlled by two adjustable limit switches which are actuated by a notched cam. Figure 6 schematically illustrates the

electrical circuit that interprets the inputs from these limit switches and controls the cover motion. When no rain is present, this circuit prevents the cover from being opened. If the cover is forced open, the cover motor will attempt to return it to the closed position. When the rain sensor relay is energized, indicating the presence of rain, the cover opens until the appropriate limit switch breaks the electrical circuit driving the motor. Forced attempts to close the cover will be resisted by the motor. Changes in the rain sensor status while the cover is in motion will cause the motor to reverse direction.

The cover mechanism is mounted to a pole to reduce the possibility of sample contamination due to rain splatter. The funnel height is variable and was located about two meters above the ground for this study. Splatter from the cover mechanism itself into the funnel was not observed.

Autosampler Design

The autosampler is comprised of a refrigerator, a carousel containing sample bottles, a sample reservoir and liquid level sensor, the controlling electronic circuitry, and a printer. The carousel and reservoir are located inside the refrigerator so that the collected samples may be refrigerated. The electronics and printer are located above the refrigerator in an isolated compartment of the main housing to protect them from moisture.

The carousel assembly is shown in detail in Figure 7. The carousel holds twenty 60 ml narrow–mouth polyethylene bottles. An indexing assembly consisting of a 4 rpm AC motor, a 20:1 worm gear reducer, a notched cam, and a microswitch, drive and precisely position the carousel. A shear pin on the main drive shaft between the indexer and the carousel protects the indexer from damage if the carousel becomes jammed. The carousel can be removed from the sampler by removing the knurled screw located in the center of the assembly.

The reservoir and liquid level sensor assembly is shown in Figure 8. Rain collected

by the funnel flows into the 125 ml polyethylene reservoir. As the sample level rises in the reservoir, it also rises in the Teflon side tube. The liquid level sensor (Skan–a–Matic model S19081), which consists of a small lamp and photodetector mounted in a fixture that clamps to the side tube, detects reflected light from the lamp when water in the side tube rises to the sensor position. The position of the sensor is variable and is adjusted to give the desired sample volume. Triggering the sensor activates a time–delay relay, which holds the Teflon solenoid drain valve open for a sufficient length of time to allow the sample to drain into the current sample bottle. For a 60 ml sample, this time delay is about 15 seconds. The drain valve then closes and collection resumes.

The collection interval can also be controlled by elapsed time. In this mode, a repeat–cycle timer with an adjustable time delay controls the drain valve. After a selected time delay, the drain valve opens for 15 seconds, dispensing the sample. The sequence repeats until the event ends or until all of the bottles have been used. This mode should only be used in conjunction with the liquid level sensing mode to ensure that the sample bottles will not be overfilled.

If all of the sample bottles are full, the liquid level sensor and the repeat–cycle timer are turned off. Sample accumulating in the reservoir is stored there until manually removed. If the volume of this sample exceeds 125 ml, the sample will flow out the overflow tube and, if provided, into a large bottle, siphoning the reservoir empty. Sample collected in the overflow bottle represents a composite of all the rain collected after the carousel was filled.

Overflowing the reservoir in this manner is also used to manually rinse the system between events. Distilled water is used to flush the reservoir several times, and then a sample of the rinse water is collected to check the cleanliness of the reservoir system components which contact the sample. All components of the reservoir assembly are made of either Teflon or polyethylene, to avoid sample contamination, and each can be easily removed for periodic cleaning.

The electronic circuitry that controls operation of the sampler is illustrated schematically in Figure 9. Test switches are included to manually rotate the carousel, to open the drain valve, and to simulate the presence of rain on the rain sensor. Power to the liquid level sensor and repeat–cycle timer is controlled by the sample counter. When all of the bottles have been used, power is removed from these devices.

The printer (Hecon model AO544) provides a record of the time and sequence of events occurring within the sampler. The printer monitors up to 8 available switch–type input channels and records the time, date, channel number, and channel status (high or low) whenever a given channel changes state. For this sampling system, the liquid level sensor status, the sample timer status, and the rain sensor status are continuously monitored. A backup battery on the printer protects its internal clock if a power failure occurs. Loss of power is also indicated on the printer tape.

Automated Fogwater Collection

The automated fractionating sampler described in the previous section was modified to provide automated sub–event sequential fogwater sampling at several sites for the South Coast Air Quality Study (SCAQS). In this configuration, the sampling system is comprised of a Caltech Active Strand Collector (CASC), a fog sensor with heated sensing grid, and the previously described autosampler. The assembled system is shown in Figure 10.

The fog collector has been used in previous studies and is described in detail in United States Patent No. 4,697,462 [Daube, Jr., et al., 1987]. Figure 11 is a diagram of the collector assembly. Table 1 lists the CASC's operating parameters. Fog or cloud water samples are obtained by drawing the droplet–laden (droplet diameters of 2 to 50 μm) air through an angled bank of 510 μm diameter Teflon strands with a 14 volt DC fan located at the back of the collector. The droplets collect on the strands by inertial impaction.

coalesce with other collected droplets, and are drawn down into a Teflon collection trough by gravity and aerodynamic drag. A Teflon tube carries the sample down to the reservoir in the autosampler. Figure 12 shows the theoretical collection efficiency of the CASC as a function of droplet diameter [Friedlander, 1977]. The 50% efficiency size cut based on droplet diameter is approximately 3.5 μm, indicating that most of the droplets in the activated size region (droplet dia. > 1 μm) are collected efficiently, while non–activated, sub–micron aerosol particles are not collected.

The collection rate of the collector is described by:

$$\text{Coll. Rate, ml/min} = (n_1)\,(n_2)\,(Q)\,(LWC)$$

Where:

n_1 = Strand efficiency

n_2 = Percent of air sampled

Q = Collector flowrate, m^3/min

LWC = Fog liquid water content, g/m^3

The percentage of air sampled by the collector is a function of the strand geometry and can be approximated using:

$$n_2 = \{1 - (1 - \frac{\text{strand dia.}}{\text{strand spacing}})^N\}$$

Where:

N = No. of rows of strands

For the CASC, with 6 rows of 510 μm diameter strands spaced 1.8 mm apart, 86% of the air passing through the collector is sampled. Assuming that the overall strand efficiency is 85%, corresponding to a 10 μm diameter droplet, the collection rate equation

yields:

$$\text{Coll. Rate, ml/min} = 17.9\ (\text{LWC})$$

Figure 13 is a plot of the expected time required to fill all of the bottles in the carousel as a function of the liquid water content (LWC) of the fog. For a typical LWC of 0.2 g/m^3, the carousel will fill in about 6 hours.

The fog sensor used for SCAQS is essentially a miniature version of the CASC. Figure 14 is a diagram of the sensor assembly and Table 2 lists its operating parameters. The sensor consists of a 15 W AC fan, 6 angled rows of 280 μm diameter nylon strands, and a heated stainless steel (Type 304, passivated) detection grid. The sensor fan runs continuously. When fog is present, it is drawn into the sensor where it collects by inertial impaction onto the strands. The collected droplets coalesce, run down the strands, and drip onto the detection grid. The grid is controlled by a circuit identical to that used for the rain sensor. When water bridges the grid, the main system is activated. Power is applied to the fan on the CASC and sample collection begins. When fog is no longer present, the heater, typically operated at 2 W, dries off the detection grid and turns off the main system and the CASC.

The collection efficiency of the sensor was designed to match that of the CASC. This ensures that all events that can be sampled by the CASC are sampled. In a fog with a LWC of 0.2 g/m^3, the sensor collects approximately 0.2 ml/min of liquid, which is sufficient to activate the main system within 10 minutes after the start of the event. After the event ends, the main system is turned off within 20 minutes.

Automated Aerosol Sampler Design

Aerosol and gas phase samples were obtained using a filter pack technique. To

obtain sequential samples at several sites simultaneously, an automated aerosol sampler was developed. The instrument, illustrated in Figure 15, consists of a vacuum pump, flow–controlling critical orifices, a four channel programmable timer, three solenoid valves, a cooling fan, and nine 47 mm open–faced filter holders mounted in a covered sampling head. Three sets of three filter packs can be installed at a time. The start and stop times of each of the three possible sampling periods is programmed into the timer.

When activated, the vacuum pump draws air through one of three possible solenoid valves, as selected by the timer, and through the corresponding 3 filter packs. A critical orifice connected in line with each filter pack maintains the air flow through the pack at 10.8 l/min. Previously used filter packs are covered to prevent wet and/or dry deposition from contaminating the top filter. For a portion of this project, the cover was painted white to reduce solar heating of the exposed filters which could volatilize some of the collected chemical species.

Summary

An instrument for the collection of sub–event sequential samples of rain was designed and ten units were constructed. The automated fractionating sampler is a general purpose sampling instrument with a total sample capacity of 1200 ml distributed among 20 sample bottles. It can be used on a time and/or volume fractionating basis and it provides overflow protection when all of the sample bottles are full. The collected samples are refrigerated at 4 C to preserve their chemical integrity. The sampler will collect sequential rain samples for approximately 8 hours during an event with an average rainfall intensity of 5 mm/hr and stores any subsequent collection in an overflow bottle. During this study, an overflow bottle was not used and collected sample exceeding the capacity of the system was not saved.

The sampler is readily modified for automated collection of sequential fog or cloud

samples. By changing sensors, removing the funnel and cover mechanism, and installing a fog collector, the sample collected by the fog collector can be directed into the autosampler and fractionated in the manner described above for rain. In this arrangement, the sampler will collect sequential fog samples for about 6 hours during an event with an average liquid water content of 0.2 g/m^3.

An instrument for the collection of aerosol samples by a filter pack technique was also developed and seven units were constructed. Three sets of three open–faced filter holders may be installed at a time. A timer, programmed by the operator, controls the sampling period for each filter set. The filter packs are covered when not in use to avoid contamination.

References

Daube, B. C., Jr., Flagan, R. C., and Hoffmann, M. R. (1986) *Active Cloudwater Collector* United States Patent #4,697,462 Oct. 6, 1987.

Friedlander, S. K., (1977) *Smoke, Dust and Haze*, John Wiley & Sons, New York, 107.

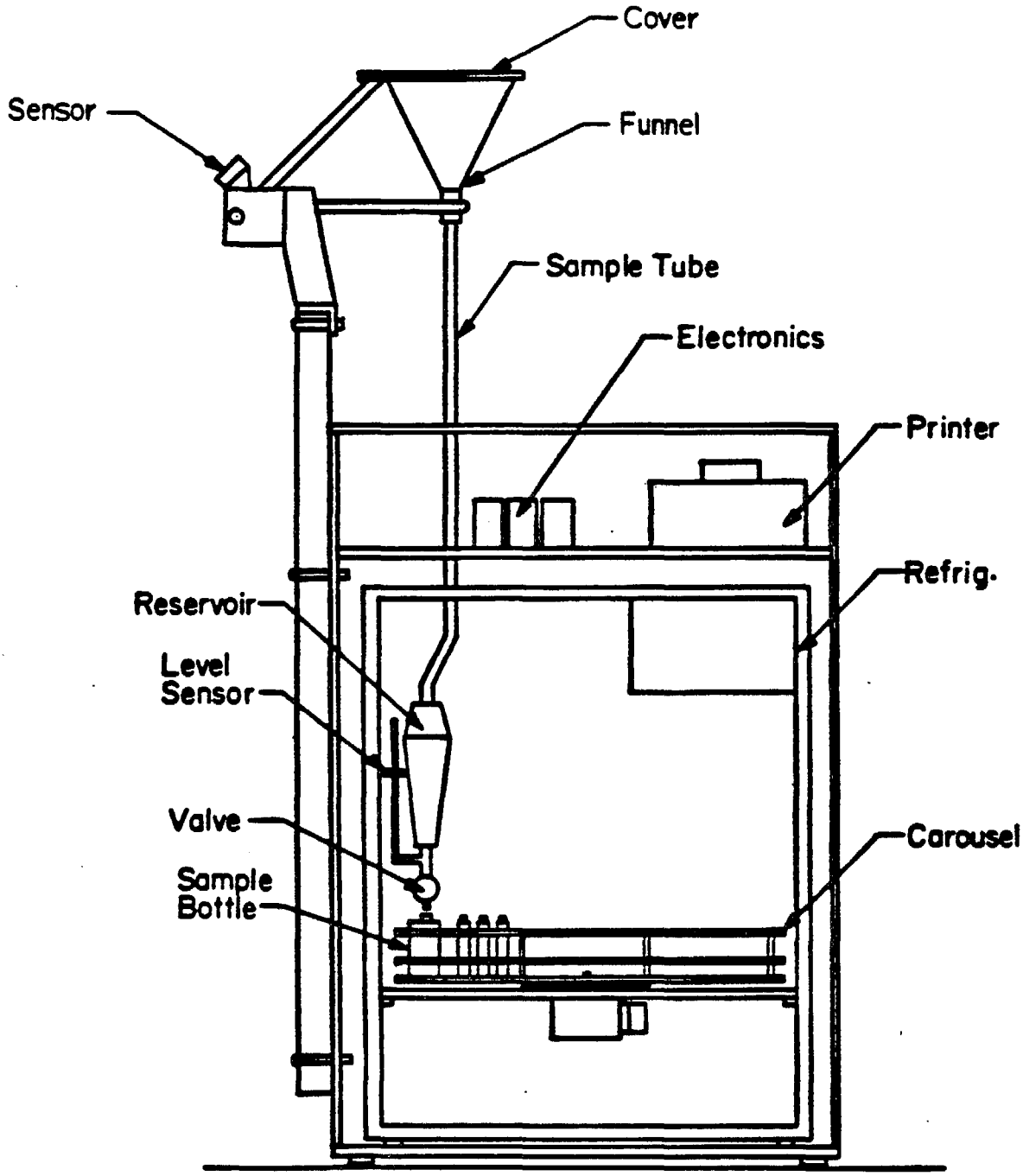

Figure 1. Automated fractionating sampling system for rainwater.

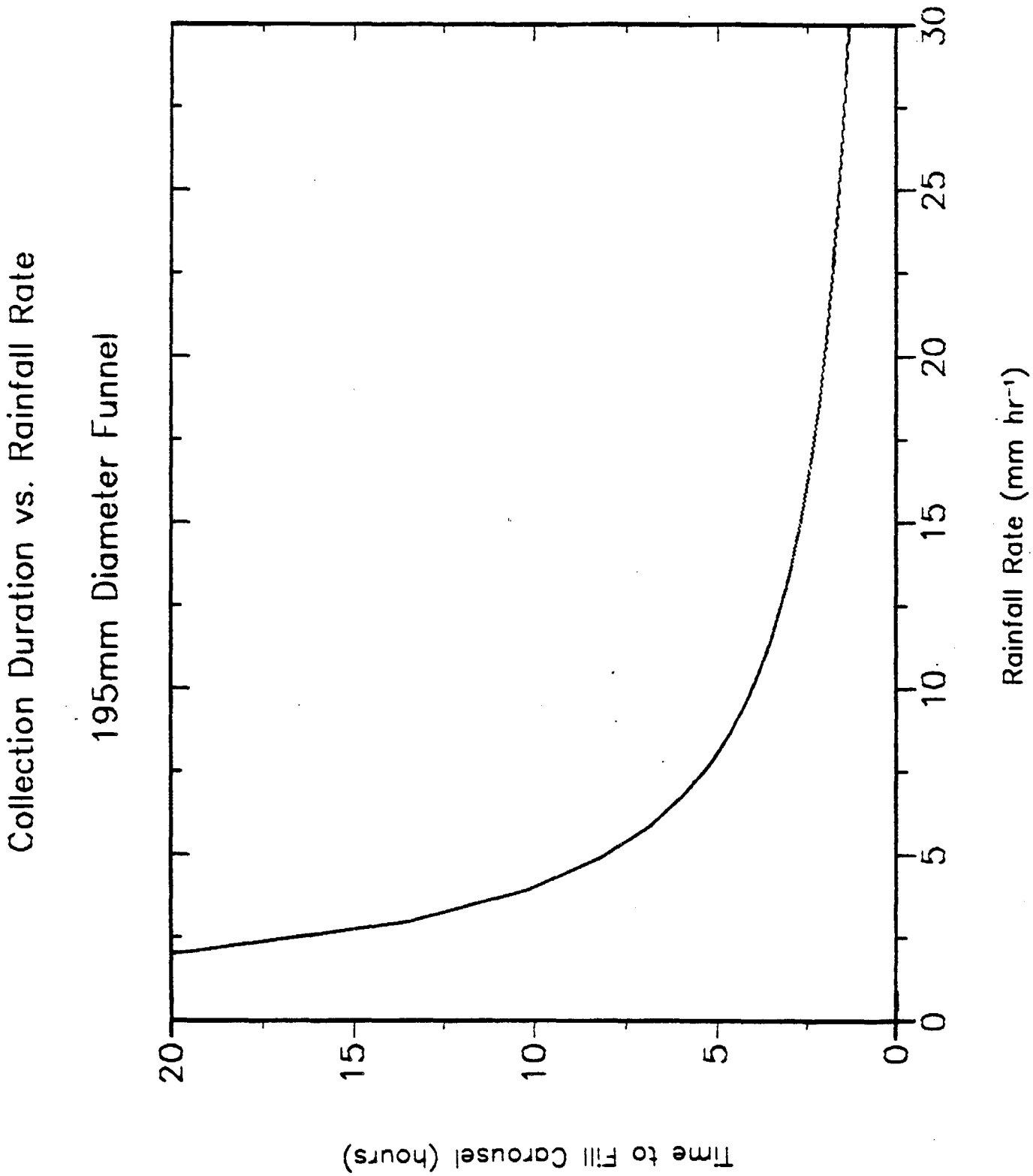

Figure 2. Time required to fill the autosampler carousel as a function of rainfall intensity.

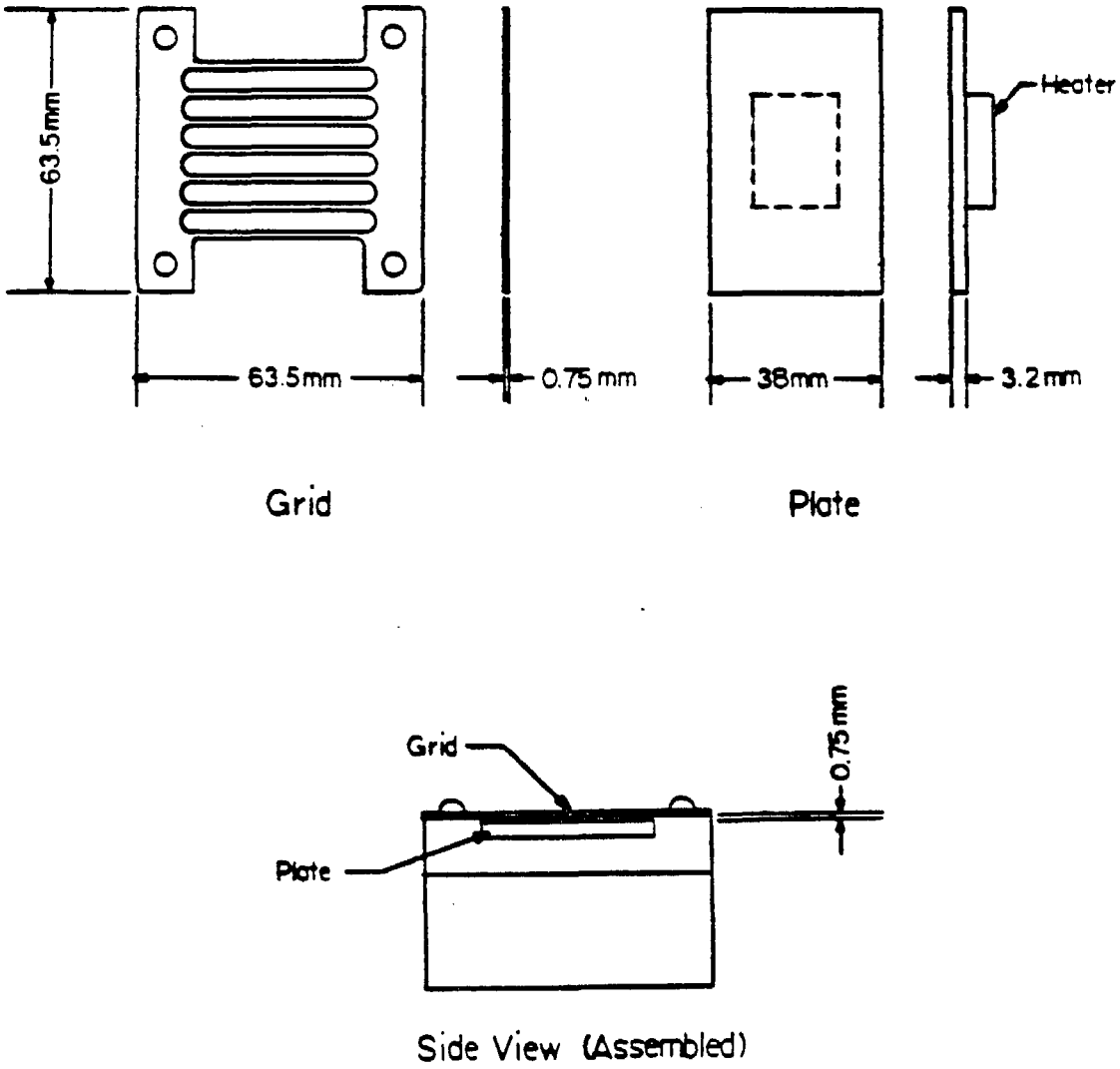

Figure 3. Rain sensor grid, plate, and assembly.

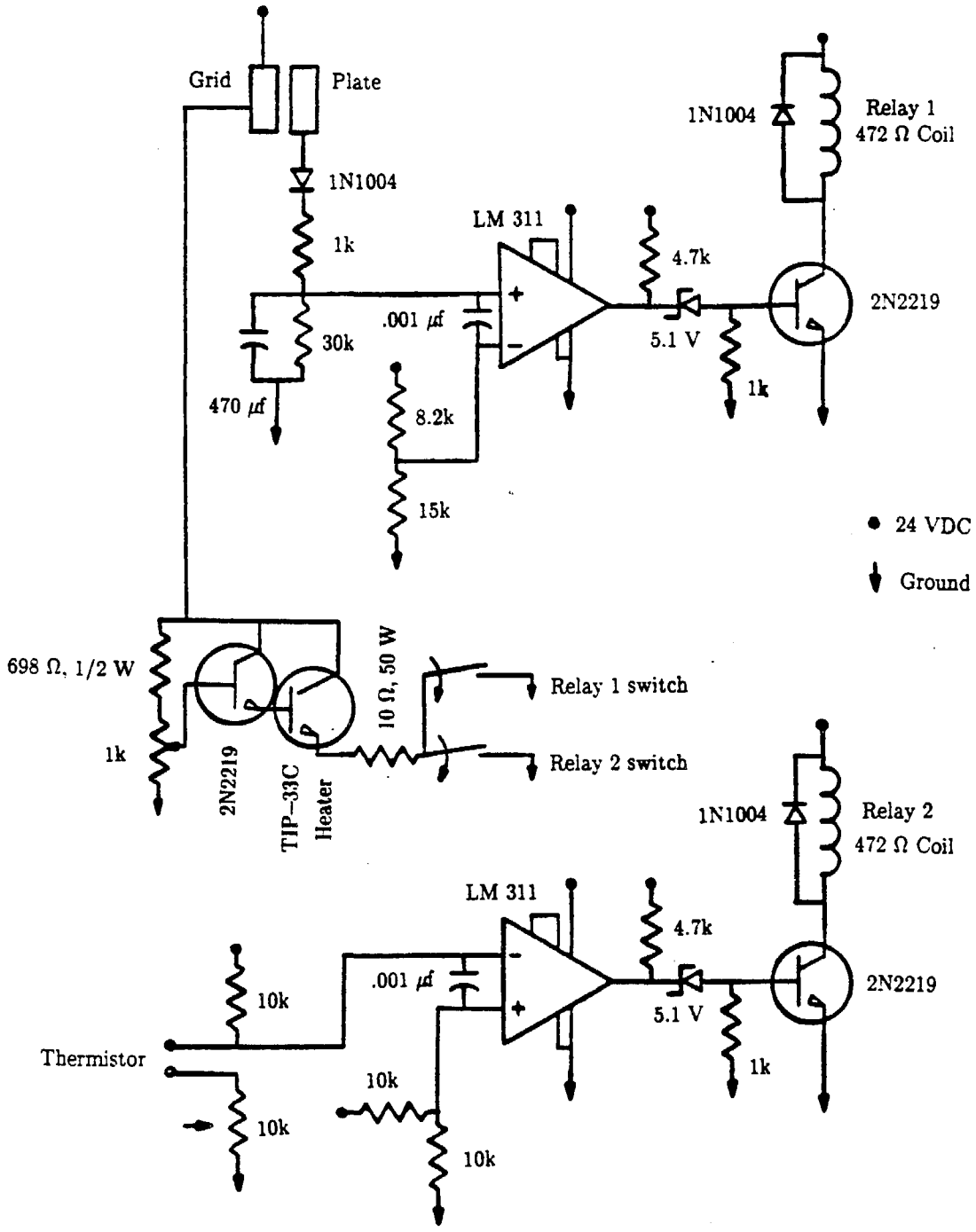

Figure 4. Rain sensor control circuitry.

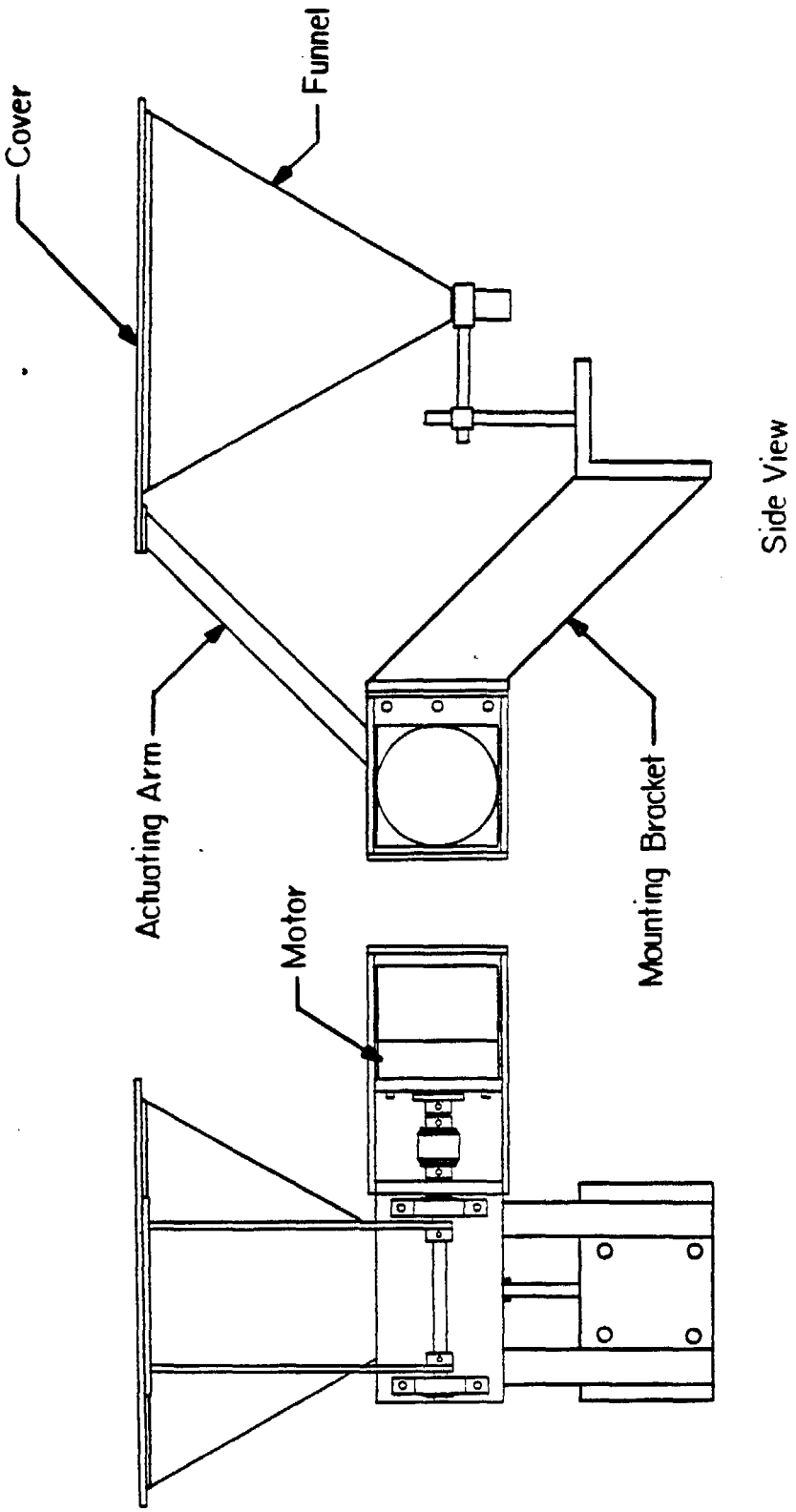

Figure 5. Funnel cover mechanism assembly.

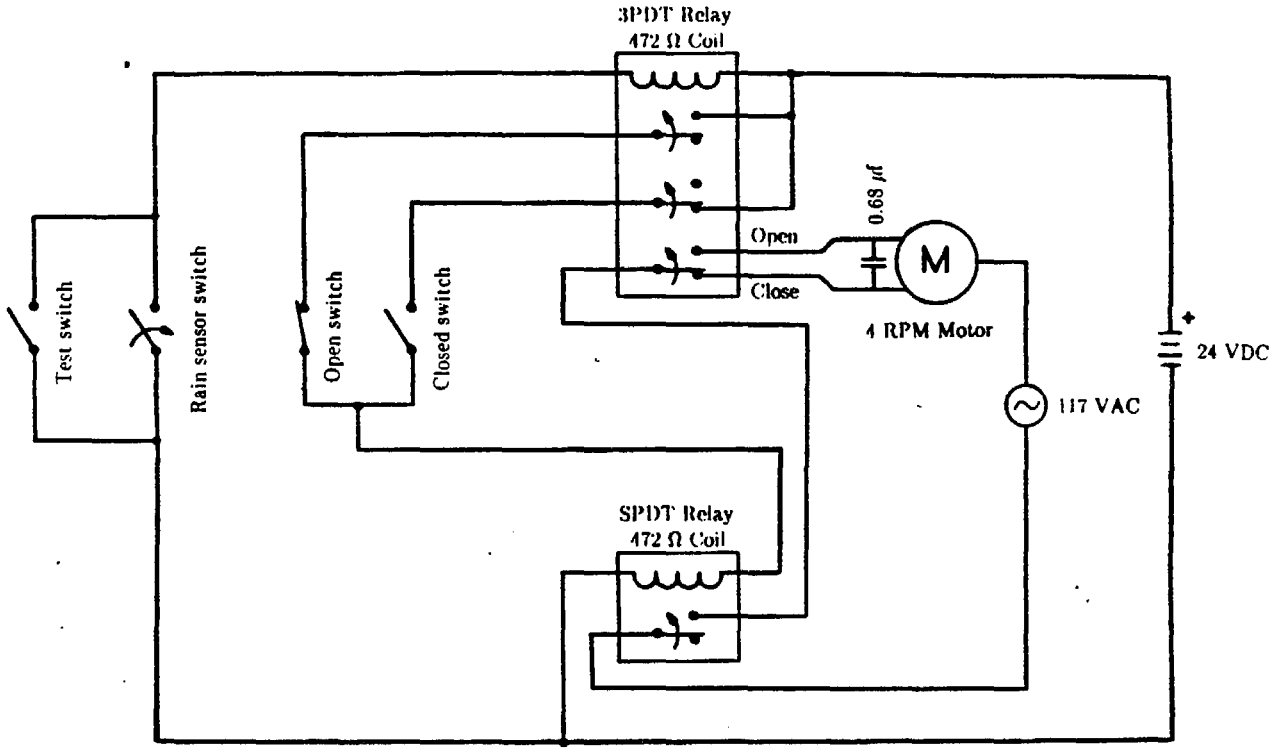

Figure 6. Funnel cover mechanism control circuitry.

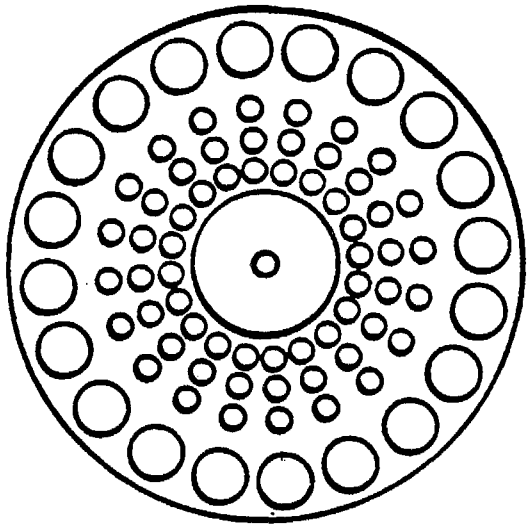

Top View

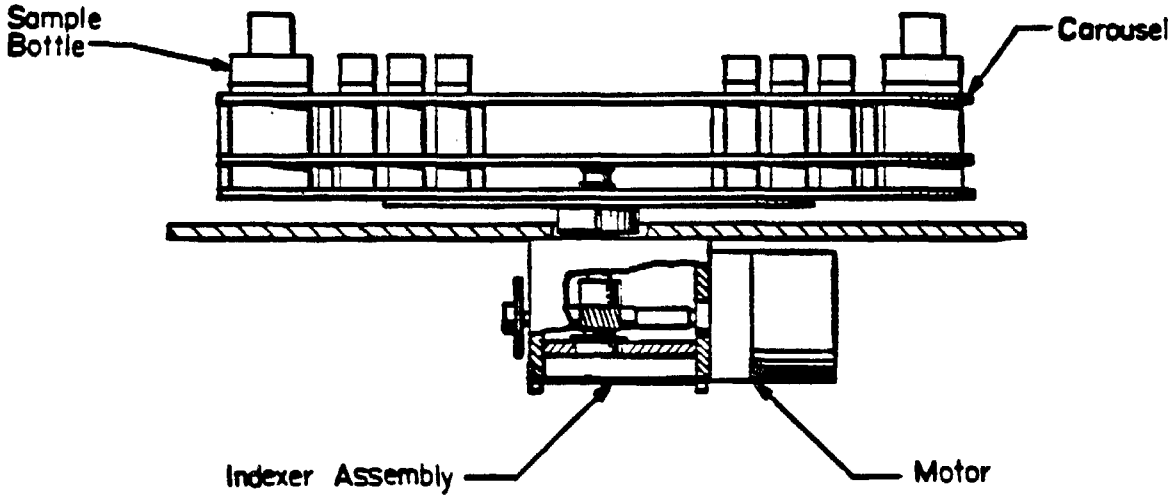

Figure 7. Carousel assembly with sample bottles and indexer.

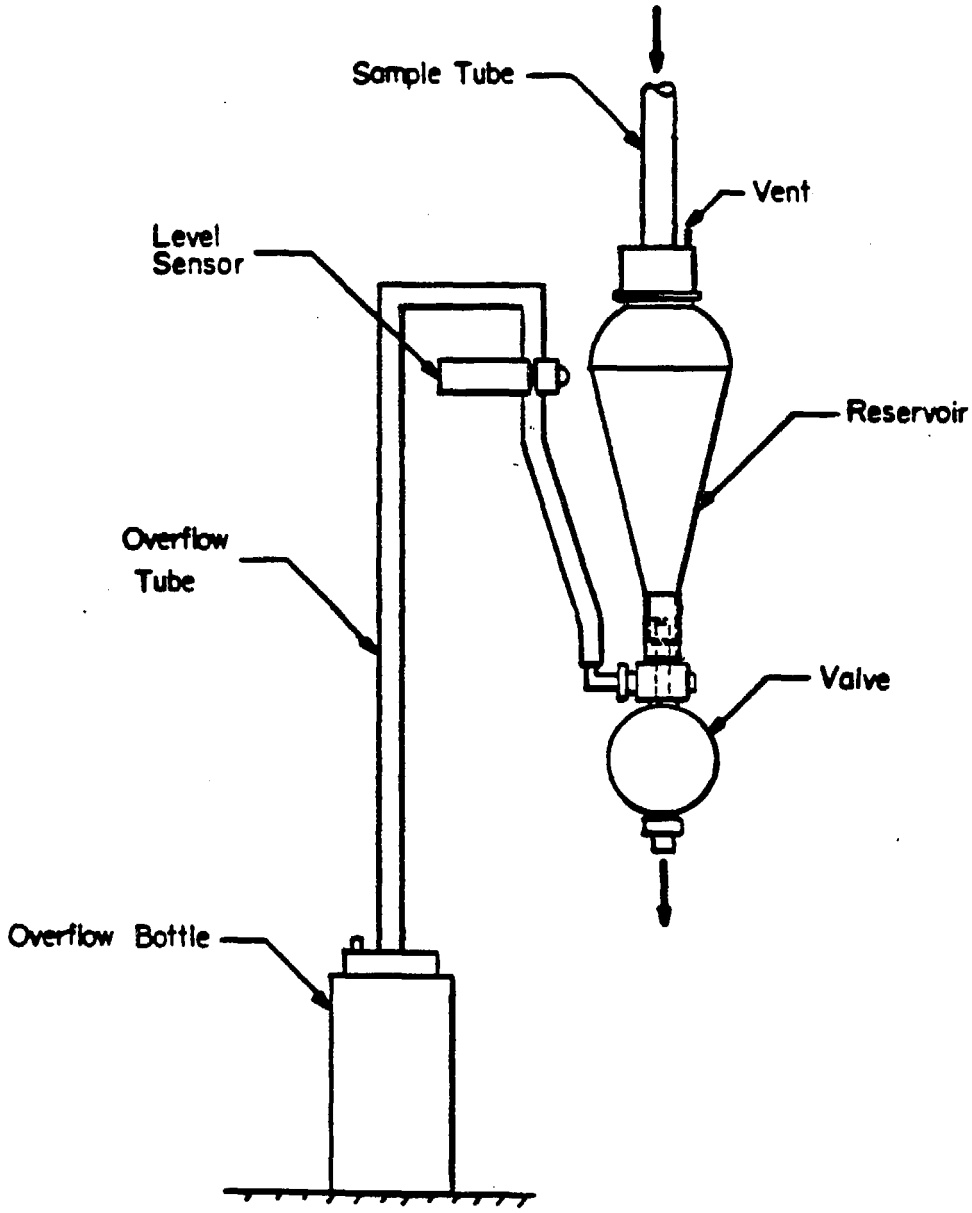

Figure 8. Autosampler reservoir assembly.

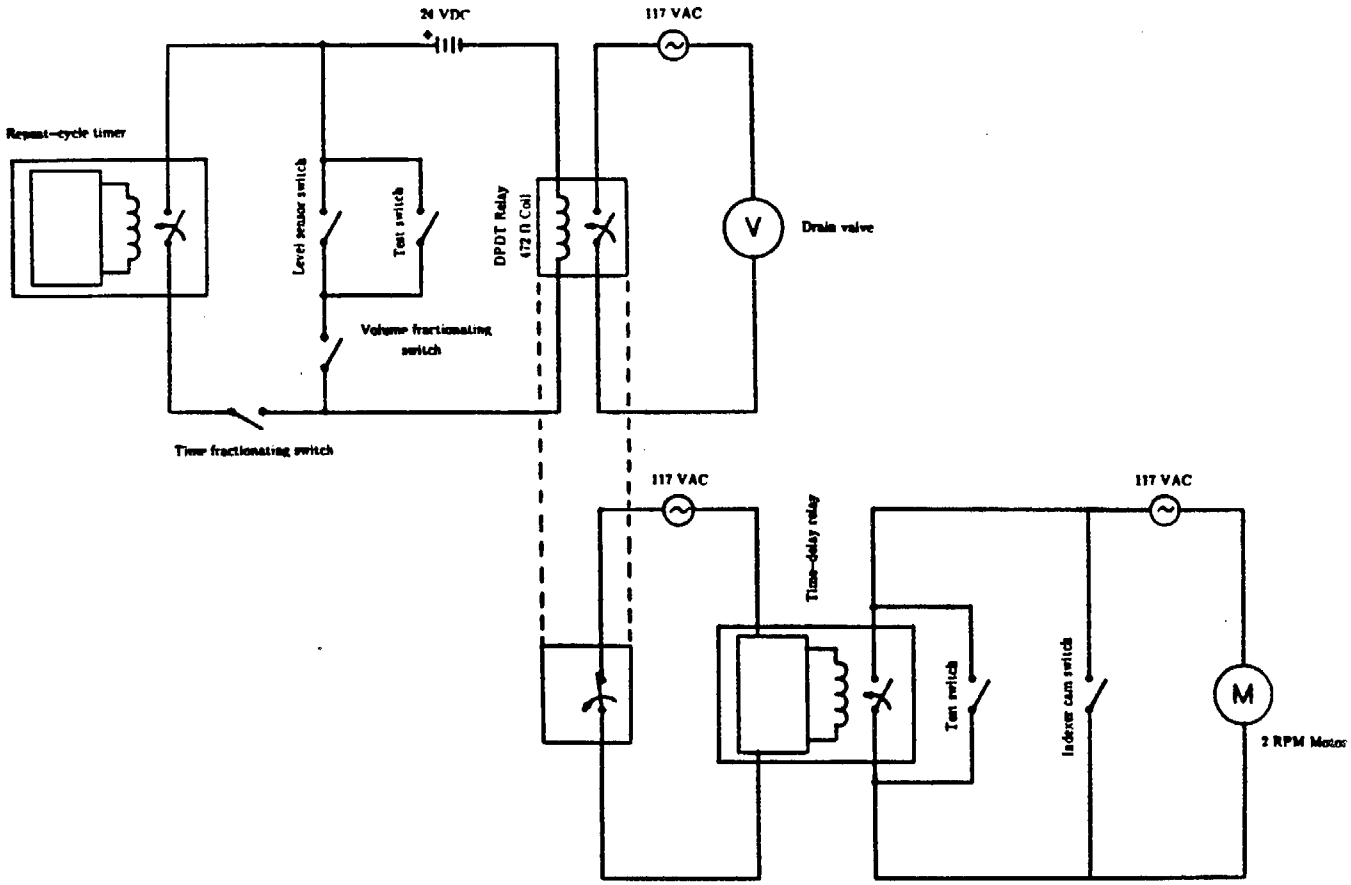

Figure 9. Autosampler carousel and drain valve control circuitry.

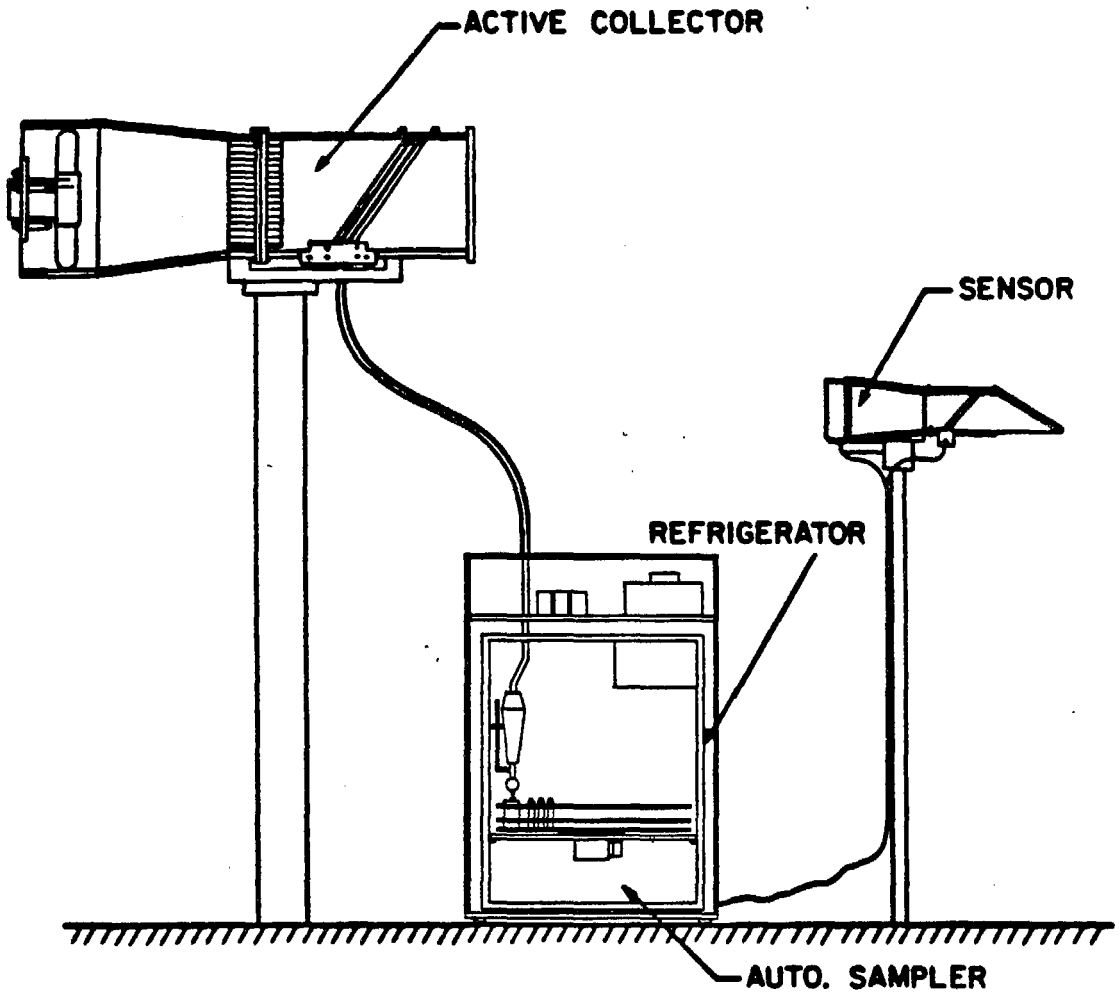

Figure 10. Automated fractionating sampling system for fogwater.

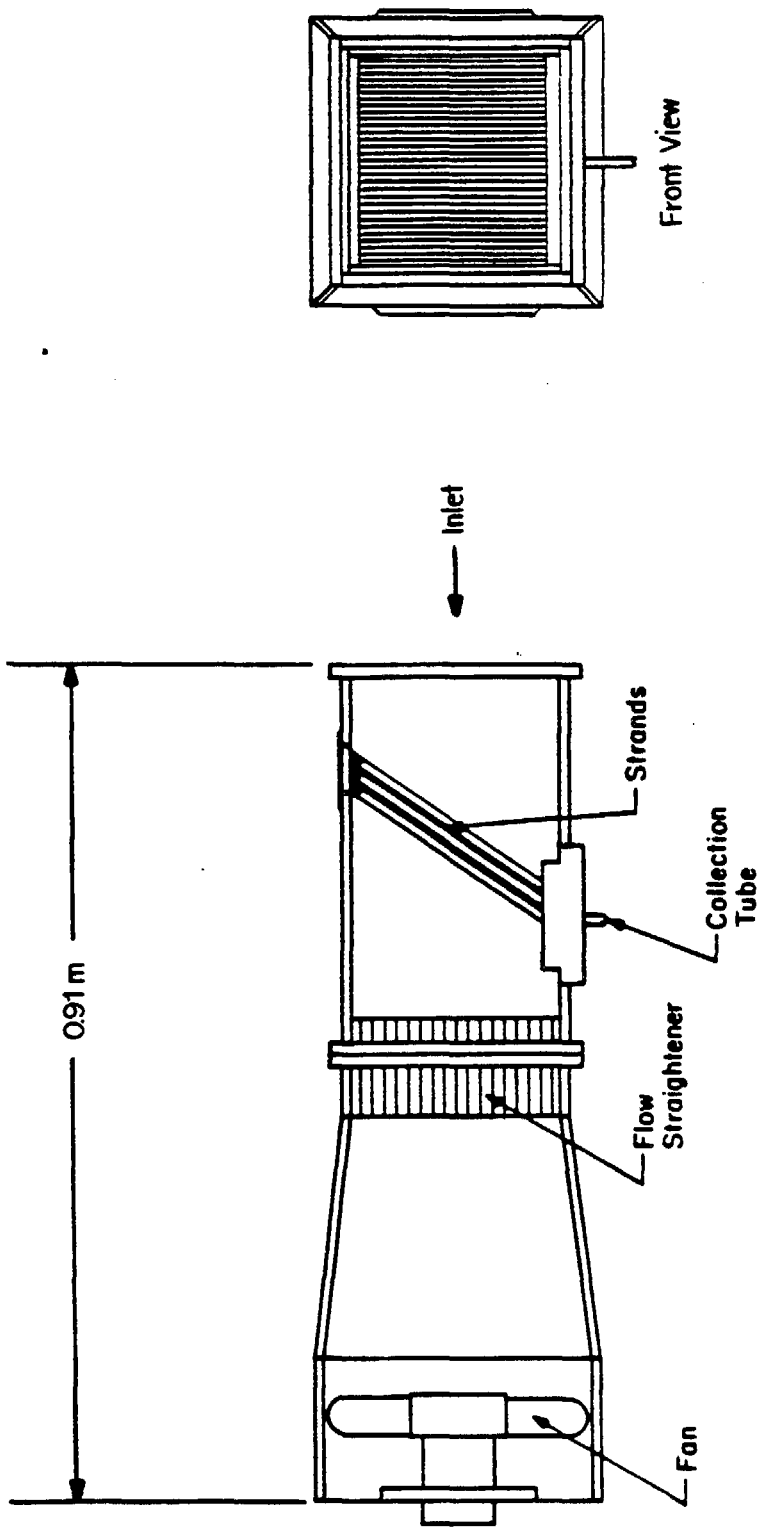

Figure 11. Caltech active strand collector (CASC) assembly.

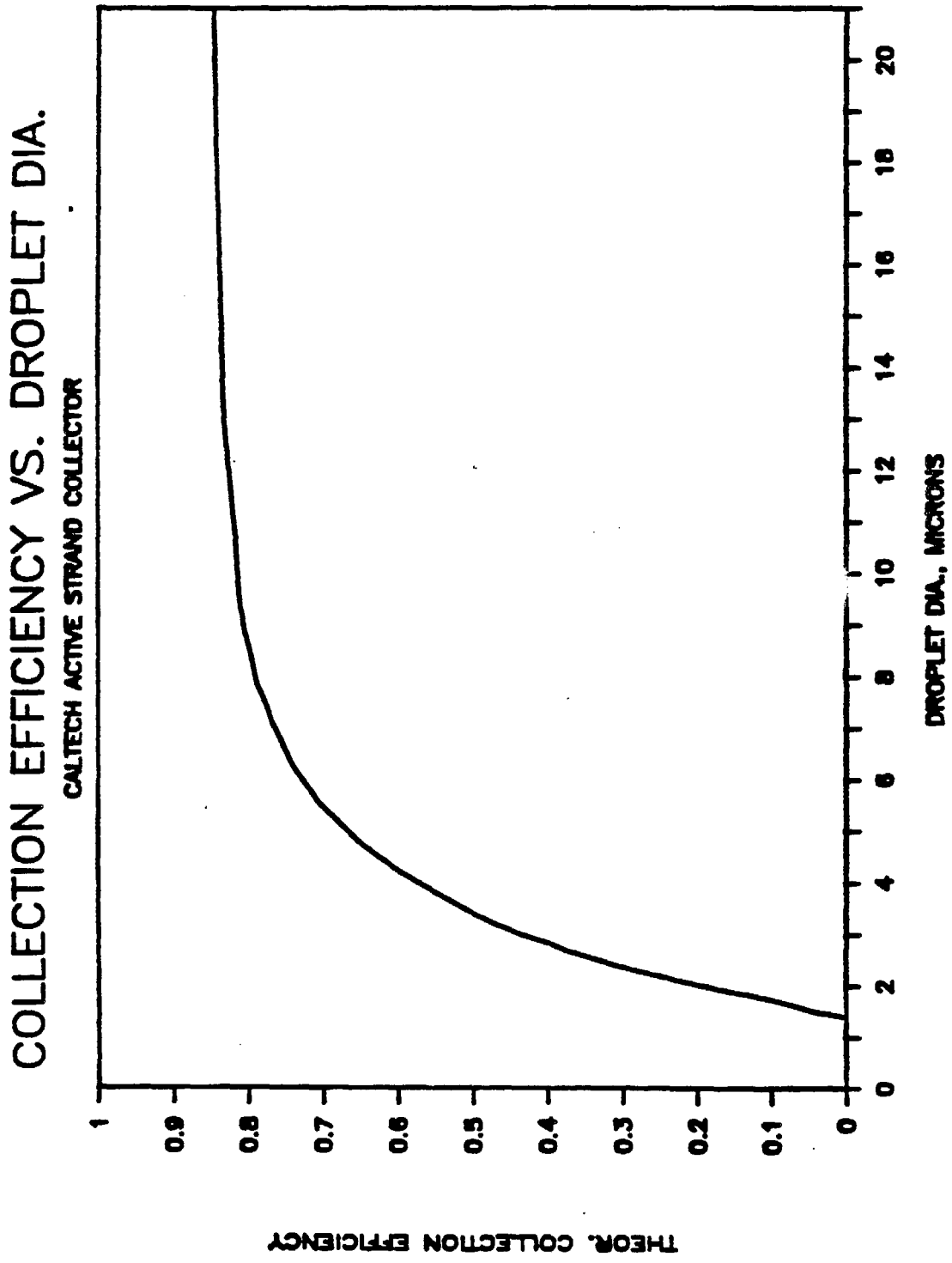

Figure 12. Theoretical collection efficiency of the CASC.

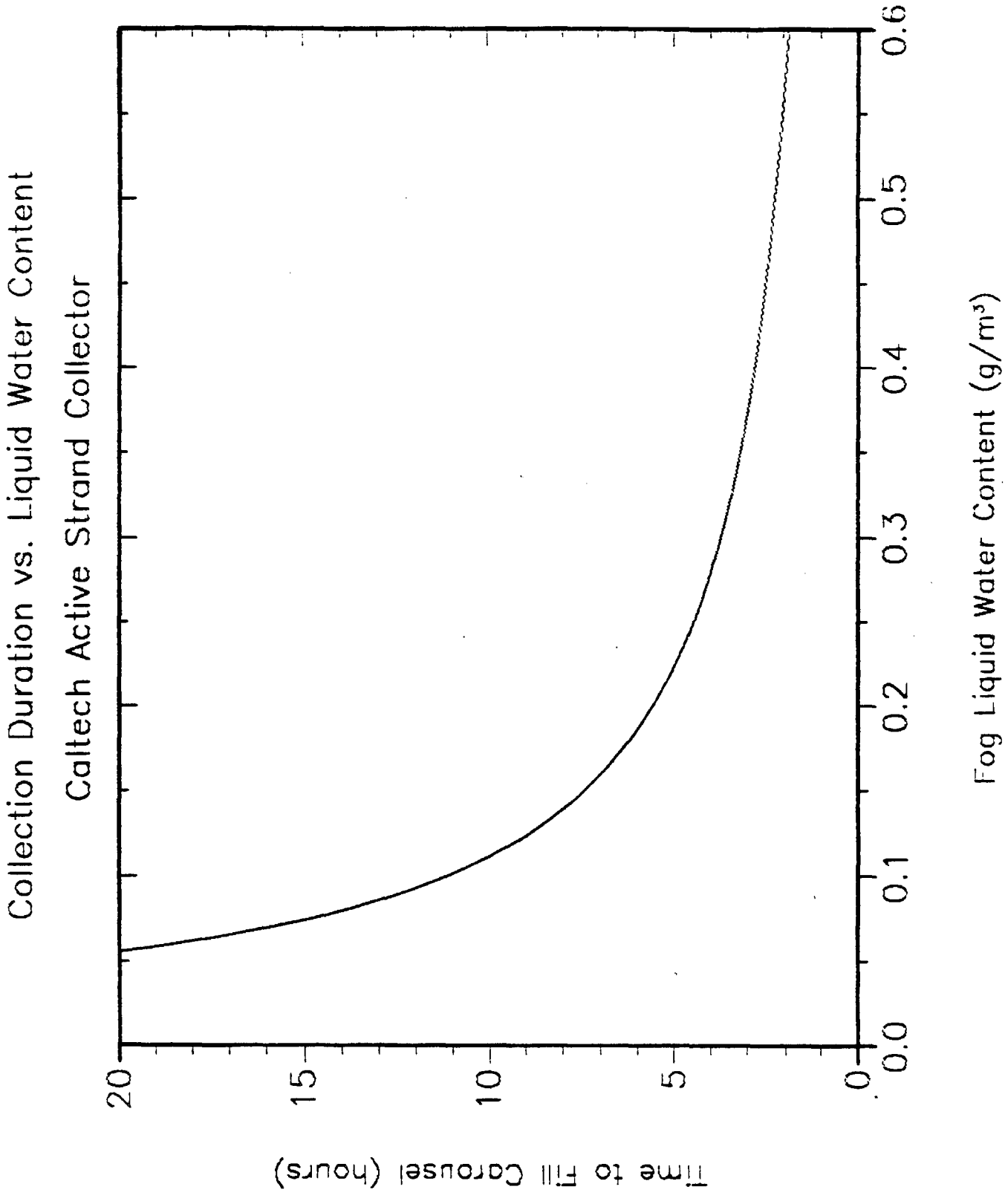

Figure 13. Time required to fill the autosampler carousel as a function of fog LWC.

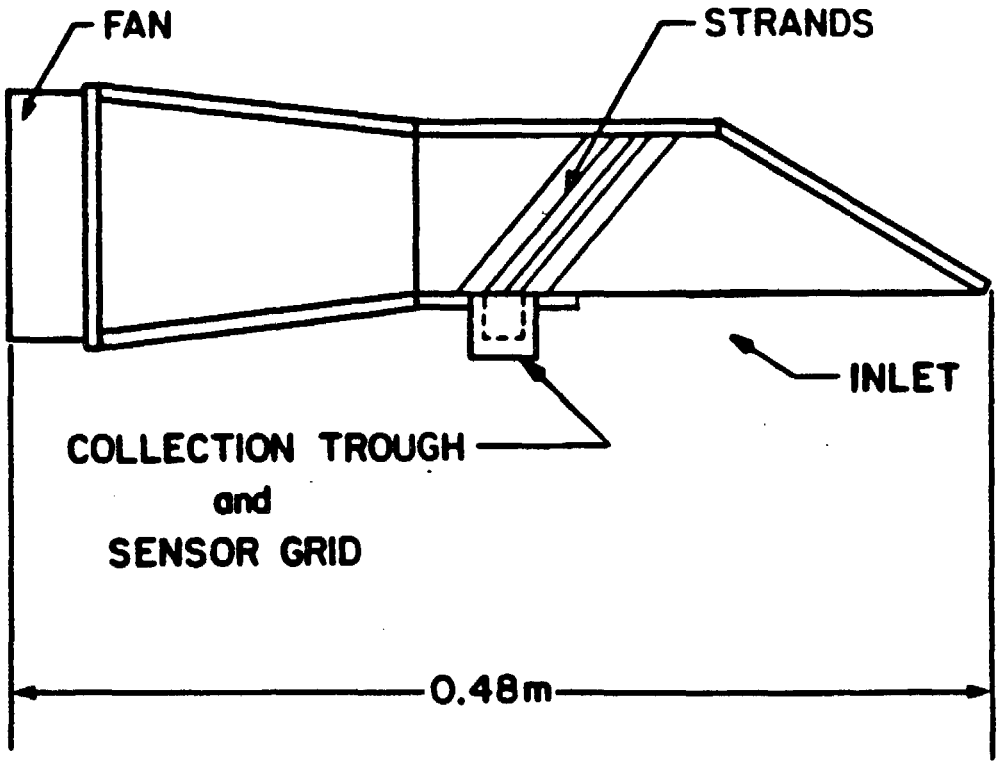

Figure 14. Fog sensor assembly used for SCAQS.

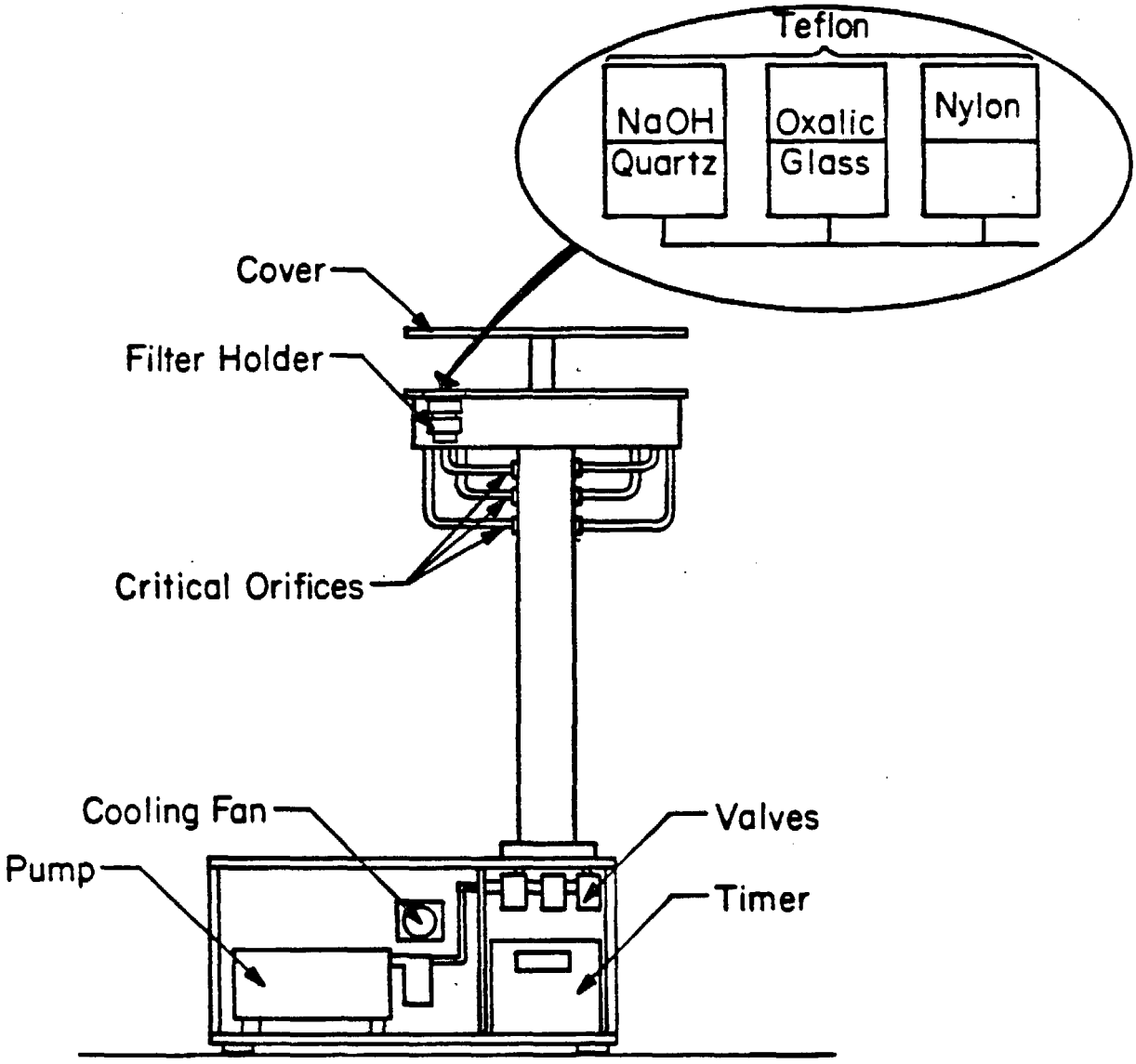

Figure 15. Automated aerosol sampler assembly.

Parameter	Value
Strand diameter, μm	510
Strand length, m	190
No. of rows of strand	6
Strand spacing, mm	1.8
Air flowrate, m^3/min	24.5
Percent of air sampled, first row	27.9
Percent of air sampled, total	86.0
Total sampled flow, m^3/min	21.1
Droplet diameter size cut (50% efficiency), μm	3.5
Average velocity at strands, m/s	8.5
Pressure drop, mm Hg	0.93
Operating voltage, VDC	14.0
Theor. collection rate, (0.5 g/m^3 LWC), ml/min	9.0

Table 1. Operating parameters of the Caltech Active Strand Collector (CASC).

Parameter	Value
Strand diameter, μm	280
Strand length, m	25
No. of rows of strand	6
Strand spacing, mm	1.1
Air flowrate, m^3/min	1.7
Percent of flow sampled, first row	26.4
Percent of flow sampled, total	84.0
Total sampled flow, m^3/min	1.4
Droplet diameter size cut (50% efficiency), μm	3.5
Average velocity at strands, m/s	6.0
Operating voltage, VAC	117
Theor. collection rate (0.5 g/m^3 LWC), ml/min	0.5

Table 2. Operating parameters of the fog sensor.

CHAPTER 2

Spatial and Temporal Variations in the Composition of Rain in the South Coast Air Basin

by

Jeff Collett, Jr., J. William Munger, Bruce Daube, Jr., and Michael R. Hoffmann

Environmental Engineering Science
W. M. Keck Laboratories, 138–78
California Institute of Technology
Pasadena, CA 91125

March 1988

Introduction

In Los Angeles, storm systems normally originate over the Pacific Ocean and have little or no contact with polluted air masses until they reach the South Coast Air Basin. Once over Los Angeles, the storm serves both to cleanse pollutants from the atmosphere and to deposit them at the ground. Several processes are important in determining the efficiency of atmospheric cleansing and the total deposition of each species of interest. Processes of interest within the cloud include scavenging of aerosol by nucleation, diffusion, and impaction, scavenging of gases, and reaction within the aqueous phase. Below the cloud, raindrops will continue to scavenge gases and aerosol, and reaction may continue within the droplets as they fall to the ground. The relative importance of in–cloud vs. below–cloud processes can be evaluated by examining vertical profiles of rainwater concentrations and deposition rates for each species of interest.

Also of interest is the amount of each species deposited to the ground during the course of the storm, relative to the quantity of that species present in the air mass over the basin prior to the onset of rain (referred to here as the pre–storm atmospheric burden of that species). If the deposition of a given species is seen to be greater than its pre–storm atmospheric burden, then some inferences about the emission rate of that species, or its production rate in the atmosphere, may be drawn, giving proper consideration to the potential for transport of the species from other locations. Questions about transport during the storm are further related to local emissions influences, which affect the composition of rainfall on a distance scale much smaller than the South Coast Air Basin.

In order to properly investigate the issues discussed above, simultaneous measurements of rainfall rate and composition are needed, as a function of time, at several sites throughout the basin. Compositional measurements of the aerosol and gas phases as a function of time are also needed at the same sites. The development of both an automated sub–event precipitation sampler and an automated aerosol collector (both described in

Chapter 1) enabled the current study to meet these requirements and proceed to address these issues.

Site Description and Measurement Techniques

Sampling Sites

Five sites were selected for use in the study. These sites, depicted in Figure 1, were located at West Los Angeles, Pasadena, Henninger Flats, Mount Wilson, and Riverside. West Los Angeles, Pasadena, and Riverside were selected to provide a sampling transect from east to west in the South Coast Air Basin (SoCAB). Pasadena, Henninger Flats, and Mount Wilson were chosen to represent a vertical profile. The elevation of the land rises from just over 200 m at Pasadena to approximately 1700 m at Mount Wilson, 12 km farther inland. Henninger Flats is located at an elevation of approximately 700 m.

The site at Mt. Wilson is located on the grounds of the Mt. Wilson Observatory. The site at Henninger Flats is located on the grounds of a nursery operated by the Los Angeles County Fire Department. Both the Mount Wilson site and the Henninger Flats site are located in areas away from regular vehicle travel. The site in Pasadena is located on the roof of the three–story W. M. Keck Laboratories building on the Caltech campus. A paved parking lot is located 75 m to the north of the building. The West Los Angeles site is located on the grounds of the Veterans Administration Hospital. The 405 freeway was located approximately 1 km to the east. The sampling equipment was situated near a lightly used corner of the hospital's paved parking lot. The Riverside site is on the roof of a one–story trailer on the eastern edge of the campus of the University of California at Riverside. A small dirt parking lot, used by three or four vehicles, is situated on one side of the trailer and a lightly used paved campus road is located on the opposing side.

Sampling Techniques

Rain samples were collected at the five sites using a 195 mm funnel mounted on a Caltech Automated Fractionating Sampler (CAFS) deployed in the rain configuration (see Chapter 1). The sampler is equipped with a plexiglas cover which closes over the funnel when it is not raining. A resistance grid sensor, described in detail in Chapter 1, is used to detect the presence of rain. When rain is detected the cover is opened so that sample can be collected. The rain sensor is continuously heated to evaporate sedimenting rain drops. The heating level is set so that 10 to 15 minutes after the rain stops the sensor is dry. When the sensor dries the funnel cover is closed.

The sampler is equipped with a carousel which holds twenty 60 ml sample bottles. Rain collected by the funnel is stored in a reservoir until either enough is collected to trigger an optical level sensor or until a break occurs in the rain. A rain break is defined as a period when the sensor dries off and the cover is closed over the funnel. The level sensor is set to activate the reservoir drain valve when the reservoir contains 60 ml (60 ml of collected rain corresponds to just under 20 mm of rainfall). When the level sensor is triggered or rain is sensed following a rain break, the sample collected in the reservoir is dumped to a collection bottle. The carousel then indexes, bringing the next bottle into position under the reservoir to receive the subsequent sample. Once the carousel has indexed twenty times, indicating that all of the sample bottles have been used, no more sample is released from the reservoir. This prevents the contamination of samples already collected. Samples are stored refrigerated in the CAFS until picked up by a research staff member. Samples were normally picked up within 12 hours after an event occurred. During extended events it was necessary to pick up collected samples and re–load the carousel with empty bottles while the event was in progress.

Each of the five sampling sites was also equipped with an automated aerosol sampler (see Chapter 1). This sampler can be programmed to collect samples over three different time periods. We employed a filter pack method for obtaining samples of aerosol

and gas phase species. Teflon filters (Zefluor, 1 μm pore size) were used to collect the aerosol for the determination of major ion concentrations. Two oxalic acid impregnated glass fiber back–up filters were used in series to collect $NH_3(g)$. A nylon back–up filter was used to collect $HNO_3(g)$. A flow rate of 10.8 liters per minute through each filter pack was maintained by a critical orifice. Filter samples were normally collected over four hour periods with two hour intervals between samples. Samples were normally picked up within a couple of hours after the last set was run.

Upon return to the laboratory each rain sample was weighed to determine its volume. An aliquot of each was then used to determine the sample pH. pH measurements were made using a Radiometer PHM82 Standard pH meter and a GK2320C semi–micro combination electrode calibrated with pH 4 and 7 buffers. Following the pH measurements, the samples were refrigerated until further analyses could be made. The major ions, Cl^-, SO_4^{2-}, and NO_3^-, were measured using a Dionex 2020i ion chromatograph, equipped with a Dionex AS–4 column, using a carbonate–bicarbonate eluent. NH_4^+ was measured by the phenol–hypochlorite method (Solorzano, 1967) using an Alpkem flow injection analyzer. Na^+, Ca^{2+}, and Mg^{2+} concentrations were measured using a Varian Techtron AA6 atomic absorption spectrophotometer. Filters were extracted in a known volume of liquid on a reciprocating shaker. The extracting liquid was carbonate–bicarbonate IC eluent for the nylon filters, water for the oxalic acid impregnated glass fiber filters, and water with 2% EtOH (to help wet the surface) for the teflon filters. The extracts were analyzed by the same methods used for the rain samples.

Results

Six rain events were sampled during the period from January 1, 1987 to April 30, 1987. During this period nearly 300 samples were collected at the five sampling sites and analyzed in our laboratory. Tables 1 through 5 list the data obtained for those samples.

Included in these five tables are the date and collection period for each sample, the sample volume, the amount of rainfall the sample represents, the sample pH, concentrations of major inorganic ions in the sample, and the ion charge balance for the inorganic species measured. A few entries in the tables are marked "NA" for not available. These represent times when (1) the sample volume was too small to allow all of the measurements to be made, (2) no sample was collected for a period during which it was raining at the site because the capacity of the sampling carousel had been exceeded, or (3) the sample was contaminated during handling.

Table 6 provides a brief summary of the data. Listed here are the number of events sampled and samples obtained, the range of pH observed, and the range of concentrations measured for each ion at each site. pH values at West Los Angeles and Henninger Flats ranged from 4.1 to approximately 6. At Pasadena the range extended from slightly below 4 to about 5.5. Mount Wilson rainwater pH values varied from 4.3 to 5.7 while values at Riverside were observed to fall between 4.5 and 6.8. The highest concentrations of Na^+ and Cl^-, derivatives of sea salt, were measured in the early part of a storm at Henninger Flats. Concentrations of these species on average, however, were highest at the West Los Angeles site, which is closest to the ocean. By far the highest concentrations of NH_4^+ were seen at Riverside. This is not surprising since the nearby dairy operations in Chino are the dominant source of $NH_3(g)$ emissions in the SoCAB. The highest NO_3^- and SO_4^{2-} concentrations were observed in samples collected in Pasadena, although concentrations nearly as high were measured in samples from West Los Angeles, Henninger Flats, and Riverside. Maximum concentrations of Ca^{2+} and Mg^{2+} were measured at Pasadena and Henninger Flats respectively. For most samples the dominant inorganic ions were H^+, NO_3^-, SO_4^{2-}, and NH_4^+. In some samples Na^+ and Cl^- were also important contributors.

Ratios of nitrate to sulfate varied considerably between sites, from storm to storm, and even within a single storm at a given site. In Figure 2 the concentration of nitrate has been plotted vs. the sulfate concentration for each sample collected at the West Los

Angeles site. The different symbols represent samples collected in different rain events. Also plotted here is a linear regression line fitted to the data using the method of ordinary least squares. The data, which fit closely to the regression line (slope = 0.86, 95% confidence limits of 0.79 and 0.92) indicate that a slight excess of sulfate over nitrate is typical of West Los Angeles rainwater. Figures 3 through 6 present similar plots for the other four sites. The data for Pasadena indicate considerably more variation in the ratio of these two species in the rainfall there. Looking closely at Figure 3, it is evident that much of the variation occurs between storms. Two of the sampled storms show considerably higher nitrate to sulfate ratios than the 1.07 suggested by the regression line. One storm shows considerably less. Samples within a given storm, however, seem to maintain a fairly constant ratio.

The nitrate to sulfate ratios at Henninger Flats, depicted in Figure 4, are even more variable than those at Pasadena. The ratio not only varies from one event to another, considerable variation is observed even within a single event. Figure 7 illustrates the changes that occurred during a storm on March 5 and 6, 1987. Data points connected by lines represent samples that were collected over periods of fairly continuous rain. Breaks in a line indicate breaks in the rainfall. Several dramatic changes were observed in the ratio of nitrate to sulfate over the course of this storm, with the range of ratios stretching from less than one–half to nearly five. The largest changes generally followed a break in the rain. Ratios of the two species at Mount Wilson were similarly variable as illustrated by Figure 5.

Riverside rain samples had, on average, a slight excess of sulfate over nitrate as seen in Figure 6. This is somewhat surprising since past work has indicated that fogwater sampled at the site generally has a large excess of nitrate (Munger et al., 1987).

Electroneutrality requires that the sum of negative charges in the rainwater equals the sum of positive charges. Clearly the data listed in Tables 1 through 5 do not always conform to this requirement as indicated by the preponderance of $-/+$ ratios (representing

the ratio of total measured negative charge concentration to total measured positive charge concentration) considerably different from one. Two reasons may be hypothesized to explain this discrepancy: (1) errors in analytical measurements of ion concentrations and (2) failure to include important species in the ion balance. For several of the samples, concentrations of most species are near our detection limit (see Chapter 3 for information on detection limits). For these samples it is not surprising to see the ion balance differ significantly from 1.0 since relative error in concentration measurements increases near the detection limit. Removing these dilute samples from consideration, however, leaves a number of samples with ion balances considerably less than one. This anion deficit suggests that lower molecular weight organic acids may be important contributors to the composition of the samples. Formic and acetic acid have been shown to be important components in rainwater collected in remote as well as urban areas, including Los Angeles (Galloway et al., 1982; Keene and Galloway, 1984; Kawamura and Kaplan, 1984). At the pH levels found in many of the rain samples, both formic and acetic acid will exist largely in their deprotonated form (pK_a^{298} of 3.74 and 4.76, respectively, Martell and Smith, 1977). Samples with the highest pH values also tended to exhibit the largest anion deficits, consistent with the hypothesis that formate and acetate are the missing anions. Since no one was generally present at each site to take the steps necessary to preserve unstable species such as acetic and formic acid which undergo biodegradation, we cannot positively confirm that acetate and formate were present at the levels necessary to correct the calculated anion deficit. During the ion chromatographic analysis of NO_3^-, SO_4^{2-}, and Cl^-, however, we did observe significant concentrations of "formate + acetate", which elute in a peak before chloride, despite the fact that the samples had not been preserved. These concentrations have not been reported here because of the instability of the species. They are indicators, however, of the presence of significant levels of low molecular weight organic acids in the collected samples.

During the study 100 filter sets were run in an attempt to define aerosol and gas

phase concentrations prior to, during, and following rain events. Approximately one–half of these were used in an intensive monitoring effort during the period from March 4 to March 8. Results of the filter analyses are listed in Table 7. Highest concentrations of $NH_3(g)$ and $HNO_3(g)$ were seen at Riverside and Pasadena, respectively. Na^+ and Cl^- aerosol concentrations were highest at West Los Angeles followed by Pasadena. The ratio of Na^+/Cl^- was seen frequently to significantly exceed the sea–salt ratio of 0.86. This suggests that much of the original Cl^- in the aerosol may have been volatilized as HCl via acid exchange with nitric acid. The highest concentrations of aerosol NO_3^- and SO_4^{2-} were observed at Pasadena. NH_4^+ concentrations in the aerosol were highest at Riverside and Pasadena. Occasional high NH_4^+ aerosol concentrations were also observed at West Los Angeles. During all periods sampled, ammonia was predominantly found in the aerosol phase at Pasadena and West Los Angeles. At Riverside, it was predominantly located in the gas phase. Concentrations of $HNO_3(g)$ at Riverside were always fairly small during the periods sampled due to the high levels of $NH_3(g)$ and the tendency of these species to form ammonium nitrate aerosol.

Discussion

Two storms were selected for more detailed consideration: February 13, 1987 and March 5–6, 1987. The February 13 event was selected because it provided the most complete data set for the vertical profile from Pasadena to Mt. Wilson. This event also provided a significant number of samples for the horizontal transect from West Los Angeles to Riverside. The discussion in the following section will consider the pattern of deposition and rainfall for these two transects. The second storm, March 5–6, will be addressed in the subsequent section. Here the discussion will focus on the relationship between the aerosol and gas phase compositions and the composition of the rainfall.

The Storm of February 23, 1987

The storm of February 23 was the second wettest event at Pasadena during the period studied. 25.1 mm of rainfall were recorded by the Los Angeles County Flood Control District rain gauge on the Caltech campus. This rain gauge is located approximately 100 m south of the study site on another three story building. The Pasadena study site recorded 24 mm of rainfall during the storm. Cumulative rainfall as a function of time at Pasadena, Henninger Flats, and Mount Wilson, is depicted in Figure 8. Both the total hydrologic deposition and the pattern in which it occurred are remarkably similar for the three sites. For most of the storm the rain fell at all three sites at a rate of approximately 4 mm/hr.

The similarity in rainfall deposition patterns at the three sites facilitates the comparison of deposition rates of the major ionic species. Plots of the deposition patterns for NO_3^-, NH_4^+,SO_4^{2-}, H^+, Na^+, Cl^-, Mg^{2+}, and Ca^{2+} at the three sites are presented in Figures 9 through 12, respectively. Deposition of nitrate was 530 μeq/m^2 at Pasadena, 40% higher than at Henninger Flats and 380% higher than at Mt. Wilson (see Figure 9). Deposition of most species at these three sites was in fact observed to be highest at Pasadena and lowest at Mt. Wilson. Deposition of NH_4^+ was approximately 580 μeq/m^2 at Pasadena, 130% higher than at Henninger Flats and more than 1000% higher than at Mt. Wilson (see Figure 9); for SO_4^{2-} the enhancement at Pasadena was 150% compared to Henninger Flats and 600 % compared to Mt. Wilson (see Figure 10). Since the rainfall patterns were essentially identical at all three sites, and the sites are located within 12 km of one another, these differences in deposition indicate that much of the loading of these species in the rain collected at Pasadena was picked up in the lowest 500 m of the atmosphere. Likewise, much of the loading in the rain collected at Henninger Flats was picked up in the 1000 m between there and Mt. Wilson.

Deposition of H^+ was only slightly higher at Pasadena than at Henninger Flats (approximately 475 vs. 425 μeq/m^2, see Figure 10), suggesting that the net acidity of the

rain droplets was not affected significantly as they fell through the lowest portion of the atmosphere. A substantial increase in deposition of H^+ was observed between Mt. Wilson and Henninger Flats, however. Na^+ deposition at all three sites followed the same hierarchy and at each site was substantially less than Cl^- deposition (Figure 11), suggesting that HCl(g) was probably being scavenged by the cloud and/or rain droplets. Deposition of Mg^{2+} was relatively small at all three sites, but was still significantly higher at Pasadena than at the other two sites (Figure 12), while Ca^{2+} deposition was somewhat higher, contributing 130 $\mu eq/m^2$ at Pasadena and 30 to 40 $\mu eq/m^2$ at both Henninger Flats and Mt. Wilson.

For most species, 75% of the deposition, or more, occurred during the first two hours of the storm. After this time, deposition rates dropped off considerably, despite the fact that average rainfall rates increased over the subsequent two hours of the storm. Mg^{2+}, Cl^-, and Na^+ were seemingly almost completely washed out of the air column by this point. Deposition of NO_3^-, SO_4^{2-}, and NH_4^+ continued at reduced, but roughly constant, rates during the remainder of the storm. Ca^{2+} was the only ion which continued to be deposited at a rate even close to its initial deposition rate, and this occurred only at Pasadena. At Henninger Flats and Mt. Wilson, deposition of Ca^{2+} was essentially finished after the first three hours.

The rainfall deposition patterns at West Los Angeles and Riverside were somewhat different than those observed at Pasadena, Henninger Flats, and Mt. Wilson (see Figure 13). The rain began an hour earlier at West Los Angeles than at Pasadena, while at Riverside the rain began three hours later. Total rainfall at West Los Angeles was approximately 16 mm while Riverside received less than 5 mm, predominantly in two short rainy periods. Figure 14 presents the deposition of NO_3^- and NH_4^+ vs. time at the three sites. Deposition of NO_3^- at both West Los Angeles and Riverside was considerably less than at Pasadena. The amount of nitrate deposition normalized by rainfall at Riverside was roughly equivalent to that at Pasadena. Normalized nitrate deposition at West Los

Angeles, however, was much less, despite the fact that the rain began there earlier than at any of the other sites. Normalized NH_4^+ deposition at Riverside was more than twice that at Pasadena, while at West Los Angeles it was considerably less (see Figure 14). It is interesting to note that the deposition patterns of both species at West Los Angeles and Riverside closely paralleled the rainfall patterns at the same sites. Unlike Pasadena, neither site experienced a dramatic drop in the deposition rate as the storm progressed, aside from periods of reduced rainfall rate.

The patterns of cumulative deposition for SO_4^{2-} and H^+ are shown in Figure 15. Deposited amounts of both species, normalized by the amount of rainfall, are considerably less at both West Los Angeles and Riverside than they are at Pasadena. The high level of $NH_3(g)$ at Riverside essentially neutralized all of the acidity in the rain there, leaving raindrops of pH > 6 and almost no H^+ deposition.

Deposition of Na^+ and Cl^- were, as expected, highest at West Los Angeles (see Figure 16). The increase in the deposition rate of each of these species at this site, shortly after 1400, occurred despite a decrease in the rainfall rate and seems more closely correlated with a change in the wind direction at the site from southerly to southwesterly at about the same time (SCAQMD, 1987).

Figures 17, 18, and 19 depict the washout of the major ionic species at Pasadena, Henninger Flats, and West Los Angeles, respectively. Also plotted here are the rainfall intensities as a function of time for each site. Lines drawn between data points indicate periods of fairly continuous rain. Concentrations of all measured species dropped rapidly in the first part of the storm, although somewhat less rapidly at West Los Angeles than at the other two sites. The concentrations of H^+, NO_3^-, SO_4^{2-}, and NH_4^+ are remarkably similar during all phases of the storm in Pasadena. A decrease in the Pasadena rainfall rate after 1600 coincided with an increase in the rainwater concentrations of these four species, and Ca^{2+}. Little change was observed in the concentrations of Na^+, Cl^-, or Mg^{2+} during this same period. At West Los Angeles, a drop in the rainfall intensity at approximately 1400

coincided with an increase of all species concentrations except Ca^{2+}. Most of these species concentrations climbed to 50% or more of their initial rain sample levels during this period. A similar drop in rainfall intensity at Henninger Flats in the late stages of the event was accompanied by only slight increases in rainwater concentrations of the major species.

The Storm of March 5 and 6, 1987

Upon forecast that a rainstorm was headed for the Los Angeles area, an intensive aerosol and gas phase monitoring program was begun on March 4 to characterize pre–storm conditions throughout the SoCAB. The monitoring was continued during and after the storm as well. Plots of the observed concentrations of aerosol NH_4^+, NO_3^-, and SO_4^{2-}, and of $NH_3(g)$ and $HNO_3(g)$ as a function of time at the five sites are presented in Figures 20 through 24 (note the different scales used for the different sites). Also shown in each figure is a plot of the cumulative rainfall deposition at the site as a function of time. Most of the rain event was not sampled at Pasadena due to an unusually long period of light rain "sprinkles" which used up the twenty bottles in the carousel before most of the rainfall occurred. Data on rainfall deposition for Pasadena was taken from the Los Angeles County Flood Control District (LACFCD) recording rain gauge also located on the Caltech campus. During other events the rainfall observed by this gauge and the study rain sampler were closely correlated.

Concentrations of all measured species were seen to drop at all of the sites except West Los Angeles following the onset of the rain. At West Los Angeles, the aerosol SO_4^{2-} concentration dropped immediately, as did the concentration of $HNO_3(g)$. Concentrations of $NH_3(g)$ and aerosol NO_3^- and NH_4^+ were seen to increase at West Los Angeles during the early part of the storm. These increases are most likely due to a change in wind direction that coincided roughly with the time the rain began. During the morning the wind had been primarily blowing lightly from the west. After noon, however, the wind shifted to the east and began to blow more strongly (SCAQMD, 1987). Since the

production of NO_3^- and NH_4^+ occurs predominantly in the central and eastern portions of the SoCAB, the rise in concentrations of these species in the air mass at West Los Angeles is consistent with the change in wind direction.

With the rain essentially over by mid–morning on March 6, concentrations of aerosol NO_3^-, SO_4^{2-}, and NH_4^+ began to increase at Pasadena, Henninger Flats, and Riverside. By early morning on March 7, NO_3^- and NH_4^+ concentrations had achieved their pre–storm levels at all three sites. Concentrations of aerosol SO_4^{2-} also achieved pre–storm levels by this time at Pasadena and Henninger Flats, but required a few extra hours at Riverside. Concentrations continued to rise through noon of March 7 when monitoring was discontinued at all of the sites except Pasadena, where concentrations were seen to drop off substantially on March 8. Aerosol concentrations were seen to rise following the end of the rain event at West Los Angeles as well, however, during the period sampled, they never significantly exceeded their pre–storm levels. SO_4^{2-} did not quite even reach that level. Concentrations at Mt. Wilson were observed to increase slightly following the storm and never came close to reaching their pre–storm levels by noon of March 7.

Rainfall deposition amounts during the storm were highest at Mt. Wilson, followed by Henninger Flats, West Los Angeles, and Riverside, in that order (see Figure 25). Data from the LACFCD rain gauge in Pasadena place that site closely behind West Los Angeles in rainfall for this storm. Compared to the storm of February 13, rainfall was much higher at Mt. Wilson and Riverside, slightly higher at Henninger Flats, slightly lower at West Los Angeles, and substantially lower at Pasadena during this event.

The deposition patterns of the major ionic species in the rainwater are shown for West Los Angeles, Henninger Flats, Mt. Wilson, and Riverside in Figures 26 through 29. Despite somewhat lower concentrations of nitrate and sulfate in the Mt. Wilson samples than in those from other sites, deposition of these species was highest here through the bulk of the storm due to higher rainfall amounts (see Figures 26 and 27). A late spurt of rain at Henninger Flats brought the total nitrate deposition there slightly above that at Mt.

Wilson around noon on March 6. H^+ concentrations, which were nearly equal at all four sites, led to deposition patterns that closely resembled those for rainfall (Figure 27). NH_4^+ concentrations were substantially lower at Mt. Wilson than at the other sites, leading to a third place finish for the site in deposition of this species. The highest NH_4^+ deposition was observed at Henninger Flats, followed by West Los Angeles (see Figure 26). Deposition of Na^+ and Cl^- was, not surprisingly highest at West Los Angeles (Figure 28). Like the event of February 13, the ratio of Cl^- to Na^+ deposition at Henninger Flats and Mount Wilson was seen to significantly exceed the sea salt ratio, suggesting the incorporation of HCl(g) into the rain droplets. Deposition of Ca^{2+} and Mg^{2+} was comparable at all four sites (see Figure 29).

By comparing the measured flux to the ground of the different species in rainwater to the pre–storm concentrations in the aerosol and gas phase, we can determine whether the rain flux during the storm is more or less than the atmospheric burden over the basin prior to the storm's onset. The concentrations of the nine species measured in the gas and aerosol phases prior to the storm at Pasadena, Henninger Flats, and Mt. Wilson are depicted in Figure 30. The data chosen for this plot are those collected from 0200–0600 on March 5. The data for the period 0800–1200 are similar. The former period was chosen because some rainfall did occur at Mt. Wilson and Henninger Flats during the latter period. The general trend observed for most species is that concentrations are highest at Pasadena (elev. 200 m) and lowest at Mt. Wilson (elev. 1700 m), with concentrations at Henninger Flats (elev. 700 m) falling in between. Using the observed concentrations at these three elevations, we can estimate the atmospheric burden of the measured species over the Pasadena area.

Since no information is available on the gradient of each species between sites we choose to assume that the concentration in each portion of the air column is equivalent to that measured at the closest site with a lower elevation. For example, between 200 and 700 m we assume the concentration of aerosol NO_3^- to be equal to that measured at

Pasadena: approximately 88 neq/m^3. Between 700 and 1700 m the concentration measured at Henninger Flats (49 neq/m^3) is used. From 1700 m, the elevation of the Mt. Wilson site, up to the top boundary of the air column of interest, the concentration is assumed to be equivalent to that measured at Mt. Wilson: approximately 27 neq/m^3. Since the concentrations really drop more gradually with elevation, this method of estimating the atmospheric burden should tend to overestimate it somewhat.

At 0800 on the morning of March 5, the cloud base was observed to be at approximately 3000 m. Assuming the cloud to extend 1000 m upward from its base, we can estimate the upper boundary of the air column accessible to processing by the cloud droplets and rain droplets to lie at about 4000 m. Given the preceding observations and assumptions, the calculated burdens of N(V), S(VI), and N(–III) over the Pasadena area are 160, 170, and 390 μeq/m^2, respectively. Estimates of the burdens of N(V) and N(–III) include not only contributions from aerosol NO_3^- and NH_4^+, but also from HNO_3(g) and NH_3(g). A similar estimate for Na^+ yields a burden of 24 μeq/m^2 in the air column above Pasadena.

For a given species, Z, if (1) all of available Z is removed from the air column in the rain (by some combination of in–cloud and below–cloud scavenging) (2) no production of Z in the air column occurs, (3) no emission of Z into the air column occurs, and (4) there is no net transport of Z into or out of the air column during the storm except in the rainfall, then the deposition of Z in the rain at the base of the air column should be equal to the calculated atmospheric burden of Z prior to the onset of the storm. Looking at the data from Henninger Flats and Mt. Wilson, since no deposition data is available for this storm at the base of the column in Pasadena, we can compare the observed deposition to the calculated burdens for each species of interest. Neglecting the last portion of rain that occurred around noon on March 6, deposition amounts of N(V) at Henninger Flats and Mt. Wilson are 310 and 380 μeq/m^2, respectively. For N(–III) the amounts are 700 and 450

μeq/m^2; for S(VI) they are 360 and 425 μeq/m^2; and for Na^+ they are 40 and 30 μeq/m^2.

While it is somewhat higher, the Na^+ deposition is not unreasonably different from the calculated pre–storm atmospheric burden. Calculations for Ca^{2+} and Mg^{2+} give similar results: the calculated pre–storm atmospheric burden is comparable to the observed deposition. The same is obviously not true for N(V) and S(VI). Observed deposition rates for both these species were approximately 150% higher than the corresponding calculated pre–storm atmospheric burdens. N(–III) deposition at Mt. Wilson was approximately equal to the calculated pre–storm burden of N(–III), however at Henninger Flats deposition of N(–III) showed an 80% excess.

Surface level winds at Pasadena were generally from the east during the afternoon of March 5. Since the rain did not begin in earnest until somewhat later in the eastern portions of the SoCAB, as evidenced by the rain record from Riverside, it is possible that some contributions to the deposition were made by transport of species from the east which were incorporated into the clouds or rainwater over Pasadena, Henninger Flats, and Mt. Wilson and rained out on these sites. It is unlikely that this explains all of the excess S(VI) deposition observed since this excess was larger than that for N(–III) which was much higher in concentration than S(VI) in the eastern part of the SoCAB, during the entire period monitored. Upper level winds may have, in fact been coming from some other direction where the relative concentration of atmospheric S(VI) was higher. Even in the western part of the basin during this storm, however, atmospheric loadings of N(–III) exceeded those of S(VI) by 200%.

Since both SO_4^{2-} and NO_3^- are secondary pollutants, no direct emissions from ground level sources could contribute to their presence in the atmosphere. Emissions of their primary pollutant precursors, NO(g) and SO_2(g), followed by oxidation in the atmosphere during the storm may play some role. While the heavy cloud cover over the basin should have reduced the gas phase production of S(VI) and N(V), we should not discard these pathways entirely as possible contributors to production of these species

during the rain event. Aqueous phase mechanisms, either in the cloud droplets, or in the falling rain drops, are probably more likely contributors. We can estimate whether in–cloud oxidation is important by looking at the amounts of these species going into the bottom of the cloud vs. the amounts of the same species in the rain drops as they emerge from the base of the cloud.

Over the period from 1500 on March 5 to 0200 on March 6, the rainfall rate and the deposition rates of SO_4^{2-}, NO_3^-, and NH_4^+, were observed to be fairly constant at both Henninger Flats and Mt. Wilson. Data from the period 2000 to 0600 indicate that the concentrations of aerosol NO_3^-, SO_4^{2-}, and NH_4^+, and of $NH_3(g)$ and $HNO_3(g)$ were constant at Mount Wilson. An observation at 1700 on March 5 placed the cloud base at the same elevation as the Mount Wilson site. Using the data for rainfall deposition at Mt. Wilson, along with the rate of transport into the base of the cloud, and the observed Mt. Wilson gas and aerosol concentrations, we can estimate whether any production of SO_4^{2-} or NO_3^- is taking place in the cloud. Since no data is available on the velocity up into the base of the cloud we will have to estimate it. Using N(–III) as a conservative tracer, we can determine what flux of N(–III) into the base of the cloud is necessary to equal the return flux of N(–III) out of the base of the cloud in the rain. The air velocity at cloud base will then be defined by the quotient of the flux and the total N(–III) concentration in the gas and aerosol. Performing this calculation yields an average velocity of 0.7 m/s. This value, which is not unreasonable for a convective cloud, is calculated assuming 100% scavenging of the N(–III) by the cloud (also reasonable for a cloud of this type). Using this updraft velocity for transport of the measured concentrations of aerosol and gas phase S(VI) and N(V) into the cloud base indicates that 92% of the N(V) flux out of the cloud in the rain is accounted for, but slightly less than 40% of the S(VI) rain flux is accounted for.

The apparent net flux of S(VI) out of the base of the cloud suggests that there is probably substantial production of S(VI) taking place in the cloud. With assumptions about cloud depth and liquid water content, we can estimate the production rate needed to

account for this efflux. During the eleven hour period from 1500 to 0200, 200 $\mu eq/m^2$ of S(VI) were deposited in the rainfall at Mt. Wilson. With the calculated updraft of 0.7 m/s, only 39%, or approximately 180 $\mu eq/m^2$, of this flux could be accounted for by in–cloud scavenging of aerosol SO_4^{2-}. This leaves about 120 $\mu eq/m^2$ to account for. If we assume that the cloud was 1000 m deep with a liquid water content of 0.5 g/m^3, then a production rate of 3.0×10^{-9} **M** sec^{-1} of S(VI) is required. The pH of the rain falling at Mt. Wilson at this time was approximately 5. Typically cloudwater has been observed to be approximately 0.5 pH units lower than simultaneously collected rainwater. For only moderate levels of $SO_2(g)$ and $O_3(g)$ of 5 ppb and 50 ppb, respectively, the aqueous phase oxidation rate of S(IV) to S(VI) is on the order of 10^{-8} **M** sec^{-1} at pH 4.5 (Seinfeld, 1986), making the required S(VI) production rate calculated for the Mt. Wilson cloud seem quite reasonable. Aqueous–phase oxidation of S(IV) by H_2O_2 may also make some contributions to S(VI) production in this environment.

Summary

Automated sub–event sequential rain samplers were used to sample rain during the winter and spring of 1987 in the South Coast Air Basin. The five sites used in the study were located at West Los Angeles, Pasadena, Henninger Flats, Mount Wilson, and Riverside. These sites were specifically chosen to represent a vertical profile in the basin (Pasadena to Henninger Flats to Mt. Wilson) and an east–west profile (Riverside to Pasadena to West Los Angeles). Measurements of aerosol and gas phase species were also made at the five sites using filter pack methods and an automated sampler.

The highest rainwater concentrations of NO_3^- and SO_4^{2-} were observed at Pasadena; highest NH_4^+ levels were measured at Riverside; highest average levels of rainwater Na^+ and Cl^- were found at West Los Angeles. Rainwater pH levels varied from 4 to 6 at West Los Angeles and Henninger Flats, from 4 to 5.5 at Pasadena, from 4.3 to 5.7 at Mt. Wilson,

and from 4.5 to 6.8 at Riverside. Rainwater concentrations at all five sites were generally dominated by NH_4^+, SO_4^{2-}, NO_3^-, and H^+. Na^+ and Cl^- were important contributors in some samples. Highest deposition rates of most species were sometimes observed at the site with the lowest rainwater concentrations, Mt. Wilson, due to the heavier rainfall there.

Rainfall concentration data from the vertical profile indicate that much of what is in the rain at Henninger Flats (700 m) was picked up between there and Mt. Wilson (1700 m), while much of what is in the rain at Pasadena (200 m) was picked up between there and Henninger Flats.

Measurements of the atmospheric burdens of aerosol and gas phase species prior to a storm indicated that considerably more NO_3^- and SO_4^{2-} were being deposited in the rainfall than could be accounted for by pre–storm burdens. Pre–storm burdens of Ca^{2+}, Mg^{2+}, and Na^+ were roughly consistent with the measured deposition of these species in the rainfall. Evidence was seen for in–cloud production of SO_4^{2-} which may account for at least a portion of the additional SO_4^{2-} deposition. No evidence was seen for in–cloud production of NO_3^-.

References

Galloway, J. N., Likens, G. E., Keene, W. C., and Miller, J. M. (1982) The compo precipitation in remote areas of the world, *J. Geophys. Res.* **87**, 8771–8786.

Kawamura, K. and Kaplan, I. R. (1984) Capillary gas chromatography determinat volatile organic acids in rain and fog samples, *Anal. Chem.* **19**, 175–188.

Keene, W. C. and Galloway, J. N. (1984) Organic acidity in precipitation of North America, *Atmos. Environ.* **18**, 2491–2497.

Martell, A. E., and Smith, R. M. (1977) "Critical Stability Constants, Vol. 3" Ple New York.

Munger, J. W., Collett, J. L., Daube, B. D., Jr., and Hoffmann, M. R. (1988) Fog Chemistry at Riverside California, submitted to *Atmos. Environ.*

SCAQMD (1987) Meteorological data obtained from the South Coast Air Quality Management District, Los Angeles, California.

Seinfeld, J. H. (1986) "Atmospheric Chemistry and Physics of Air Pollution," Wiley–Interscience, New York.

Solorzano, L. (1967) Determination of ammonia in natural waters by the phenol–hypochlorite method, *Limnol. Oceanogr.* **14**, 799–801.

West Los Angeles Rain Samples - 1987

Date	Start	Stop	Vol (ml)	Rain (mm)	pH	NH4+ (uN)	Na+ (uN)	Ca2+ (uN)	Mg2+ (uN)	Cl- (uN)	NO3- (uN)	SO42- (uN)	H+ (uN)	-/+
02/13	11:12	11:53	57	1.76	5.36	36.5	32.1	7.0	7.2	42.1	12.3	24.4	4.37	0.90
02/13	11:53	13:00	69	2.13	5.45	16.5	11.7	2.0	2.6	17.1	4.5	11.2	3.55	0.90
02/13	13:00	13:22	69	2.13	5.66	10.5	3.2	0.0	0.4	3.5	1.5	4.7	2.19	0.59
02/13	13:22	13:38	59	1.82	5.61	6.8	0.7	0.0	0.0	1.0	1.6	3.3	2.45	0.58
02/13	13:38	13:48	30	0.93	5.53	6.8	0.9	0.0	0.0	1.0	1.6	3.6	2.95	0.59
02/13	13:48	14:07	58	1.80	5.45	7.3	2.2	0.0	0.4	0.7	1.6	3.3	3.55	0.41
02/13	14:07	15:00	58	1.77	5.6	18.3	23.5	0.0	4.9	35.8	5.7	12.5	2.51	1.10
02/13	15:02	15:49	59	1.82	5.73	12.7	12.0	0.0	2.6	16.1	2.5	7.0	1.86	0.88
02/13	15:49	16:23	26	0.80	5.85	22.2	20.5	2.7	4.4	29.2	5.9	12.2	1.41	0.93
02/13	17:21	18:10	31	0.96	6.1	32.4	24.9	3.3	5.5	34.1	5.8	14.4	0.79	0.81
02/15	07:13	08:52	35	1.06	4.68	47.3	46.6	6.4	10.4	61.4	27.8	41.1	20.89	0.99
02/15	09:15	09:53	6	0.19	4.19	105.6	NA	NA	NA	67.1	69.4	73.0	64.57	NA
03/05	11:11	11:49	1	0.03	4.1	68.5	55.6	25.0	0.7	49.6	80.5	98.0	79.4	1.00
03/05	12:01	14:42	5	0.15	4.1	68.5	55.6	25.0	0.7	49.6	80.5	98.0	79.4	1.00
03/05	14:42	15:29	68	2.10	4.67	25.9	3.9	8.5	2.4	4.9	15.9	22.1	21.4	0.69
03/05	15:34	16:45	8	0.24	5.1	42.4	13.2	11.0	0.7	5.4	18.9	22.7	7.9	0.62
03/05	17:01	17:24	36	1.10	5.62	67.3	4.5	9.3	2.6	7.1	17.4	28.6	2.4	0.62
03/05	17:30	19:38	1	0.04	5.62	67.3	4.5	9.3	2.6	7.1	17.4	28.6	2.4	0.62
03/05	19:38	20:17	70	2.15	5.33	58.6	7.1	6.2	2.7	9.2	17.4	28.6	4.7	0.70
03/05	20:17	20:41	63	1.93	5.03	26.4	4.2	5.7	1.9	5.3	13.2	19.5	9.3	0.80
03/05	20:41	20:44	37	1.15	5.69	28.8	4.7	4.6	2.2	5.3	12.9	13.5	2.0	0.75
03/05	20:44	21:08	1	0.03	5.45	NA	NA	NA	NA	NA	NA	NA	3.5	NA
03/05	22:24	00:26	55	1.70	5.01	52.3	7.0	4.3	2.1	14.6	18.2	33.1	9.8	0.87
03/06	00:33	00:44	2	0.07	5.33	86.9	NA	NA	NA	6.7	20.0	37.0	4.7	NA
03/06	03:05	05:08	46	1.42	4.65	38.7	1.7	3.7	1.2	3.9	23.5	25.5	22.4	0.78
03/06	05:21	06:12	15	0.45	4.66	38.7	2.3	4.2	2.1	4.2	24.5	23.9	21.9	0.76
03/06	06:22	07:48	22	0.67	4.76	46.8	5.9	5.1	2.6	5.9	20.7	30.1	17.4	0.73
03/14	22:13	22:32	67	2.07	5.47	8.0	13.1	4.8	3.9	16.0	9.9	7.4	3.4	1.00
03/14	23:32	00:14	7	0.22	5.67	12.4	6.8	8.0	3.3	6.4	6.8	9.4	2.1	0.69
03/21	08:58	10:04	68	2.11	4.72	65.0	86.6	15.5	21.0	86.0	42.2	55.8	19.1	0.89
03/21	10:04	10:41	64	1.97	5.36	11.4	20.8	5.0	5.4	27.7	4.8	12.7	4.4	0.96
03/21	10:41	11:05	68	2.11	5.19	14.0	8.4	5.0	5.4	11.5	3.9	14.3	6.5	0.75
03/21	11:05	11:22	65	2.02	5.09	17.6	8.8	2.3	2.5	11.6	6.9	15.1	8.1	0.86
03/21	11:22	12:37	49	1.52	4.88	22.6	31.5	4.2	7.8	39.6	12.2	26.2	13.2	0.98
03/21	13:20	14:14	14	0.42	5	14.2	24.5	5.3	6.6	31.5	11.1	15.6	10.0	0.96

Table 1. Composition of rain samples collected at West Los Angeles during the winter of 1987. The last column denotes the charge balance for the measured species.

Pasadena Rain Samples - 1987

Date	Start	Stop	Vol (ml)	pH	NH4+ (uN)	Na+ (uN)	Ca2+ (uN)	Mg2+ (uN)	Cl- (uN)	NO3- (uN)	SO42- (uN)	H+ (uN)	-/+
01/04	05:33	05:43	NA	NA	NA	NA	NA	NA	NA	NA	NA	NA	NA
01/04	05:43	06:30	59.5	4.3	91.2	12.1	4.5	2.4	12.3	96.4	42.7	50.12	0.94
01/04	06:30	07:17	63.3	4.78	92.1	3.6	2.0	0.6	12.4	65.6	26.9	16.6	0.91
01/04	07:17	07:27	16.4	4.87	44.2	1.6	2.0	0.0	7.5	33.2	15.0	13.49	0.91
01/04	07:27	07:46	67.8	5.04	33.1	1.9	1.7	0.1	7.5	24.5	14.1	9.12	1.00
01/04	07:46	07:55	59.8	5.02	18.0	5.1	2.7	0.4	7.8	17.5	10.7	9.55	1.01
01/04	07:55	08:02	42.6	5.03	14.5	2.4	1.1	0.0	5.0	13.3	8.3	9.33	0.97
01/04	08:02	08:14	42.4	4.99	17.6	1.6	0.8	0.0	4.0	14.0	11.5	10.23	0.97
01/04	08:14	08:23	28.4	5.06	10.6	2.7	0.8	0.1	4.8	10.4	11.1	8.71	1.15
01/04	08:23	08:36	48.1	5.2	9.9	1.6	0.8	0.0	4.9	9.7	7.5	6.31	1.18
01/04	08:36	08:38	51.3	5.07	5.7	0.1	0.8	0.0	2.3	6.4	9.2	8.51	1.18
01/04	08:38	08:46	46.3	5.35	3.2	0.3	0.8	0.0	5.1	5.2	3.5	4.47	1.58
01/04	08:46	09:19	19.3	5.36	6.6	0.9	0.8	0.0	3.1	7.1	3.5	4.37	1.08
01/04	09:19	09:20	14.6	5.34	9.3	1.9	2.0	0.1	3.8	7.7	4.7	4.57	0.90
01/04	09:28	10:00	35.3	5.36	6.4	0.5	0.8	0.0	2.6	5.8	3.5	4.37	0.99
01/04	13:32	13:43	8.7	5.35	0.9	0.1	0.8	0.0	2.7	2.9	2.5	4.47	1.30
01/04	14:08	14:46	NA	NA	NA	NA	NA	NA	NA	NA	NA	NA	NA
01/04	15:20	15:54	NA	NA	NA	NA	NA	NA	NA	NA	NA	NA	NA
01/04	16:32	16:56	NA	NA	NA	NA	NA	NA	NA	NA	NA	NA	NA
01/04	20:33	21:08	NA	NA	NA	NA	NA	NA	NA	NA	NA	NA	NA
01/04	21:57	22:13	49.2	4.71	28.8	29.8	3.0	6.2	41.0	18.6	22.8	19.5	0.94
01/04	22:13	22:31	66.7	4.81	18.0	8.6	2.0	1.6	14.1	12.5	12.4	15.49	0.85
01/04	22:31	22:46	48.1	4.97	2.4	2.0	0.8	0.1	4.4	8.0	2.7	10.72	0.94
01/04	22:46	22:54	7.7	5.06	1.7	5.4	NA	NA	5.5	8.1	2.7	8.71	NA
01/05	02:00	02:42	47.4	4.8	2.7	8.7	2.0	1.5	13.6	13.2	8.5	15.85	1.15
01/05	02:42	02:54	11.3	4.78	2.6	9.3	2.7	1.5	11.3	11.8	10.2	16.6	1.02
01/05	03:31	03:51	NA	NA	NA	NA	NA	NA	NA	NA	NA	NA	NA
02/08	17:37	18:25	40.3	5.29	74.5	31.6	49.5	11.1	33.6	90.9	70.1	5.13	1.13
02/08	18:40	19:07	43.2	5.21	43.4	16.8	32.1	6.2	17.3	51.0	39.4	6.17	1.03
02/08	19:07	19:14	46.9	5.43	12.5	4.8	9.5	1.5	0.5	14.4	9.2	3.72	0.75
02/08	19:14	19:27	68.7	5.54	8.4	3.2	5.5	0.9	8.9	11.7	6.6	2.88	0.92
02/08	19:27	19:37	30.2	5.4	6.8	1.8	4.5	0.4	1.0	8.2	6.3	3.98	0.88
02/08	19:37	19:50	6.9	5.21	13.7	0.1	6.7	1.2	4.3	13.0	11.4	6.17	1.03
02/08	20:14	20:21	3	5.4	51.8	NA	NA	NA	22.0	59.0	43.7	3.98	NA

Table 2. Composition of rain samples collected at Pasadena during the winter of 1987. The last column denotes the charge balance for the measured species.

Pasadena Rain Samples - 1987

Date	Start	Stop	Vol (ml)	pH	NH4+ (uN)	Na+ (uN)	Ca2+ (uN)	Mg2+ (uN)	Cl- (uN)	NO3- (uN)	SO42- (uN)	H+ (uN)	-/+
02/13	12:05	13:08	45	3.95	134.2	14.8	13.2	4.4	28.1	129.0	118.0	112.2	0.99
02/13	13:08	13:41	68	4.29	62.4	7.4	8.9	2.3	10.1	60.0	51.1	51.29	0.92
02/13	13:41	13:51	43	4.6	39.2	2.8	4.5	0.7	3.0	30.2	26.7	25.12	0.83
02/13	13:51	14:05	47	4.94	22.1	5.0	13.2	2.0	5.9	27.8	21.6	11.48	1.03
02/13	14:05	14:15	48	5.18	12.9	1.9	7.6	0.7	1.1	12.5	13.0	6.61	0.89
02/13	14:15	14:33	48	5.34	13.5	1.3	5.5	0.3	1.0	8.6	8.7	4.57	0.73
02/13	14:33	15:05	45	5.24	10.2	0.9	5.1	0.3	1.0	9.0	7.2	5.75	0.77
02/13	15:05	15:19	48	5.13	10.4	0.8	3.9	0.0	1.0	9.3	9.1	7.41	0.86
02/13	15:19	15:44	47	4.94	9.6	0.5	2.4	0.0	1.0	8.4	10.9	11.48	0.85
02/13	15:44	15:57	48	5.03	8.8	0.6	2.7	0.0	1.0	6.8	9.4	9.33	0.80
02/13	15:57	16:04	49	5.09	6.1	0.7	3.3	0.0	1.0	5.2	7.7	8.13	0.76
02/13	16:04	16:08	30	NA	NA	NA	NA	NA	NA	NA	NA	NA	NA
02/13	16:08	16:23	37	5.13	6.7	1.0	3.9	0.0	1.0	6.4	9.1	7.41	0.87
02/13	16:34	16:59	16.6	4.88	15.9	1.5	7.0	0.4	1.4	15.0	17.3	13.18	0.89
02/13	16:59	16:59	4	4.9	NA	NA	NA	NA	10.6	16.4	18.3	12.59	NA
02/13	17:14	17:27	49.3	4.88	18.4	1.5	3.3	0.1	1.0	11.8	20.2	13.18	0.91
02/13	17:27	17:47	42.4	5.03	10.8	0.6	3.3	0.0	0.5	7.1	12.1	9.33	0.82
02/13	17:47	18:10	45.2	5.03	7.1	0.1	2.4	0.0	1.0	5.1	7.8	9.33	0.74
02/13	18:10	18:34	37.8	4.96	5.7	0.1	1.1	0.0	1.0	4.8	8.0	10.96	0.77
02/13	20:12	20:26	6.2	5.07	19.1	NA	NA	NA	0.4	13.9	17.8	8.51	NA
03/05	12:07	12:46	20	4.44	101.8	20.8	23.3	7.8	24.8	66.9	83.8	36.31	0.92
03/05	12:50	12:56	1.2	4.44	NA	NA	NA	NA	24.8	66.9	83.8	36.31	NA
03/05	15:45	15:52	2.5	4.76	44.7	1.0	6.8	2.4	6.0	25.4	29.7	17.38	0.85
03/05	16:25	16:49	11.5	4.76	44.7	1.0	6.8	2.4	6.0	25.4	29.7	17.38	0.85
03/05	16:56	17:12	8.2	4.76	44.7	1.0	6.8	2.4	6.0	25.4	29.7	17.38	0.85
03/05	17:36	08:11	NA	NA	NA	NA	NA	NA	NA	NA	NA	NA	NA
03/21	09:46	10:54	45.2	4.35	84.5	77.0	22.8	20.7	81.5	87.6	72.0	44.67	0.97
03/21	10:54	11:13	44	4.49	34.7	16.9	6.1	4.7	19.7	30.2	32.9	32.36	0.87
03/21	11:13	11:41	66.3	4.64	25.0	10.7	3.4	2.9	12.9	22.2	21.2	22.91	0.87
03/21	11:41	12:09	65.4	4.87	6.1	3.1	2.3	1.4	4.6	6.5	7.8	13.49	0.71
03/21	12:09	12:21	68.7	4.95	6.2	0.9	2.6	1.3	2.5	5.7	7.8	11.22	0.72
03/21	12:21	12:33	42.5	4.81	10.8	1.5	2.3	0.8	4.1	11.2	12.6	15.49	0.90
03/21	12:33	13:05	4.3	4.81	10.8	1.5	2.3	0.8	4.1	11.2	12.6	15.49	0.90
03/21	13:35	13:51	40	4.38	31.1	8.1	3.4	2.6	13.2	35.9	31.1	41.69	0.92
03/21	13:51	14:08	40.5	4.54	19.8	2.7	2.6	1.3	4.7	23.8	19.2	28.84	0.86
03/21	14:08	14:53	11.7	4.54	19.8	2.7	2.6	1.3	4.7	23.8	19.2	28.84	0.86

Table 2 (cont'd). Composition of rain samples collected at Pasadena during the winter of 1987. The last column denotes the charge balance for the measured species.

Henninger Flats Rain Samples - 1987

Date	Start	Stop	Vol (ml)	Rain (mm)	pH	NH4+ (uN)	Na+ (uN)	Ca2+ (uN)	Mg2+ (uN)	Cl- (uN)	NO3- (uN)	SO42- (uN)	H+ (uN)	-/+
01/04	03:29	03:43	2.1	0.1	4.1	NA	NA	NA	NA	NA	NA	NA	79.4	NA
01/04	05:31	06:08	63.4	2.0	4.22	53.1	15.5	8.9	3.9	10.3	94.4	30.2	60.3	0.95
01/04	06:08	06:26	33.6	1.0	4.5	10.0	2.2	2.0	0.7	4.2	23.9	14.5	31.6	0.92
01/04	06:26	06:42	24.2	0.7	4.75	4.0	1.0	1.7	0.0	2.9	11.3	7.2	17.8	0.87
01/04	06:48	07:17	64.8	2.0	4.98	3.6	0.2	0.8	0.0	3.6	8.6	4.1	10.5	1.08
01/04	07:17	07:43	60.8	1.9	5.07	1.4	0.1	0.8	0.0	2.5	5.9	2.8	8.5	1.04
01/04	07:43	07:49	59.8	1.8	5.27	0.6	0.0	0.8	0.0	2.2	4.3	3.0	5.4	1.40
01/04	07:49	08:07	67.6	2.1	5.13	0.4	0.6	0.8	0.0	2.8	3.2	5.6	7.4	1.27
01/04	08:07	08:21	52.6	1.6	5.21	0.1	1.2	0.8	0.0	3.2	3.4	5.2	6.2	1.43
01/04	08:21	08:39	63.2	2.0	5.34	0.0	0.8	0.8	0.0	3.7	2.8	4.8	4.6	1.83
01/04	08:39	08:45	53.8	1.7	5.3	0.0	0.2	0.8	0.0	0.0	0.0	3.9	5.0	0.65
01/04	08:45	08:59	29.1	0.9	5.42	0.0	0.6	0.8	0.0	3.1	3.2	2.5	3.8	1.71
01/04	09:02	09:20	22	0.7	5.27	2.2	1.3	0.8	0.0	3.2	4.2	2.9	5.4	1.06
01/04	09:28	09:55	54.2	1.7	4.93	1.8	5.7	2.0	0.0	8.8	5.3	13.3	11.8	1.29
01/04	10:09	16:50	NA	NA	NA	NA	NA	NA	NA	NA	NA	NA	NA	NA
01/04	19:36	19:55	24	0.7	4.77	7.1	29.1	1.7	6.2	35.0	13.4	13.0	17.0	1.00
01/04	20:42	21:08	22.6	0.7	4.85	2.8	24.3	1.1	5.3	31.4	9.9	10.9	14.1	1.10
01/04	21:58	22:33	67.2	2.1	4.86	5.3	11.9	0.8	2.6	15.9	12.8	9.3	13.8	1.11
01/04	22:33	22:35	22.5	0.7	5	4.6	3.4	0.8	0.7	5.8	8.4	4.7	10.0	0.97
01/04	22:35	22:41	65.8	2.0	5.04	4.4	1.9	0.8	0.4	4.4	8.7	3.7	9.1	1.01
01/04	22:41	22:52	66.7	2.1	5.04	2.8	0.8	0.8	0.1	3.2	7.1	4.0	9.1	1.05
01/04	22:52	22:53	5.5	0.2	5	3.8	NA	NA	NA	4.2	8.2	3.9	10.0	NA
01/04	22:53	23:06	40.1	1.2	5.11	1.2	0.7	0.8	0.0	2.7	7.6	3.2	7.8	1.29
01/05	01:55	02:23	22.4	0.7	4.87	0.9	14.8	0.8	2.3	15.6	10.6	7.4	13.5	1.04
01/05	04:02	04:03	41.7	1.3	4.85	0.3	12.8	0.8	2.4	17.0	10.1	7.5	14.1	1.14
01/05	04:03	04:04	4.3	0.1	4.84	NA	NA	NA	NA	15.6	9.7	7.2	14.5	NA
02/13	11:41	13:04	69	2.1	4.2	64.9	4.0	3.6	0.9	6.3	80.7	39.1	63.1	0.92
02/13	13:04	13:40	69	2.1	4.38	19.4	2.8	3.0	0.1	2.4	38.4	25.3	41.7	0.99
02/13	13:40	14:03	60	1.9	4.69	8.2	1.0	2.7	0.0	1.0	15.6	9.5	20.4	0.81
02/13	14:03	14:19	46	1.4	4.97	3.8	0.3	1.1	0.0	1.0	8.0	4.4	10.7	0.84
02/13	14:19	14:34	49	1.5	5.09	3.1	0.2	0.8	0.0	1.0	6.0	2.9	8.1	0.81
02/13	14:34	15:08	47	1.5	5.12	2.8	0.0	0.8	0.0	1.0	4.7	2.4	7.6	0.72
02/13	15:08	15:25	51	1.6	5.18	3.4	0.5	0.8	0.0	1.0	5.8	1.9	6.6	0.77
02/13	15:25	15:43	48	1.5	4.95	3.1	0.3	0.8	0.0	1.0	5.8	2.8	11.2	0.62
02/13	15:43	15:58	51	1.6	5.05	2.5	0.0	0.8	0.0	1.0	4.1	3.0	8.9	0.66
02/13	15:58	16:08	48	1.5	5.15	0.0	0.0	0.8	0.0	1.0	3.0	4.3	7.1	0.93
02/13	16:08	17:29	68	2.1	4.98	4.4	0.5	0.8	0.0	1.0	6.2	5.7	10.5	0.80
02/13	17:29	18:32	51	1.6	5.01	3.0	0.0	0.8	0.0	1.0	5.9	3.6	9.8	0.78
02/13	18:32	19:25	38.2	1.2	4.96	3.3	0.4	0.8	0.0	1.0	9.5	3.4	11.0	0.90
02/13	19:41	20:23	34.4	1.1	4.82	3.9	0.6	2.4	0.0	1.0	13.9	4.0	15.1	0.86

Table 3. Composition of rain samples collected at Henninger Flats during the winter of 1987. The last column denotes the charge balance for the measured species.

Henninger Flats Rain Samples - 1987

Date	Start	Stop	Vol (ml)	Rain (mm)	pH	NH4+ (uN)	Na+ (uN)	Ca2+ (uN)	Mg2+ (uN)	Cl- (uN)	NO3- (uN)	SO42- (uN)	H+ (uN)	-/+
03/05	09:08	09:36	3.6	0.1	4.34	57.9	NA	NA	NA	10.1	50.5	63.5	45.7	NA
03/05	11:13	11:55	14.8	0.5	4.8	128.2	17.4	26.4	7.3	22.3	89.3	108.0	15.8	1.13
03/05	12:03	12:45	45	1.4	4.7	102.8	17.6	16.3	5.8	16.4	50.2	66.0	20.0	0.82
03/05	12:45	13:23	13.3	0.4	5.37	72.2	4.9	8.5	2.2	6.3	21.8	37.0	4.3	0.71
03/05	13:50	14:14	4.3	0.1	4.99	64.0	7.9	1.2	0.7	5.1	25.8	31.2	10.2	0.74
03/05	15:13	16:14	42	1.3	4.65	15.7	1.6	4.3	1.0	5.6	16.2	15.3	22.4	0.83
03/05	16:14	17:15	67	2.1	4.86	7.0	0.0	0.0	0.0	2.0	9.6	8.4	13.8	0.96
03/05	17:15	18:19	44.5	1.4	5.09	5.6	0.0	0.0	0.0	0.8	6.1	4.2	8.1	0.81
03/05	18:19	19:20	67.8	2.1	5.02	8.5	0.0	0.0	0.0	0.3	6.4	7.2	9.5	0.77
03/05	19:20	19:53	43.3	1.3	5.07	6.2	0.3	0.0	1.0	2.0	6.2	6.4	8.5	0.92
03/05	19:53	20:57	45.4	1.4	5.18	5.8	0.8	2.6	0.0	1.6	6.3	4.1	6.6	0.76
03/05	21:44	22:28	44.1	1.4	4.79	19.5	0.0	0.0	0.0	1.7	16.0	12.1	16.2	0.83
03/05	22:28	23:32	47.6	1.5	4.82	12.9	0.0	2.3	0.0	0.5	12.8	9.0	15.1	0.73
03/05	23:32	00:16	45	1.4	4.76	8.8	0.0	2.3	0.0	0.3	9.2	9.7	17.4	0.67
03/06	00:16	01:01	12.7	0.4	4.72	13.9	0.8	2.3	0.0	1.9	14.8	16.7	19.1	0.93
03/06	01:35	02:24	9.4	0.3	4.65	11.4	0.0	2.0	0.0	1.7	12.8	15.9	22.4	0.85
03/06	02:48	03:50	45.3	1.4	4.77	7.8	0.0	0.0	0.0	1.7	7.9	10.4	17.0	0.81
03/06	03:50	04:48	44.7	1.4	4.95	7.0	0.0	0.0	0.0	0.8	6.2	8.4	11.2	0.85
03/06	04:48	05:22	46.3	1.4	5.1	7.0	0.0	0.0	0.0	0.3	4.0	8.2	7.9	0.83
03/06	05:22	05:37	43.3	1.3	5.1	7.8	0.0	0.0	0.0	1.7	3.5	8.5	7.9	0.87
03/06	05:37	06:17	46.1	1.4	5.1	7.3	0.0	0.0	0.0	0.3	3.6	8.1	7.9	0.79
03/06	06:17	07:26	45.7	1.4	5.03	6.0	0.0	0.0	0.0	0.5	4.0	6.0	9.3	0.68
03/06	07:26	08:22	42.3	1.3	5.2	7.3	0.0	0.0	0.0	1.1	4.0	6.0	6.3	0.82
03/06	08:22	08:59	14.2	0.4	5.39	8.3	0.0	0.0	0.0	0.1	5.3	4.2	4.1	0.78
03/06	13:03	14:09	29.4	0.9	4.52	34.8	0.0	3.6	0.0	1.8	35.4	15.8	30.2	0.77
03/06	14:46	15:01	18.2	0.6	4.89	97.2	0.2	4.8	1.5	3.4	53.8	26.5	12.9	0.72
03/06	15:01	15:42	23.9	0.7	5.87	140.2	0.3	4.3	1.0	3.4	54.9	24.9	1.3	0.57
03/06	17:08	17:33	1.6	0.0	5.97	NA	NA	NA	NA	NA	NA	NA	1.1	NA
03/06	21:11	21:53	9.9	0.3	4.4	100.0	1.1	8.8	2.6	3.8	97.2	22.5	39.8	0.81
03/14	21:38	22:25	4.4	0.1	NA	NA	NA	NA	NA	NA	NA	NA	NA	NA
03/14	22:30	22:50	46.1	1.4	4.49	55.0	92.4	16.9	28.1	107.8	90.0	66.6	32.4	1.18
03/14	22:50	22:56	47.5	1.5	4.78	12.6	42.4	4.5	9.9	52.5	18.7	20.2	16.6	1.06
03/14	22:56	23:04	47.8	1.5	4.85	6.8	20.2	2.6	5.4	26.3	10.2	10.4	14.1	0.95
03/14	23:04	23:07	43.2	1.3	4.87	7.4	13.3	2.1	3.6	18.1	10.1	8.3	13.5	0.91
03/14	23:07	23:21	56	1.7	5	7.4	9.8	4.0	3.2	10.0	15.0	7.6	10.0	0.95
03/14	23:21	23:44	50	1.5	NA	NA	NA	NA	NA	NA	NA	NA	NA	NA
03/14	23:44	00:37	42.3	1.3	5.16	3.9	3.6	5.0	2.3	3.1	9.4	6.9	6.9	0.89
03/21	10:27	11:09	55.5	1.7	4.62	53.3	70.3	14.7	18.3	63.6	68.4	46.1	24.0	0.99
03/21	11:09	11:30	67	2.1	4.7	16.6	12.2	4.8	3.9	13.0	20.9	18.0	20.0	0.90
03/21	11:30	12:05	67.9	2.1	4.97	7.8	4.6	2.6	1.6	6.6	10.8	8.9	10.7	0.96
03/21	12:05	13:16	>115	>3.5	NA	NA	NA	NA	NA	NA	NA	NA	NA	NA

Table 3 (cont'd). Composition of rain samples collected at Henninger Flats during the winter of 1987. The last column denotes the charge balance for the measured species.

Mount Wilson Rain Samples - 1987

Date	Start	Stop	Vol (ml)	Rain (mm)	pH	NH4+ (uN)	Na+ (uN)	Ca2+ (uN)	Mg2+ (uN)	Cl- (uN)	NO3- (uN)	SO42- (uN)	H+ (uN)	-/+
02/13	11:46	13:27	69	2.1	4.73	6.6	3.5	10.7	0.6	3.8	19.3	8.7	18.6	0.79
02/13	13:27	14:05	69	2.1	4.88	3.1	0.3	2.0	0.0	1.5	8.0	8.4	13.2	0.96
02/13	14:05	14:21	54	1.7	5.19	2.4	0.7	2.7	0.0	1.0	5.2	3.4	6.5	0.79
02/13	14:21	14:45	69	2.1	5.71	2.5	0.0	1.1	0.0	1.0	1.9	1.2	2.0	0.73
02/13	14:45	15:13	69	2.1	5.61	0.0	0.0	0.0	0.0	1.0	1.7	1.3	2.5	1.62
02/13	15:13	15:38	70	2.2	5.53	0.0	0.0	0.0	0.0	1.0	1.4	2.2	3.0	1.54
02/13	15:38	15:56	69	2.1	5.43	0.0	0.0	0.0	0.0	1.0	1.2	1.0	3.7	0.86
02/13	15:56	16:09	70	2.2	5.45	0.0	0.0	0.0	0.0	1.0	1.4	1.4	3.6	1.06
02/13	16:09	17:01	70	2.2	5.34	0.0	0.1	0.0	0.0	1.0	2.8	2.8	4.6	1.42
02/13	17:01	17:34	69	2.1	5.31	2.5	0.0	0.0	0.0	1.0	2.1	2.3	4.9	0.73
02/13	17:34	19:42	33.5	1.0	5.13	2.8	2.4	4.2	0.0	4.4	9.8	3.2	7.4	1.03
02/15	07:45	09:49	17	0.5	4.9	7.2	2.1	2.4	0.3	1.0	12.8	6.1	12.6	0.81
03/05	05:14	06:07	8.7	0.3	4.39	6.4	5.5	9.9	4.6	7.1	34.5	25.4	40.7	1.00
03/05	07:31	08:09	4.6	0.1	4.31	14.6	5.5	11.9	5.3	9.1	38.8	32.6	49.0	0.93
03/05	08:18	08:33	2	0.1	4.31	14.6	5.5	11.9	5.3	9.1	38.8	32.6	49.0	0.93
03/05	08:39	09:54	23.1	0.7	4.37	20.5	5.6	10.7	4.4	7.3	35.1	32.7	42.7	0.90
03/05	10:14	12:26	68.1	2.1	4.62	53.6	9.2	11.6	3.9	10.4	38.3	40.0	24.0	0.87
03/05	12:26	13:29	39.7	1.2	5.39	59.8	3.4	4.9	2.2	4.7	22.5	26.4	4.1	0.72
03/05	13:49	14:18	7.5	0.2	4.9	27.2	1.4	7.4	2.4	4.5	22.4	18.4	12.6	0.89
03/05	14:21	14:31	1.6	0.0	4.76	24.7	NA	NA	NA	NA	NA	NA	17.4	NA
03/05	15:15	16:33	67.4	2.1	4.8	7.2	0.8	3.6	1.0	2.3	11.6	9.8	15.8	0.83
03/05	16:33	16:52	42.3	1.3	4.83	7.5	0.0	2.9	0.9	1.3	10.5	8.5	14.8	0.78
03/05	16:52	17:44	50.7	1.6	4.95	5.6	0.0	0.0	0.0	0.7	7.4	6.7	11.2	0.88
03/05	17:44	18:27	46.5	1.4	4.94	6.4	0.0	0.0	0.0	1.2	6.3	5.8	11.5	0.75
03/05	18:24	18:54	65.2	2.0	4.9	9.2	0.0	2.3	0.0	0.7	8.1	10.1	12.6	0.78
03/05	18:54	19:24	67.5	2.1	4.84	7.6	0.0	0.0	0.0	0.5	6.4	9.2	14.5	0.73
03/05	19:24	19:57	64.9	2.0	5.01	4.7	0.0	0.0	0.0	0.2	3.5	5.7	9.8	0.65
03/05	19:57	20:20	46.9	1.4	5.19	7.5	0.0	0.0	0.0	0.3	3.4	4.4	6.5	0.58
03/05	20:20	21:30	48	1.5	4.7	18.7	0.0	2.3	0.0	2.0	16.7	12.4	20.0	0.76
03/05	21:38	22:08	48.1	1.5	4.92	8.7	0.0	0.0	0.0	1.3	8.9	6.6	12.0	0.81
03/05	22:08	22:18	56.6	1.7	4.92	7.7	0.0	0.0	0.0	0.4	9.2	7.0	12.0	0.84
03/05	22:18	22:42	55.3	1.7	4.88	7.3	0.0	0.0	0.0	1.2	8.3	7.6	13.2	0.83
03/05	22:42	23:34	61.9	1.9	4.99	4.4	0.0	0.0	0.0	0.0	4.0	5.4	10.2	0.64
03/05	23:34	00:11	42.9	1.3	5.08	4.4	0.0	0.0	0.0	0.1	2.9	4.8	8.3	0.61
03/06	00:11	00:18	68.3	2.1	4.81	7.7	0.0	0.0	0.0	0.5	6.7	10.3	15.5	0.75
03/06	01:34	02:40	67.9	2.1	4.89	6.7	0.0	0.0	0.0	0.2	5.1	8.9	12.9	0.73
03/06	02:40	03:42	34.8	1.1	5.12	4.2	0.0	0.0	0.0	0.3	3.7	4.4	7.6	0.71
03/06	03:42	04:08	55.3	1.7	5.06	6.5	0.0	1.5	0.0	0.8	3.9	9.0	8.7	0.82
03/06	04:08	05:32	68.2	2.1	5.2	4.8	0.0	0.0	0.7	0.3	2.3	5.3	6.3	0.67
03/06	05:32	05:43	49	1.5	5.34	3.0	0.0	0.0	0.0	0.0	0.9	3.0	4.6	0.52
03/06	05:43	07:03	48.5	1.5	5.33	2.8	0.0	0.0	0.0	2.4	1.6	3.0	4.7	0.84
03/06	07:03	08:02	67.8	2.1	5.29	3.3	0.0	1.5	0.0	0.1	2.0	2.8	5.1	0.50
03/06	08:02	09:14	46.6	1.4	5.39	4.2	0.0	1.5	0.0	2.6	3.2	3.0	4.1	0.90
03/06	15:14	16:10	28.6	0.9	4.96	18.5	0.0	1.2	0.0	2.9	13.9	4.5	11.0	0.70
03/06	16:35	17:45	2.8	0.1	5.06	37.5	NA	NA	NA	1.5	23.7	10.4	8.7	NA
03/06	20:35	22:00	29.8	0.9	4.68	23.1	0.0	2.3	0.2	0.6	33.7	7.3	20.9	0.90

Table 4. Composition of rain samples collected at Mt. Wilson during the winter of 1987. The last column denotes the charge balance for the measured species.

Riverside Rain Samples - 1987

Date	Start	Stop	Vol (ml)	Rain (mm)	pH	NH4+ (uN)	Na+ (uN)	Ca2+ (uN)	Mg2+ (uN)	Cl- (uN)	NO3- (uN)	SO42- (uN)	H+ (uN)	-/+
01/04	20:33	20:53	53	1.63	5.71	26.9	25.1	2.7	4.6	40.0	8.1	14.3	2.0	1.02
01/04	20:53	20:59	50	1.54	5.75	22.9	10.6	1.4	1.6	17.8	7.7	8.3	1.8	0.88
01/04	20:59	21:21	62	1.90	6	20.7	5.0	1.3	0.4	11.2	7.2	3.9	1.0	0.79
01/04	21:21	21:30	9	0.28	6	37.0	NA	NA	NA	32.4	15.3	10.5	1.0	NA
01/04	21:39	22:02	65	1.99	5.73	28.5	4.3	1.4	0.3	9.4	8.5	7.9	1.9	0.71
01/04	22:02	22:24	25	0.76	6	9.2	2.8	0.8	0.0	6.6	4.6	3.8	1.0	1.09
01/04	22:28	22:33	4	0.11	5.53	NA	NA	NA	NA	5.6	5.3	5.5	3.0	NA
01/05	00:49	01:24	53	1.62	5.82	8.4	3.8	0.8	0.3	7.1	3.0	4.8	1.5	1.01
01/05	01:59	02:22	53	1.63	5.63	29.5	5.2	0.8	0.7	10.7	5.3	5.5	1.5	0.57
01/05	02:22	02:39	52	1.62	5.87	4.8	1.5	2.7	0.0	5.0	17.1	5.2	1.4	2.65
01/05	02:39	02:48	6	0.19	5.93	17.6	NA	NA	NA	5.4	10.6	3.8	2.3	NA
02/13	14:47	15:11	6	0.19	6.33	219.5	NA	NA	NA	15.2	82.6	92.8	0.5	NA
02/13	16:21	16:30	9	0.26	6.65	174.9	NA	NA	NA	6.1	47.9	44.1	0.2	NA
02/13	16:38	17:07	36	1.11	6.72	52.1	0.7	1.1	0.0	1.4	10.0	9.9	0.2	0.39
02/13	17:08	17:33	37	1.13	6.47	32.8	0.0	1.7	0.0	1.0	5.4	5.0	0.3	0.33
02/13	18:35	19:19	43	1.33	6.6	62.8	0.1	0.0	0.0	0.7	21.3	10.2	0.3	0.51
02/13	20:34	20:45	7	0.21	6.26	80.4	NA	NA	NA	0.2	33.4	12.4	0.6	NA
03/05	09:04	09:44	6	0.18	5.01	42.1	16.2	24.5	6.3	20.2	34.3	33.4	9.8	0.89
03/05	09:49	09:57	2	0.05	5.01	42.1	16.2	24.5	6.3	20.2	34.3	33.4	9.8	0.89
03/05	10:47	11:01	1	0.02	5.01	42.1	16.2	24.5	6.3	20.2	34.3	33.4	9.8	0.89
03/05	11:54	12:27	1	0.02	4.55	84.9	14.5	0.0	6.1	19.6	60.4	60.6	28.2	1.05
03/05	12:43	13:13	4	0.13	4.55	84.9	14.5	0.0	6.1	19.6	60.4	60.6	28.2	1.05
03/05	13:26	13:45	2	0.07	4.55	84.9	14.5	0.0	6.1	19.6	60.4	60.6	28.2	1.05
03/05	17:20	17:50	2	0.06	5.45	64.0	NA	NA	NA	14.0	25.3	27.4	3.5	NA
03/05	18:06	18:51	12	0.37	5.32	61.9	6.4	19.4	2.8	8.7	29.7	33.6	4.8	0.76
03/05	20:37	21:35	19	0.59	5.1	28.9	9.6	13.0	3.1	11.8	16.2	20.2	7.9	0.77
03/05	21:44	21:56	1	0.04	5.1	48.5	NA	NA	NA	NA	NA	NA	7.9	NA
03/05	21:59	22:33	9	0.29	4.91	26.3	NA	10.2	2.1	10.1	16.2	20.8	12.3	NA
03/05	22:40	23:13	9	0.27	4.99	30.6	6.0	8.5	1.9	7.0	15.6	22.5	10.2	0.79
03/05	23:14	23:19	2	0.06	5.15	49.3	NA	NA	NA	11.4	15.5	24.6	7.1	NA
03/05	23:22	23:54	10	0.32	5.13	33.6	10.4	8.8	2.4	11.3	14.7	22.0	7.4	0.77
03/06	00:21	01:38	48	1.48	5.15	16.2	1.0	4.0	1.2	2.1	6.3	11.9	7.1	0.69
03/06	01:38	03:15	41	1.27	5.02	10.6	0.6	2.9	1.7	3.1	6.4	7.9	9.5	0.69
03/06	03:17	03:58	14	0.42	4.95	25.3	13.1	16.1	4.6	10.6	26.3	24.0	11.2	0.87
03/06	04:00	06:05	50	1.53	5.44	23.6	4.8	8.2	2.7	11.1	12.1	15.3	3.6	0.90
03/06	06:38	07:17	12	0.38	5.42	17.7	2.0	6.0	1.4	3.9	9.8	9.1	3.8	0.74
03/06	07:27	09:24	51	1.56	5.5	13.4	0.3	4.0	1.0	2.9	7.1	5.5	3.2	0.71
03/06	09:35	12:37	13	0.39	5.04	18.6	0.6	4.8	1.2	5.2	19.2	5.8	9.1	0.88
03/06	16:26	17:43	26	0.80	5.8	59.2	0.0	2.6	0.9	3.3	17.1	12.9	1.6	0.52
03/06	17:46	17:05	2	0.06	5.81	60.9	0.0	1.5	1.0	3.8	19.1	12.3	1.5	0.54
03/06	18:04	18:25	4	0.13	5.81	60.9	0.0	1.5	1.0	3.8	19.1	12.3	1.5	0.54
03/06	18:47	18:59	1	0.02	5.81	60.9	0.0	1.5	1.0	3.8	19.1	12.3	1.5	0.54
03/06	20:18	20:29	0	0.01	6.73	134.8	NA	NA	NA	4.1	45.1	18.6	0.2	NA
03/06	21:39	22:09	5	0.15	6.73	134.8	NA	NA	NA	4.1	45.1	18.6	0.2	NA

Table 5. Composition of rain samples collected at Riverside during the winter of 1987. The last column denotes the charge balance for the measured species.

Parameter	West Los Angeles	Pasadena	Henninger Flats	Mt. Wilson	Riverside
pH	4.10-6.10	3.95-5.54	4.10-5.97	4.31-5.71	4.55-6.73
H^+ (μN)	0.8-79.4	2.9-112.2	79.4-1.1	2.0-49.0	0.2-28.2
NH_4^+ (μN)	6.8-105.6	0.9-134.2	0.0-140.2	0.0-59.8	4.8-219.5
Na^+ (μN)	0.7-86.6	0.1-77.0	0.0-92.4	0.0-9.2	0.0-25.1
Ca^{2+} (μN)	0.0-25.0	0.8-49.5	0.0-26.4	0.0-11.9	0.0-24.5
Mg^{2+} (μN)	0.0-21.0	0.0-20.7	0.0-28.1	0.0-5.3	0.0-6.3
Cl^- (μN)	0.7-86.0	0.4-81.5	0.0-107.8	0.0-10.4	0.2-40.0
NO_3^- (μN)	1.5-80.5	2.9-129.0	0.0-94.4	0.9-38.8	3.0-82.6
SO_4^{2-} (μN)	3.3-98.0	2.5-118.0	1.9-108.0	1.0-40.1	3.8-92.8
# samples	35	70	81	46	44
# events	5	5	5	3	3

Table 6. Summary of rain composition for samples collected in the South Coast Air Basin during the winter of 1987. Shown in the table are the concentration ranges observed for the measured species at each site, along with the total number of events sampled and samples collected at each location.

Aerosol and Gas Phase Data - Rain Study 1987

Date	Site	Start Time	Stop Time	Na+	NH4+	Ca2+	Mg2+	Cl-	NO3-	SO42-	NH3	HNO3
				neq/m3							nmole/m3	
01/03	HF	22:00	02:00	52.0	135.6	13.5	12.8	6.9	109.2	87.6	0.8	53.3
01/04	HF	07:00	11:00	3.9	11.7	2.8	2.6	8.5	9.5	8.1	7.7	10.0
01/04	HF	11:01	15:01	3.7	8.2	3.4	2.2	12.3	6.4	7.5	12.3	9.1
01/27	HF	20:00	00:00	18.5	434.6	15.7	6.3	10.6	349.3	61.3	40.9	70.3
01/28	HF	02:00	06:00	0.6	7.5	2.5	1.0	7.7	12.5	3.8	23.1	4.5
01/28	HF	08:00	12:00	11.6	131.8	15.3	4.1	4.8	115.2	26.8	48.6	61.2
02/10	HF	15:00	18:00	19.3	198.8	16.2	7.0	0.5	155.9	52.0	159.5	27.0
02/10	HF	20:00	00:00	8.9	124.0	10.5	3.6	0.0	33.0	105.3	27.8	11.2
02/11	HF	02:00	06:00	11.8	161.1	8.1	3.9	0.0	61.3	101.3	29.3	8.7
03/04	HF	20:00	00:00	5.3	45.3	10.5	3.8	3.1	10.2	31.6	34.0	39.7
03/05	HF	08:00	12:00	9.0	67.1	11.3	8.9	3.5	31.4	33.8	51.7	20.4
03/05	HF	20:00	00:00	0.0	18.8	3.2	2.0	1.9	7.1	14.3	6.9	8.5
03/05	HF	02:00	06:00	9.5	61.8	10.7	5.1	1.5	9.1	47.8	34.7	39.7
03/06	HF	08:00	12:00	2.7	22.2	3.7	1.0	1.9	10.8	12.3	14.7	6.6
03/06	HF	02:00	06:00	2.0	20.4	2.5	2.3	0.0	4.4	16.4	0.0	5.7
03/06	HF	20:00	00:00	3.7	142.5	11.9	2.7	2.7	98.4	33.2	2.3	6.0
03/06	HF	15:15	18:00	5.1	123.7	6.7	2.6	0.0	80.2	22.4	3.4	8.2
03/07	HF	08:00	12:00	10.2	279.4	5.9	1.8	9.3	189.8	93.6	0.0	39.5
01/27	MW	20:00	00:00	5.7	19.2	10.5	2.0	8.5	14.7	8.9	3.1	9.6
01/28	MW	02:00	06:00	1.6	12.6	4.8	2.0	7.1	7.3	5.6	0.8	10.2
01/28	MW	08:00	11:00	2.8	24.7	2.6	2.7	14.9	47.8	8.7	14.4	8.3
02/10	MW	20:00	00:00	2.4	90.7	4.2	2.4	0.0	45.5	44.8	0.0	14.4
02/10	MW	14:00	18:00	4.3	186.8	7.2	2.4	2.3	134.1	47.8	44.0	9.8
02/11	MW	02:00	06:00	0.0	6.9	2.3	2.0	0.0	3.8	8.3	13.9	5.7
03/04	MW	20:00	00:00	4.0	50.9	7.9	3.4	0.8	17.9	32.2	12.3	43.7
03/05	MW	08:00	12:00	0.5	48.6	3.6	2.4	1.4	20.8	24.1	5.4	7.4
03/05	MW	20:00	00:00	0.0	7.7	2.5	2.0	8.5	3.2	2.1	0.0	3.8
03/05	MW	02:00	06:00	0.0	50.1	5.8	2.2	6.6	7.7	40.7	5.4	19.1
03/06	MW	08:00	12:00	1.7	12.1	2.5	1.0	1.9	4.8	4.2	0.0	3.4
03/06	MW	02:00	06:00	1.0	9.6	2.3	2.0	3.9	3.9	2.5	0.0	3.8
03/06	MW	14:00	18:00	0.0	17.2	0.5	1.0	0.0	10.6	6.4	1.5	4.5
03/07	MW	02:00	06:00	0.0	11.3	2.5	1.0	0.0	5.6	6.0	0.0	8.9
03/07	MW	08:00	11:15	2.3	19.6	5.0	0.8	0.6	10.2	10.2	0.0	10.0
01/04	PAS	11:01	15:01	19.2	45.9	15.8	2.0	0.0	34.5	15.4	31.6	12.3
01/05	PAS	11:00	15:00	23.6	112.2	15.3	7.4	0.6	109.0	30.9	67.1	95.5
01/27	PAS	20:00	00:00	61.4	981.7	77.0	28.4	68.7	791.7	142.6	371.1	43.5
01/27	PAS	13:00	17:00	45.5	984.8	93.3	24.5	20.8	794.8	93.7	296.3	102.1
01/28	PAS	02:00	06:00	22.1	630.4	34.4	6.2	43.2	478.0	76.0	339.5	17.2
01/28	PAS	14:00	16:50	35.2	76.0	14.2	11.0	13.8	70.3	31.2	123.1	58.7
01/28	PAS	10:00	14:00	31.4	298.6	21.4	9.2	19.7	255.6	88.0	120.4	132.5
02/10	PAS	14:00	18:00	22.0	155.3	19.4	7.9	6.2	114.0	58.3	183.6	84.3
02/10	PAS	20:00	00:00	27.7	176.8	11.7	8.2	16.6	97.6	42.4	159.0	15.3
02/11	PAS	02:00	06:00	25.8	197.0	12.9	7.3	26.0	89.5	108.6	217.6	8.3
02/14	PAS	12:00	18:00	20.2	354.4	9.4	8.3	11.2	314.3	59.9	187.2	98.9
02/14	PAS	18:00	00:00	55.5	74.9	12.8	15.9	20.6	77.0	30.1	193.4	21.8
02/15	PAS	01:00	06:00	55.2	126.8	13.0	18.8	31.8	112.0	42.7	212.3	8.5
02/15	PAS	18:00	00:00	21.9	29.1	8.4	7.0	1.4	11.8	25.8	73.6	59.6
02/15	PAS	12:00	18:00	37.6	159.8	9.0	9.9	2.1	86.5	73.0	42.2	42.0
02/16	PAS	01:00	06:00	23.8	24.7	9.3	7.6	9.1	11.6	28.4	41.4	17.8
02/22	PAS	12:00	16:00	12.8	18.1	5.7	0.9	0.0	9.6	2.2	9.3	3.6
02/22	PAS	20:00	00:00	59.8	110.3	17.5	14.7	17.7	54.8	42.2	125.0	11.3

Table 7. Concentrations of selected aerosol and gas phase species measured at the five rain study sites during the winter of 1987. HF = Henninger Flats, MW = Mount Wilson, PAS = Pasadena, RIV = Riverside, and WLA = West Los Angeles.

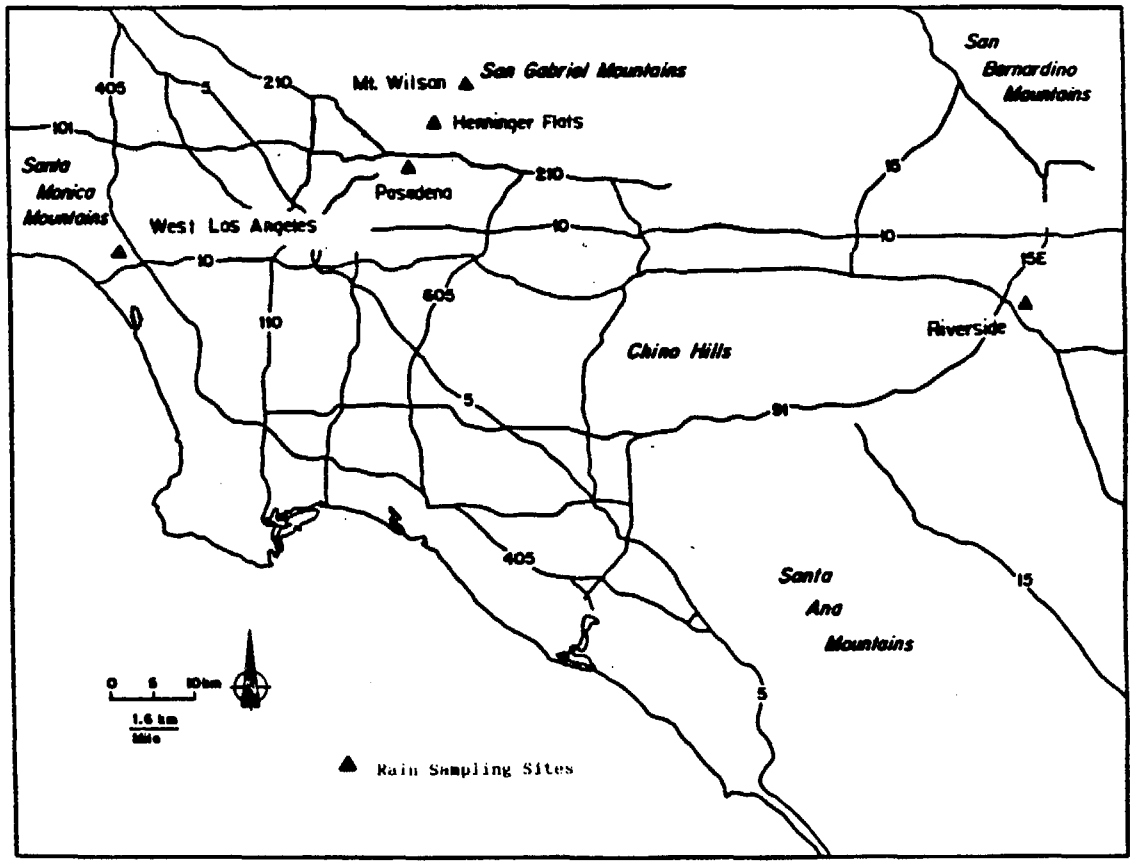

Figure 1. Map of the Los Angeles area showing the five sites used for sampling rain, aerosol, and selected gases during the winter of 1987.

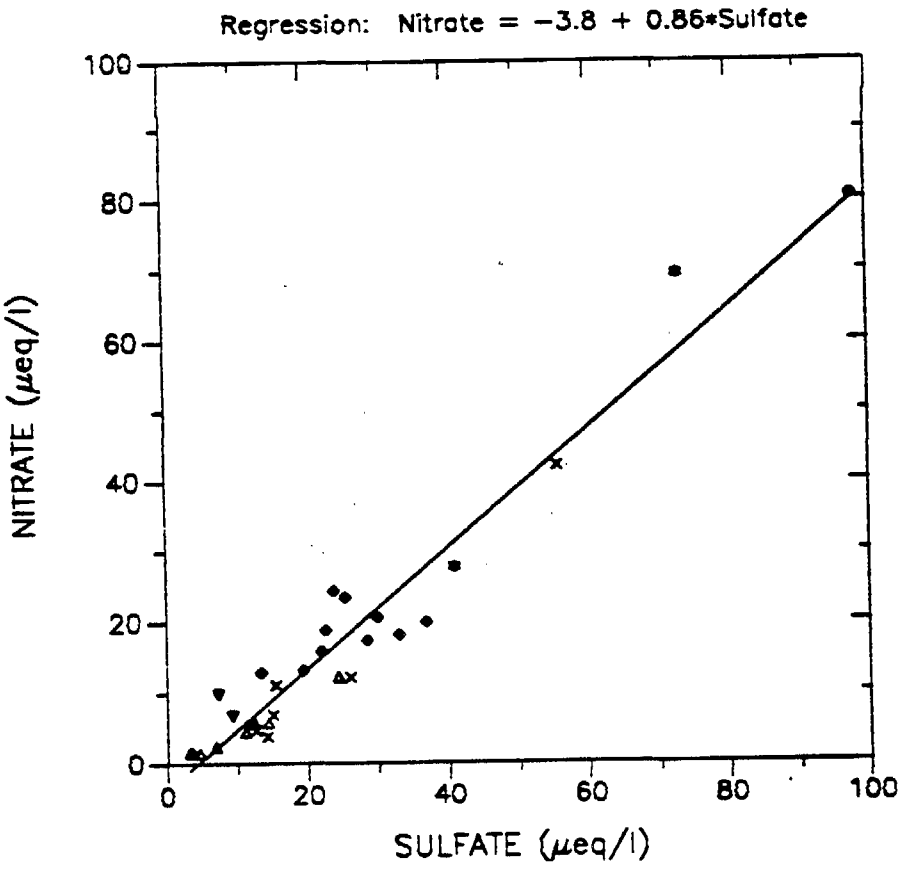

Figure 2. Comparison of nitrate and sulfate concentrations in rain samples collected at West Los Angeles during the winter of 1987. The different symbols represent samples from different storms. The least–squares regression line is included for reference.

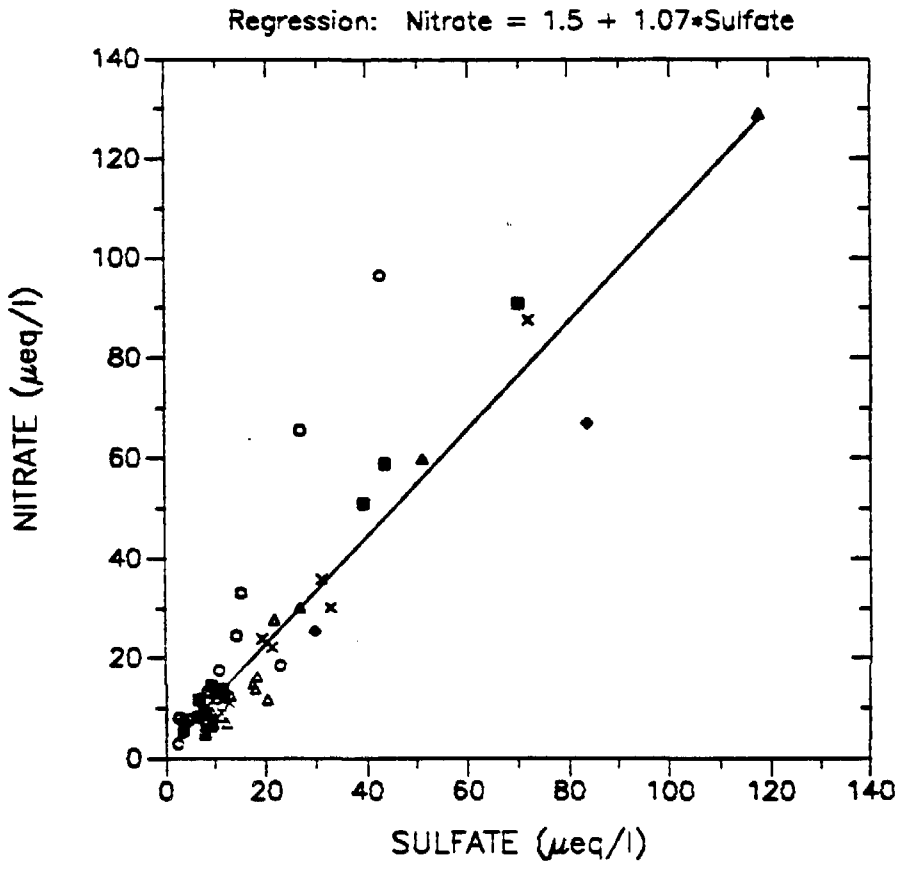

Figure 3. Comparison of nitrate and sulfate concentrations in rain samples collected at Pasadena during the winter of 1987. The different symbols represent samples from different storms. The least–squares regression line is included for reference.

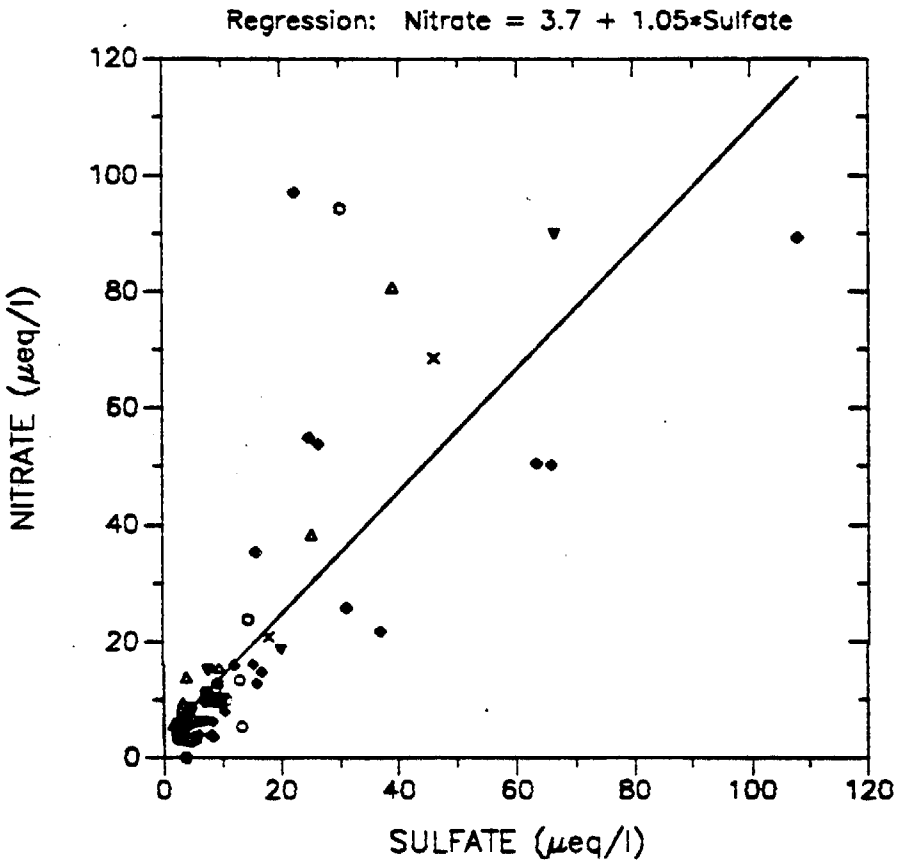

Figure 4. Comparison of nitrate and sulfate concentrations in rain samples collected at Henninger Flats during the winter of 1987. The different symbols represent samples from different storms. The least–squares regression line is included for reference.

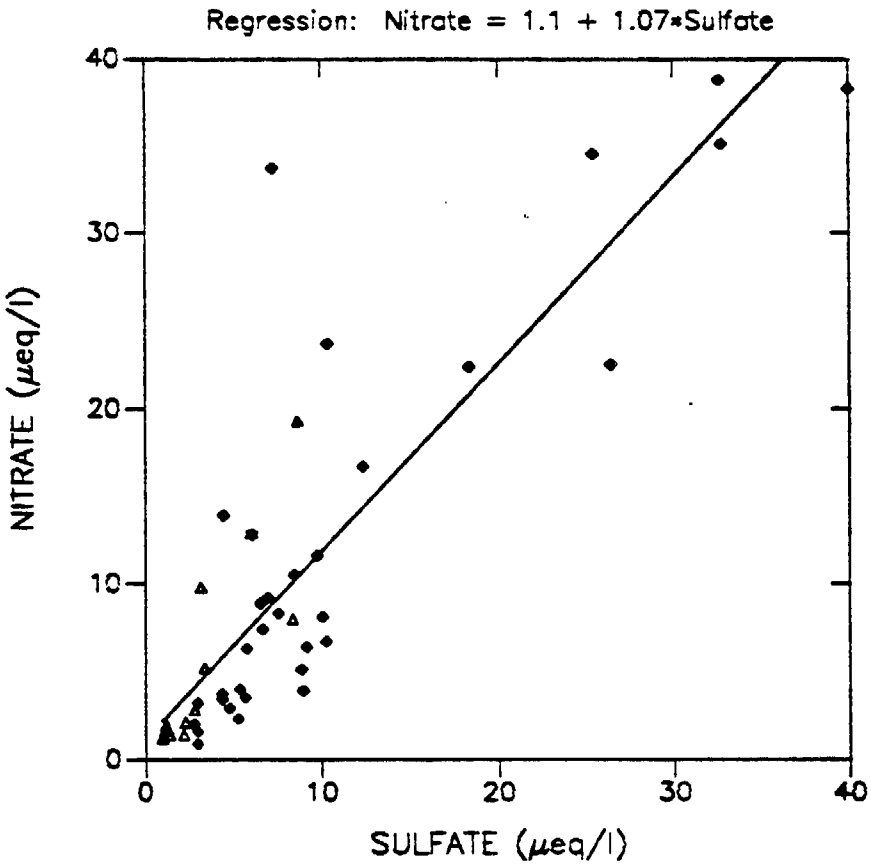

Figure 5. Comparison of nitrate and sulfate concentrations in rain samples collected at Mt. Wilson during the winter of 1987. The different symbols represent samples from different storms. The least–squares regression line is included for reference.

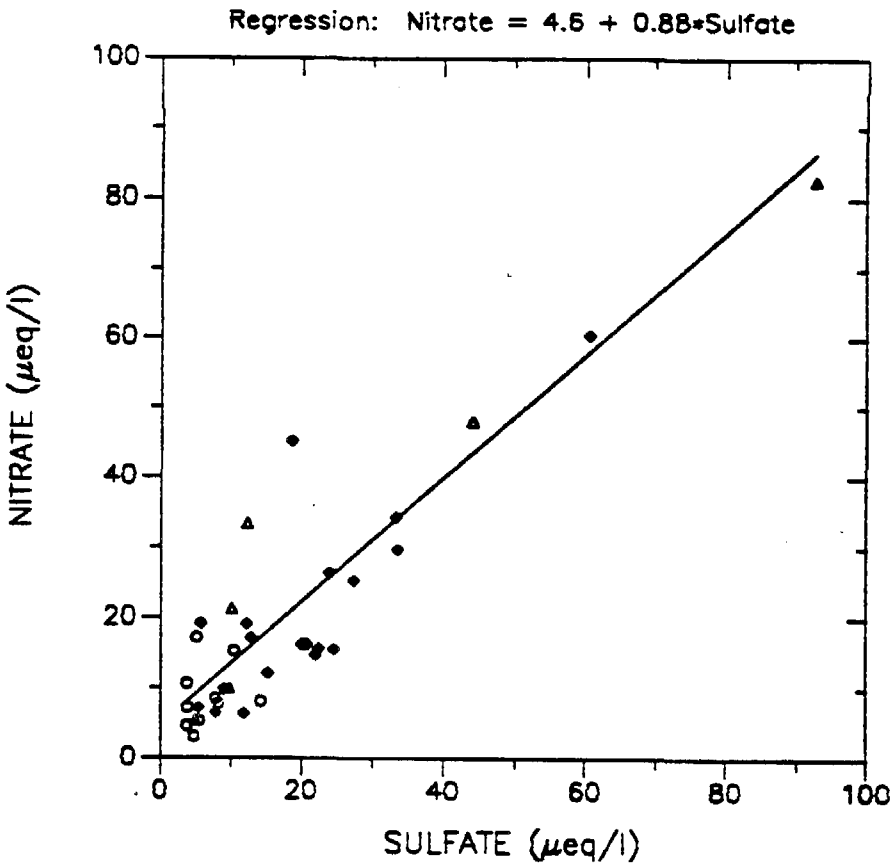

Figure 6. Comparison of nitrate and sulfate concentrations in rain samples collected at Riverside during the winter of 1987. The different symbols represent samples from different storms. The least–squares regression line is included for reference.

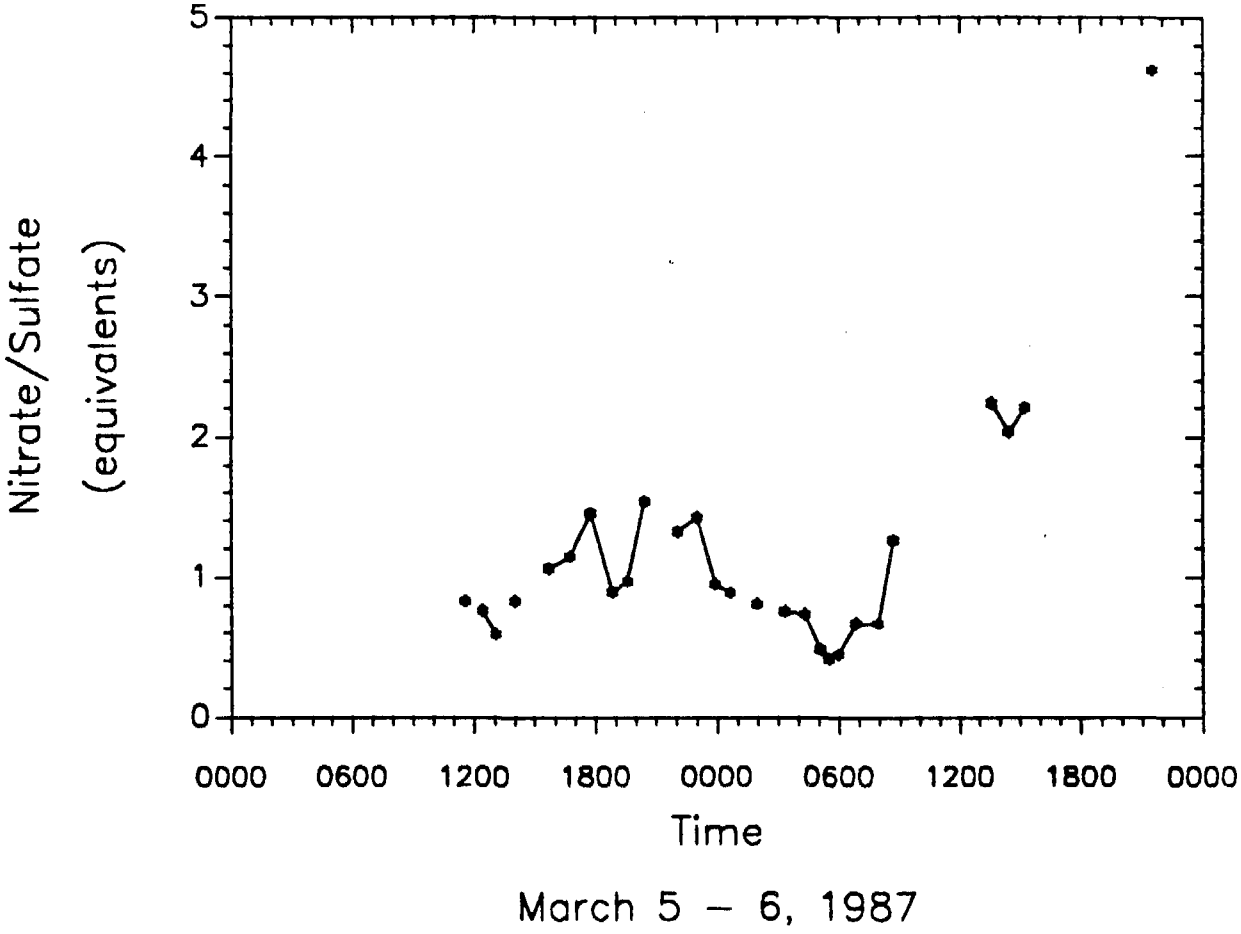

Figure 7. Variations in the nitrate to sulfate ratio observed in rain samples collected at Henninger Flats over the course of a single storm on March 5 and 6, 1987.

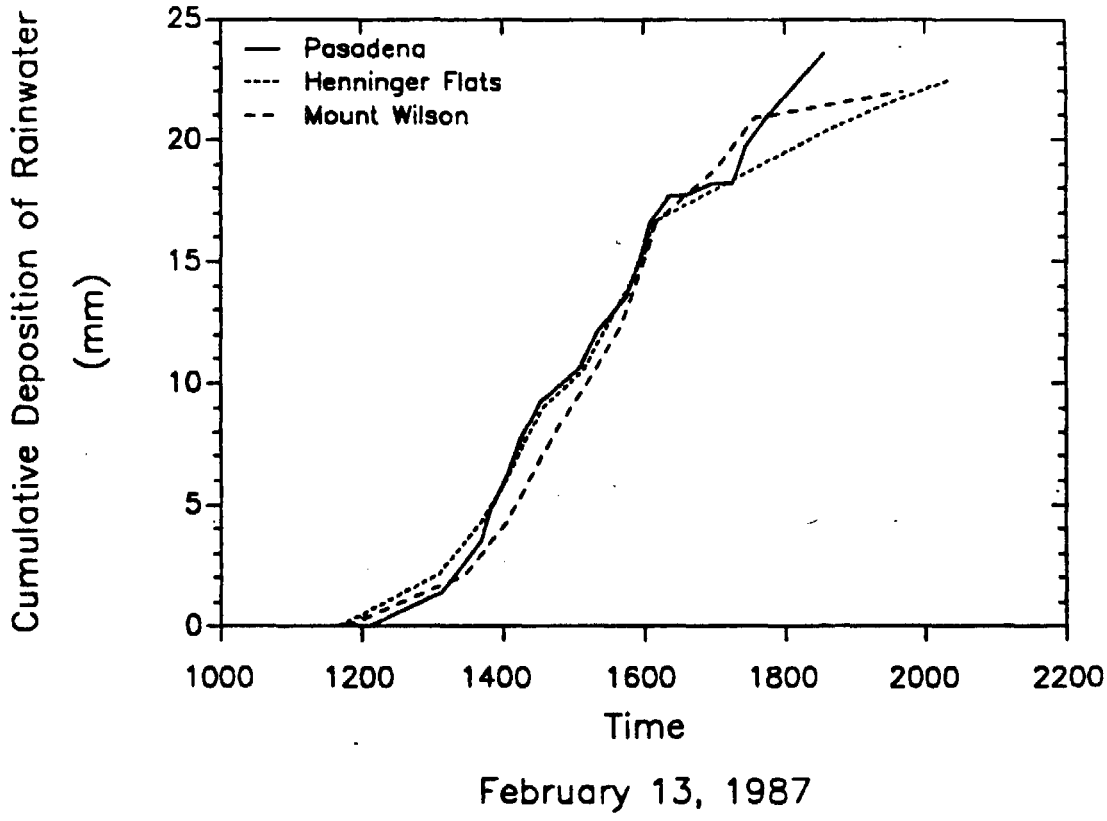

Figure 8. Cumulative rainfall measured at Pasadena, Henninger Flats, and Mt. Wilson on February 13, 1987.

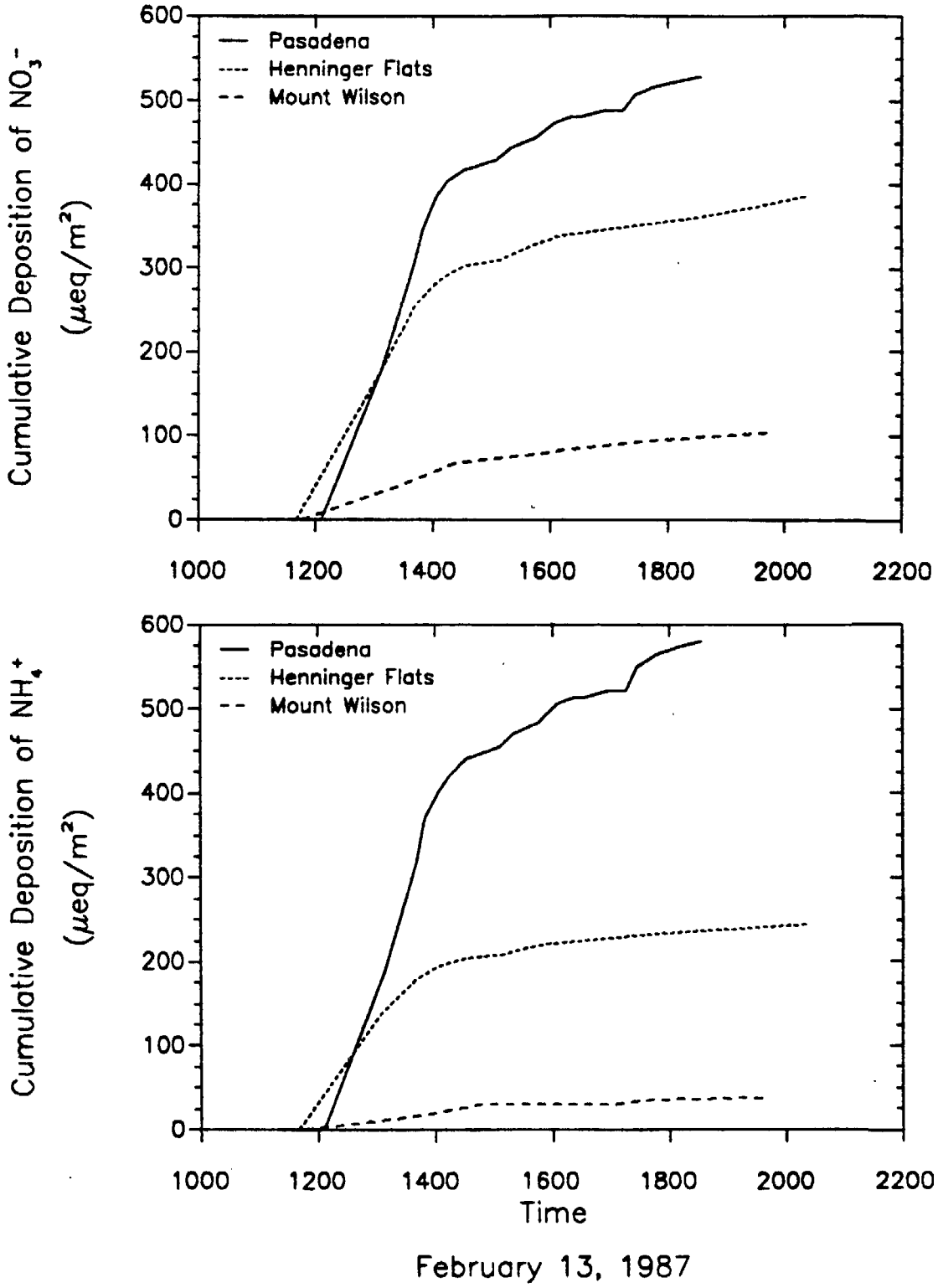

Figure 9. Cumulative deposition of NO_3^- and NH_4^+ measured at Pasadena, Henninger Flats, and Mt. Wilson on February 13, 1987.

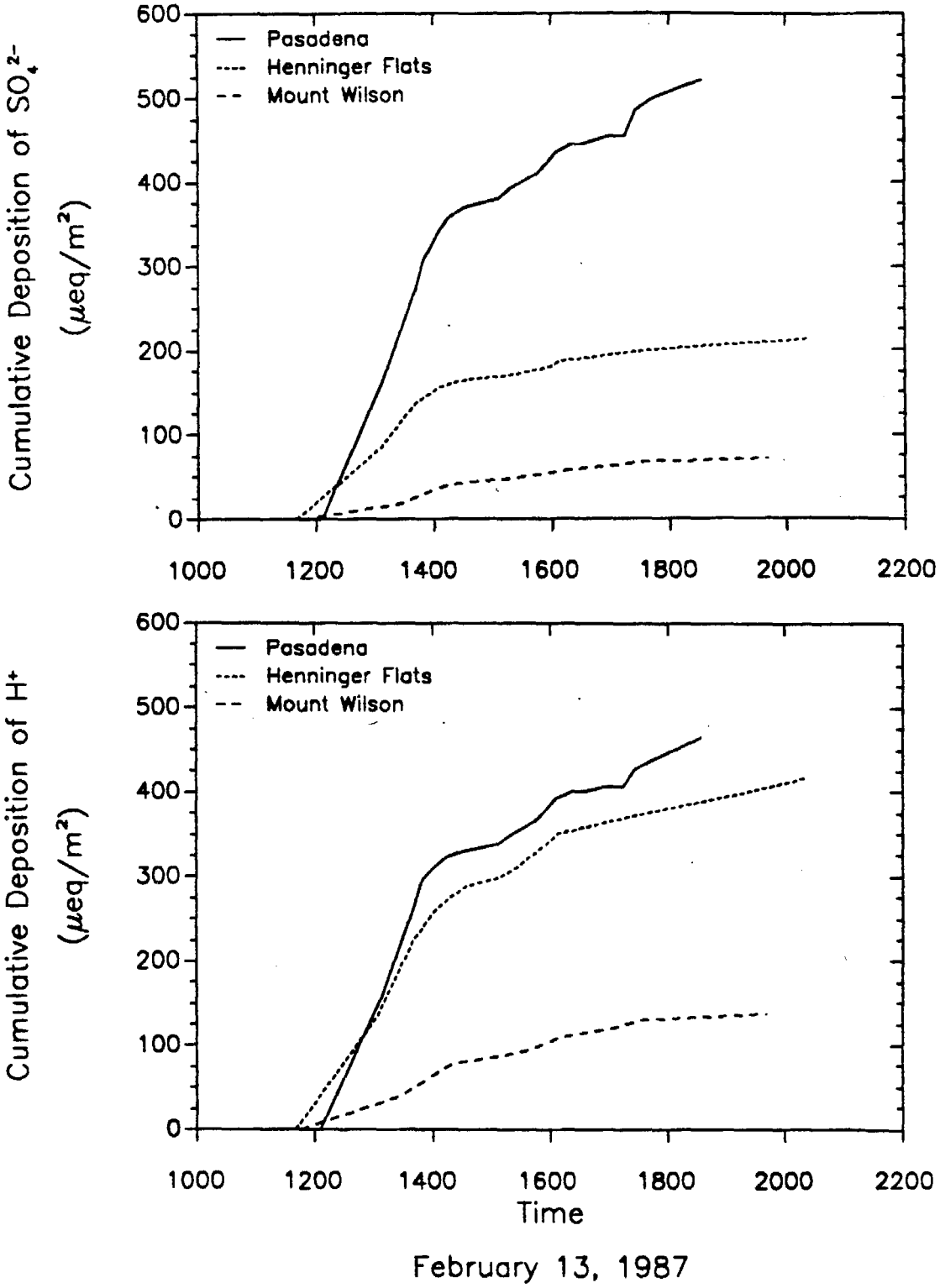

Figure 10. Cumulative deposition of SO_4^{2-} and H^+ measured at Pasadena, Henninger Flats, and Mt. Wilson on February 13, 1987.

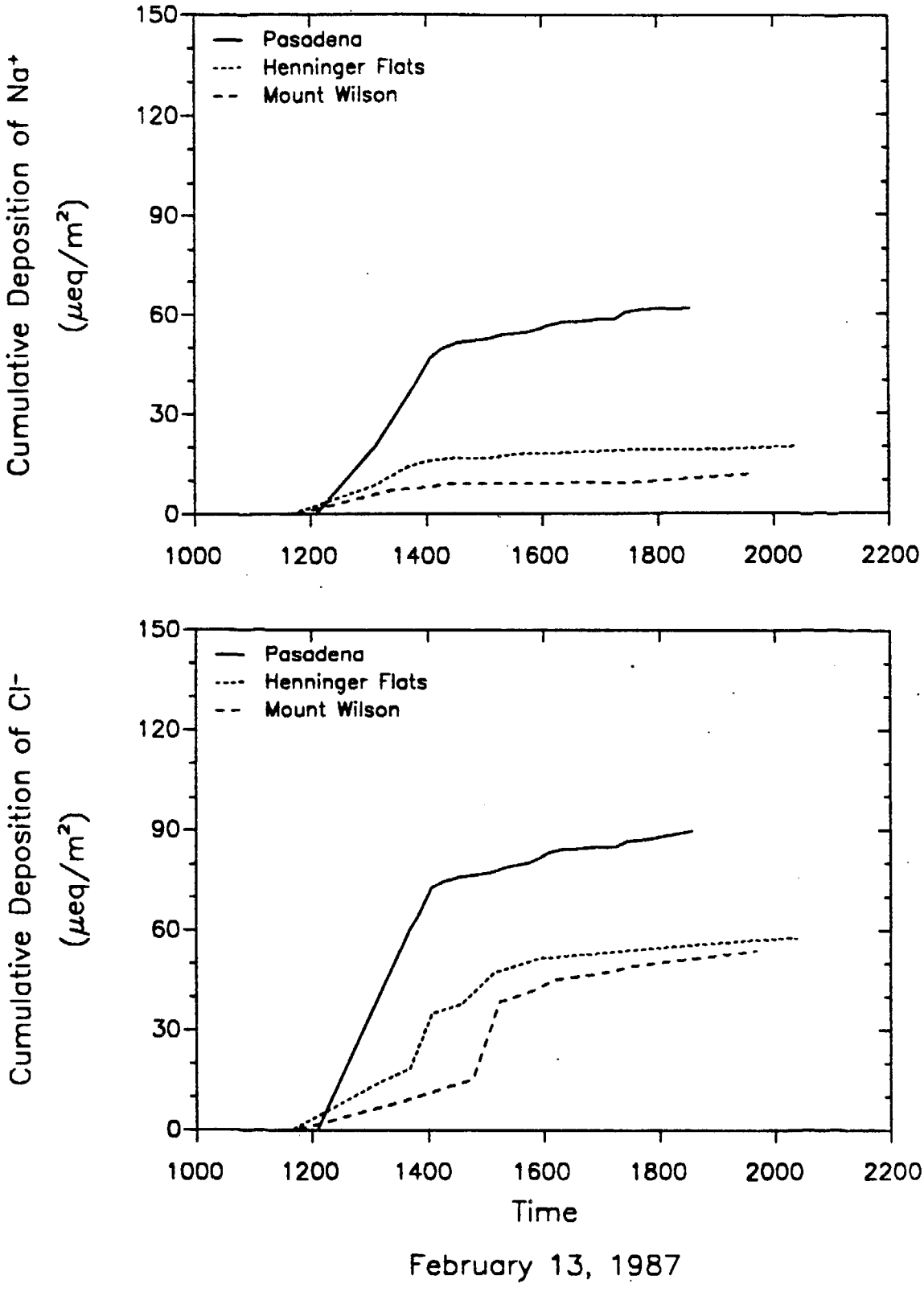

Figure 11. Cumulative deposition of Na^+ and Cl^- measured at Pasadena, Henninger Flats, and Mt. Wilson on February 13, 1987.

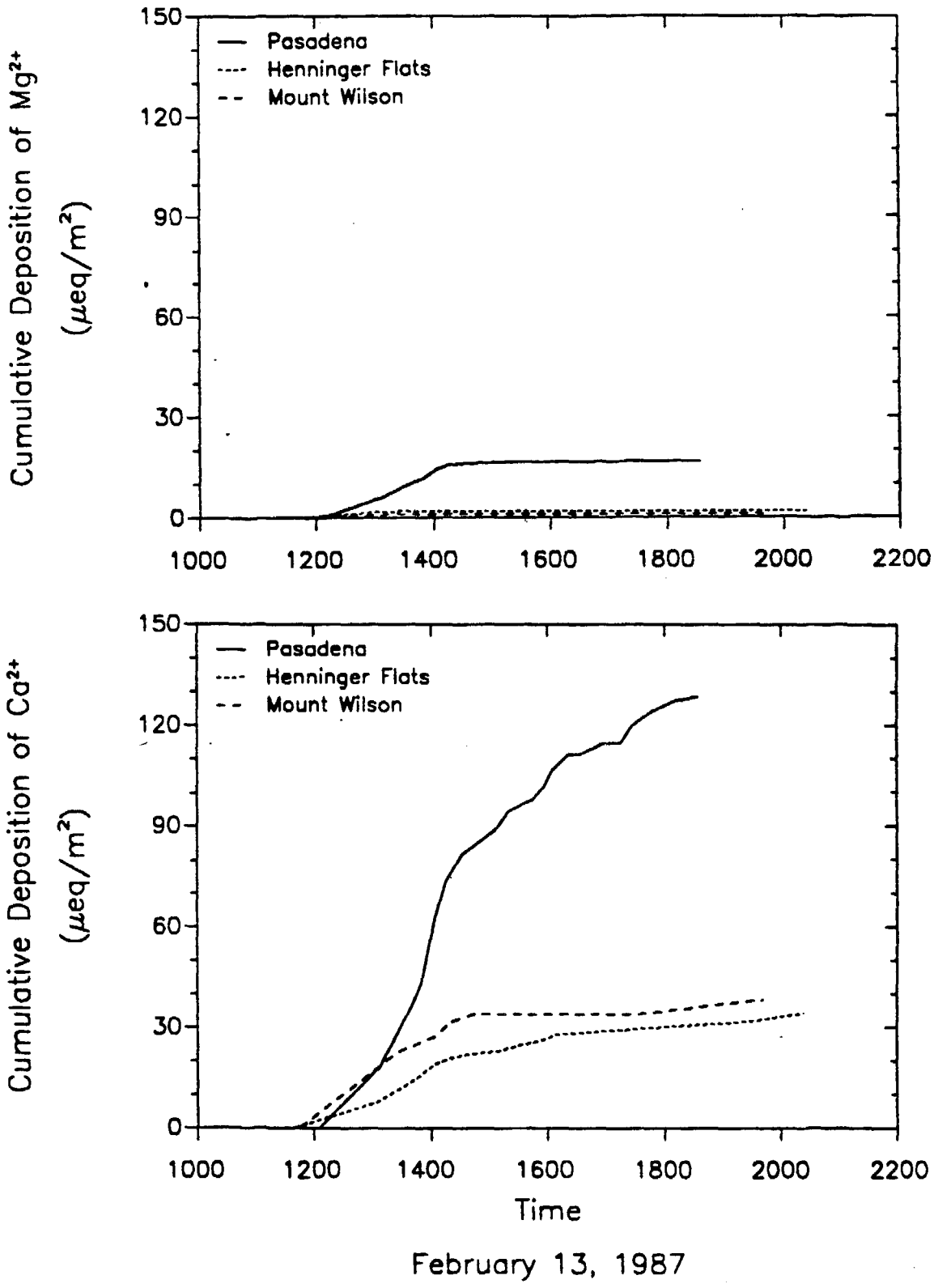

Figure 12. Cumulative deposition of Mg^{2+} and Ca^{2+} measured at Pasadena, Henninger Flats, and Mt. Wilson on February 13, 1987.

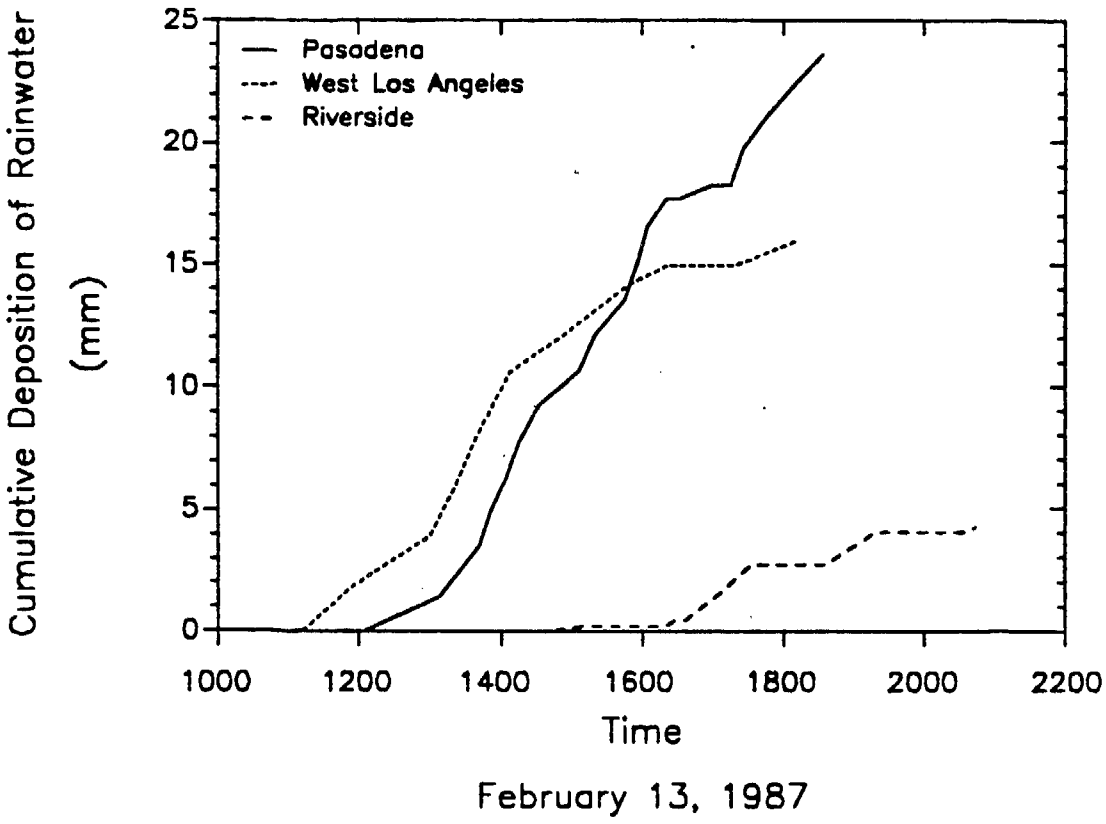

Figure 13. Cumulative rainfall measured at Pasadena, West Los Angeles, and Riverside on February 13, 1987.

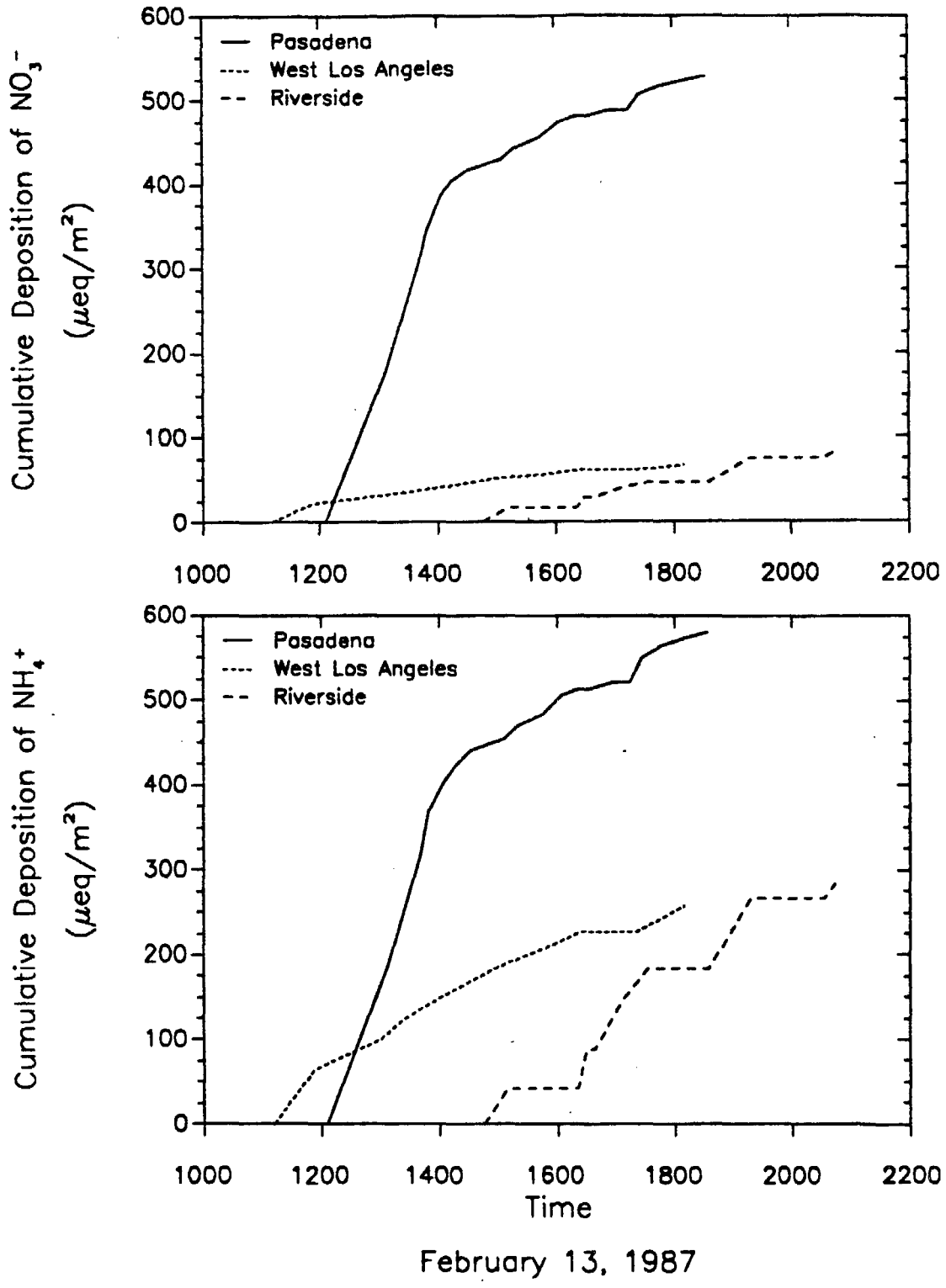

Figure 14. Cumulative deposition of NO_3^- and NH_4^+ measured at Pasadena, West Los Angeles, and Riverside on February 13, 1987.

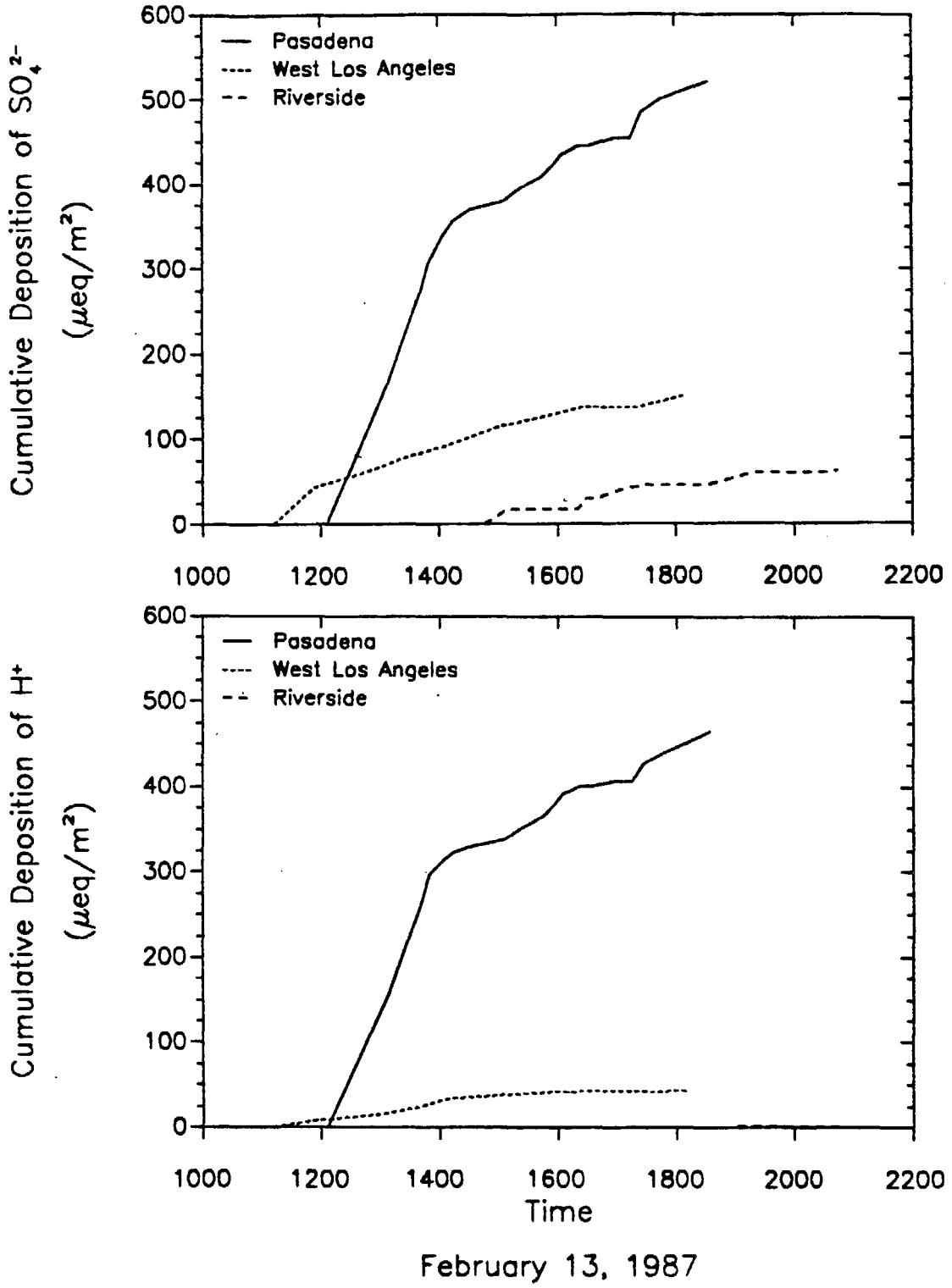

Figure 15. Cumulative deposition of SO_4^{2-} and H^+ measured at Pasadena, West Los Angeles, and Riverside on February 13, 1987.

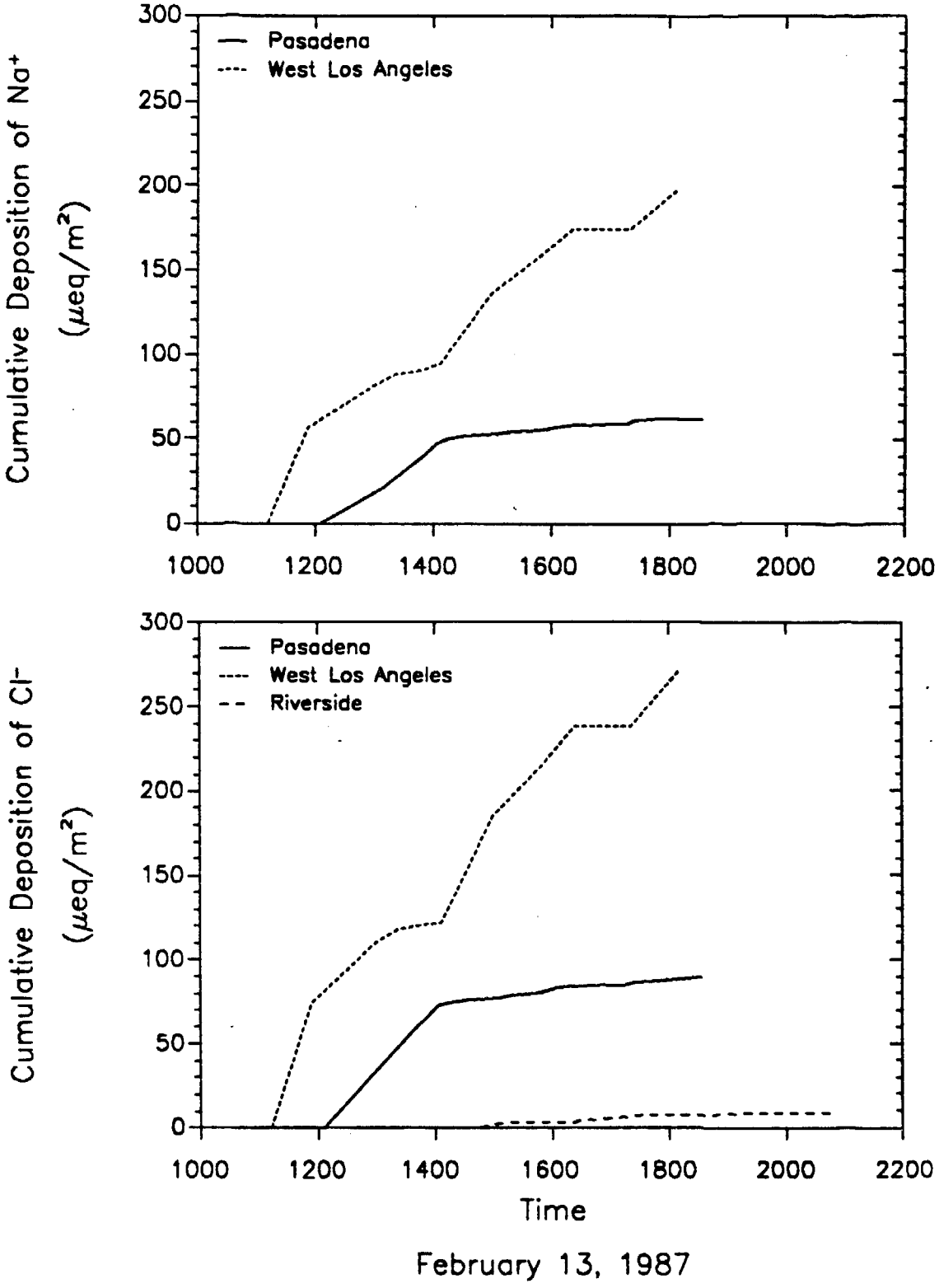

Figure 16. Cumulative deposition of Na^+ and Cl^- measured at Pasadena, West Los Angeles, and Riverside on February 13, 1987.

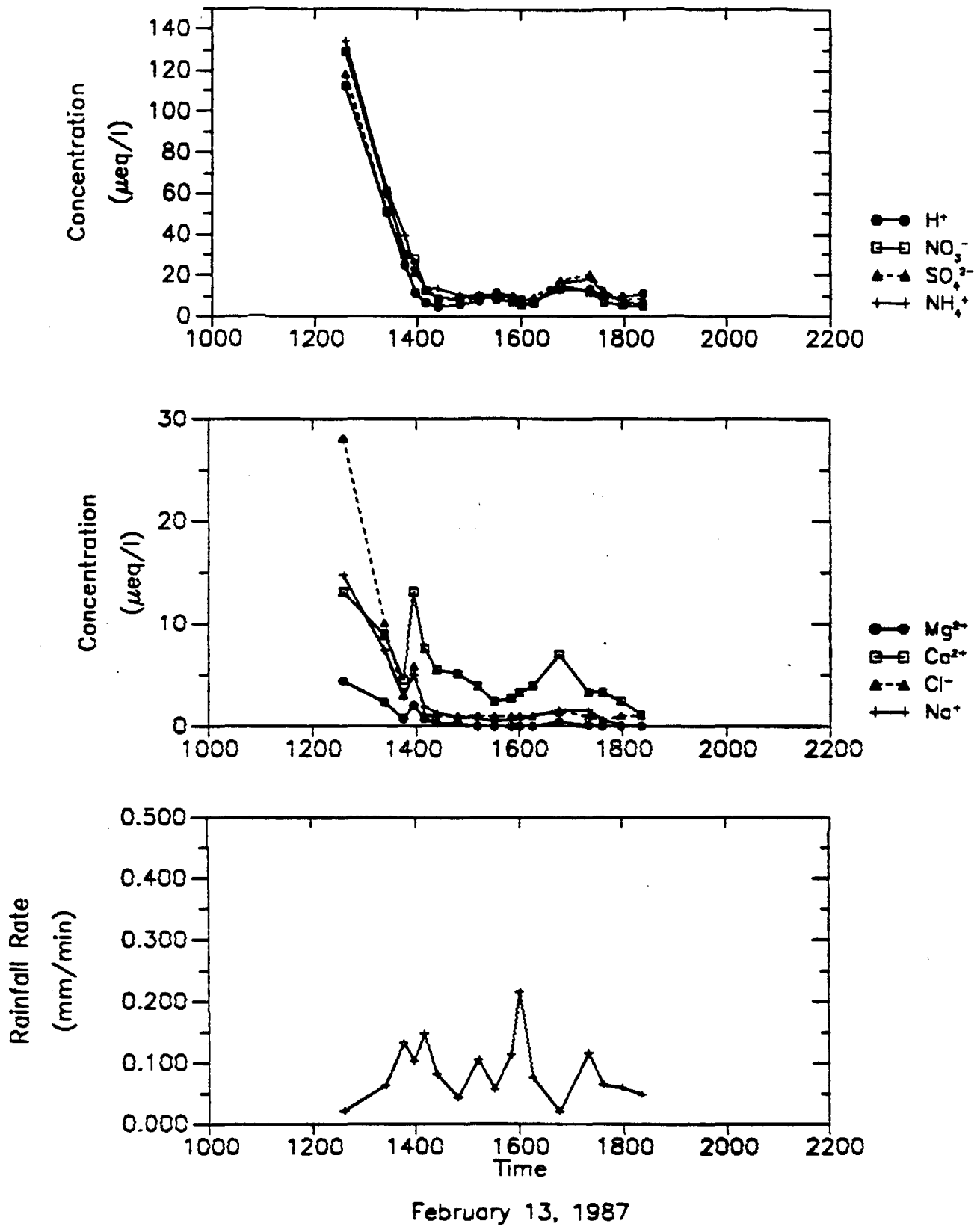

Figure 17. Concentrations of major species measured in rain samples collected at Pasadena as a function of time. Samples were collected on February 13, 1987. Also shown is a plot of the rainfall rate as a function of time (averaged over the collection period of each sample) for the same storm. No significant breaks in the continuity of the rainfall were observed during this period.

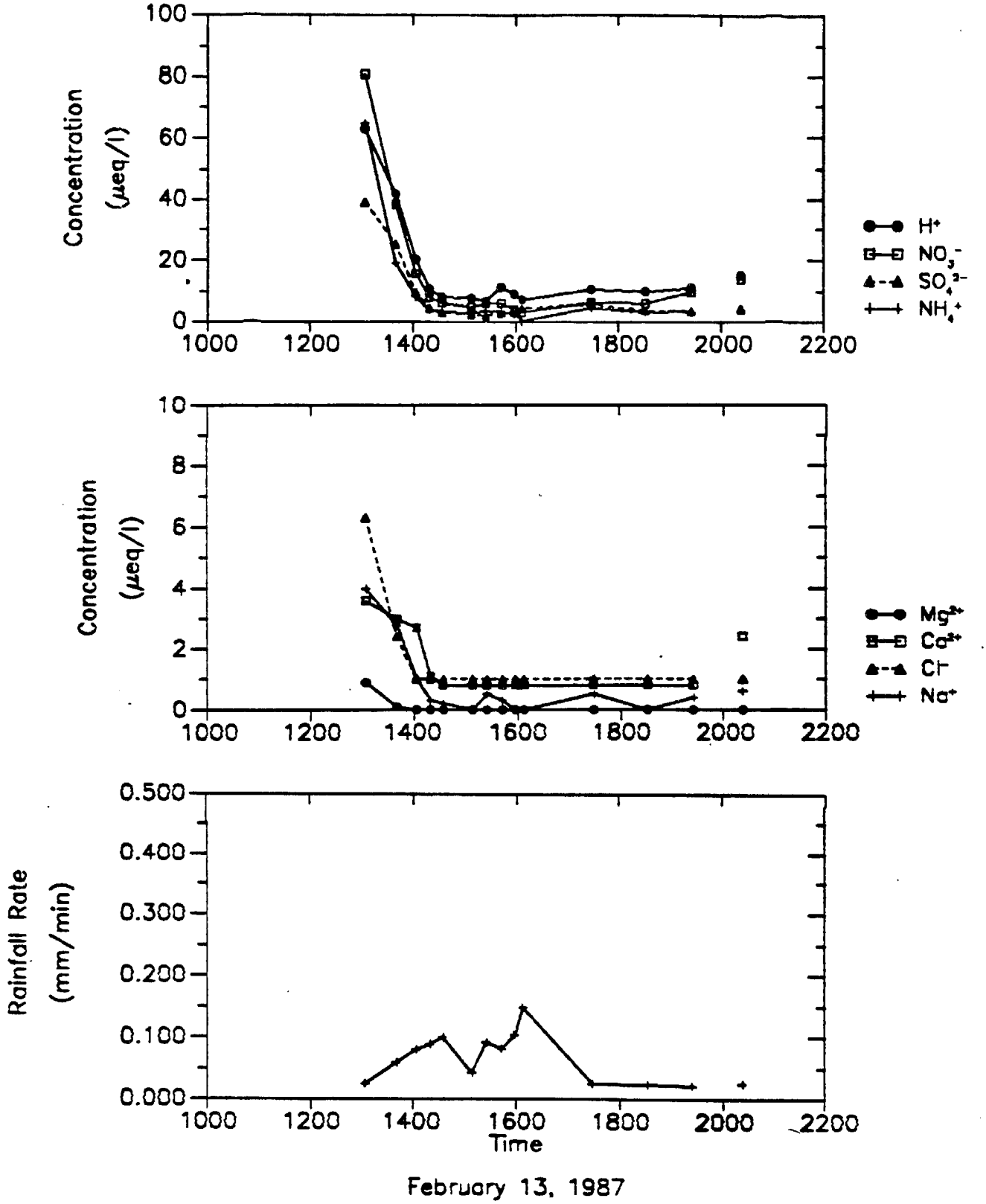

Figure 18. Concentrations of major species measured in rain samples collected at Henninger Flats as a function of time. Samples were collected on February 13, 1987. Also shown is a plot of the rainfall rate as a function of time (averaged over the collection period of each sample) for the same storm. Breaks in a line indicate breaks in the rain.

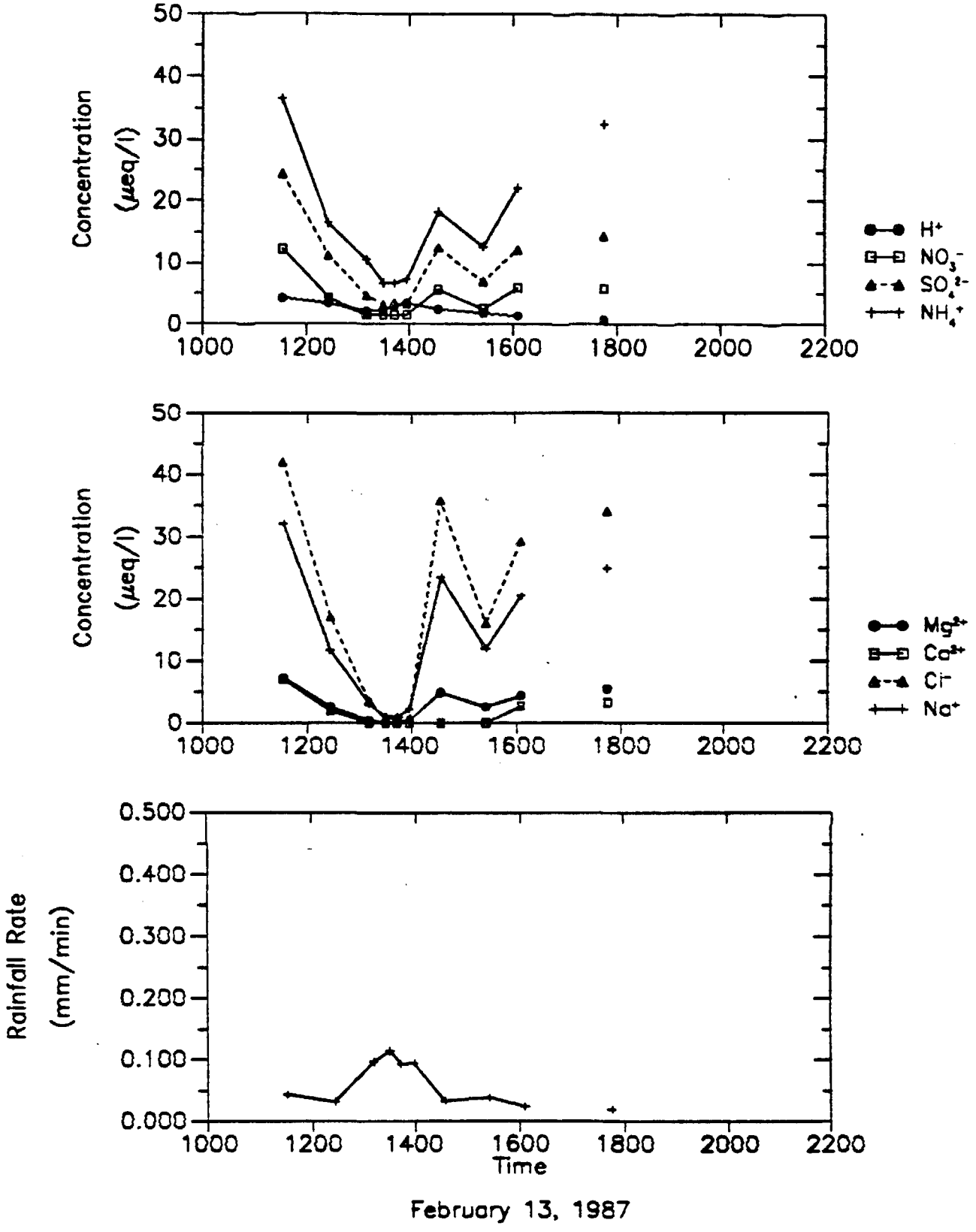

Figure 19. Concentrations of major species measured in rain samples collected at West Los Angeles as a function of time. Samples were collected on February 13, 1987. Also shown is a plot of the rainfall rate as a function of time (averaged over the collection period of each sample) for the same storm. Breaks in a line indicate breaks in the rain.

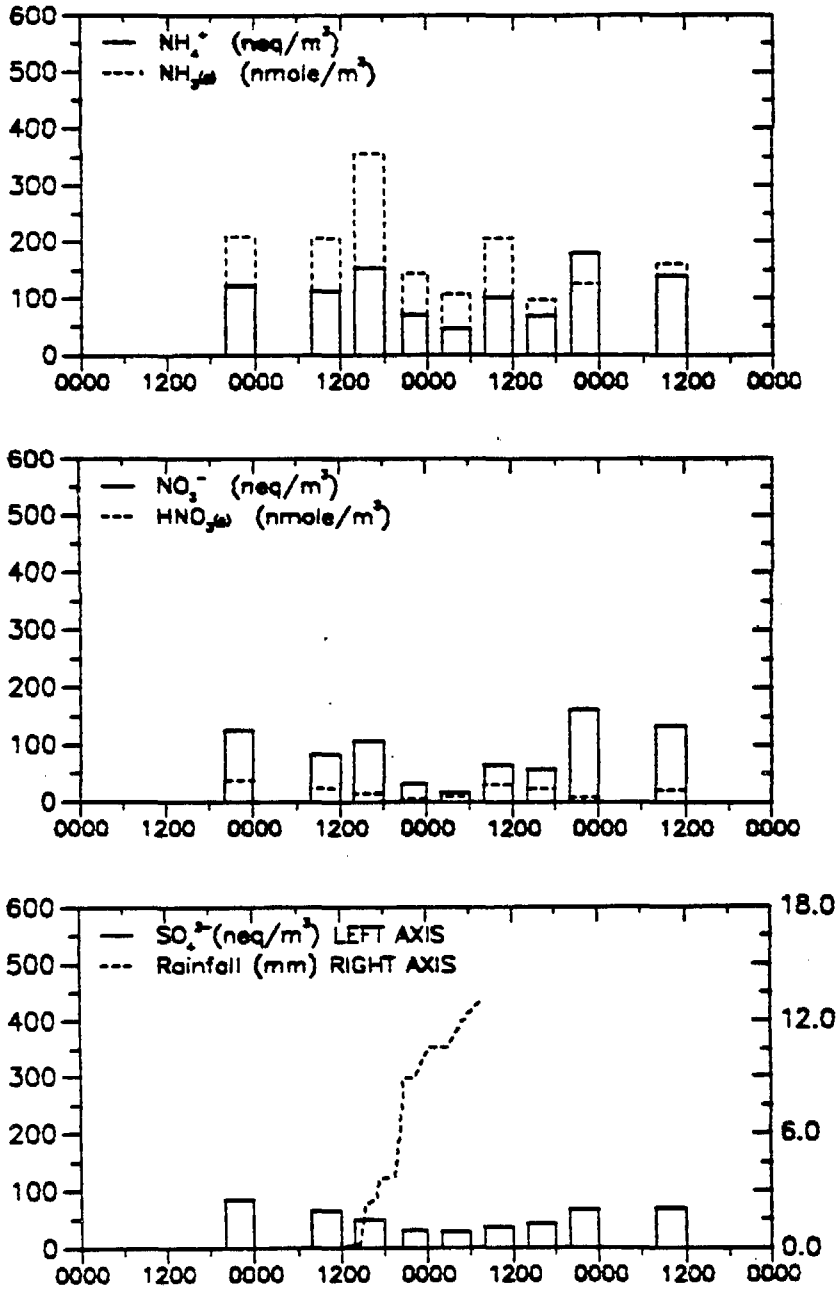

Figure 20. Concentrations of selected aerosol and gas phase species measured at West Los Angeles from March 4 through March 7, 1987. Also shown is the cumulative rainfall measured at the same site during this period.

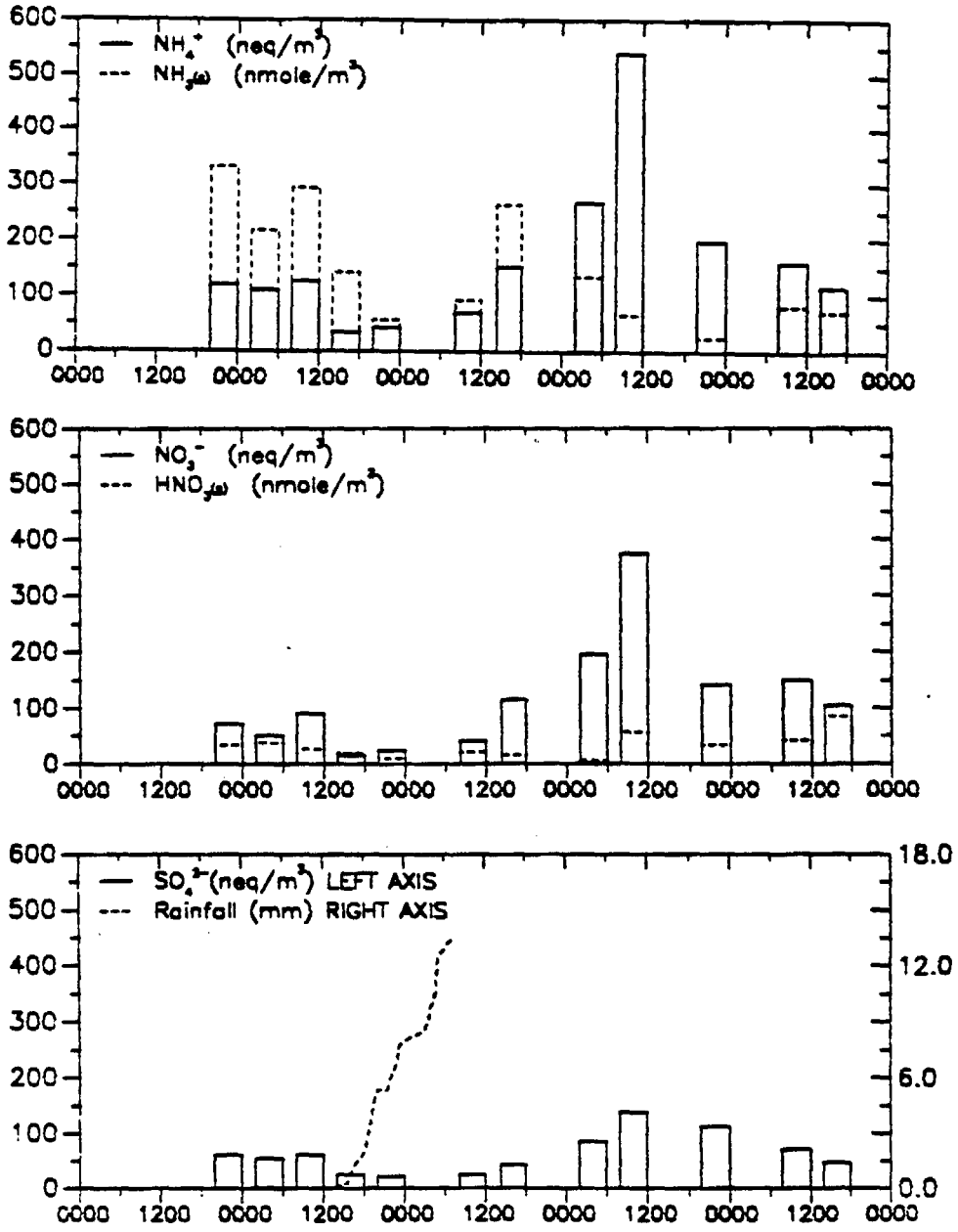

Figure 21. Concentrations of selected aerosol and gas phase species measured at Pasadena from March 4 through March 8, 1987. Also shown is the cumulative rainfall measured at the same site during this period.

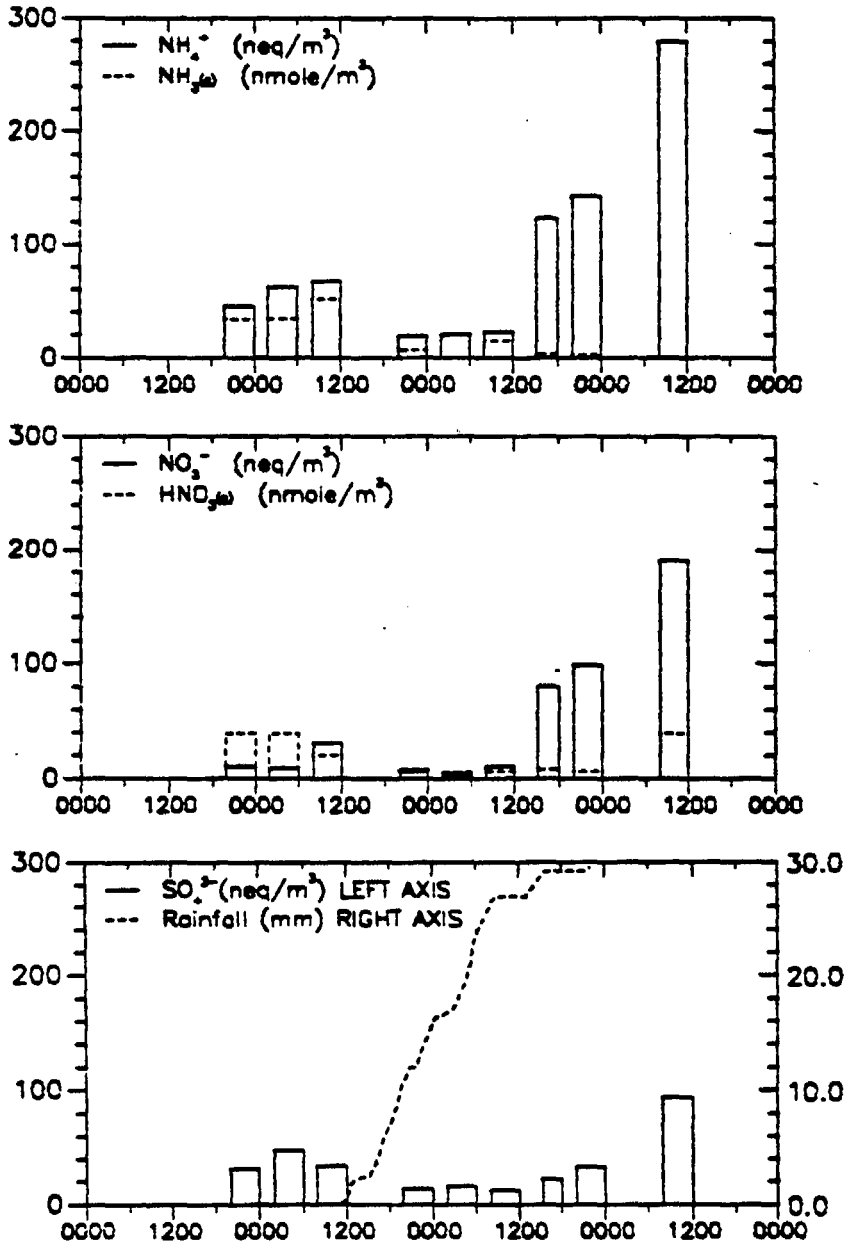

Figure 22. Concentrations of selected aerosol and gas phase species measured at Henninger Flats from March 4 through March 7, 1987. Also shown is the cumulative rainfall measured at the same site during this period.

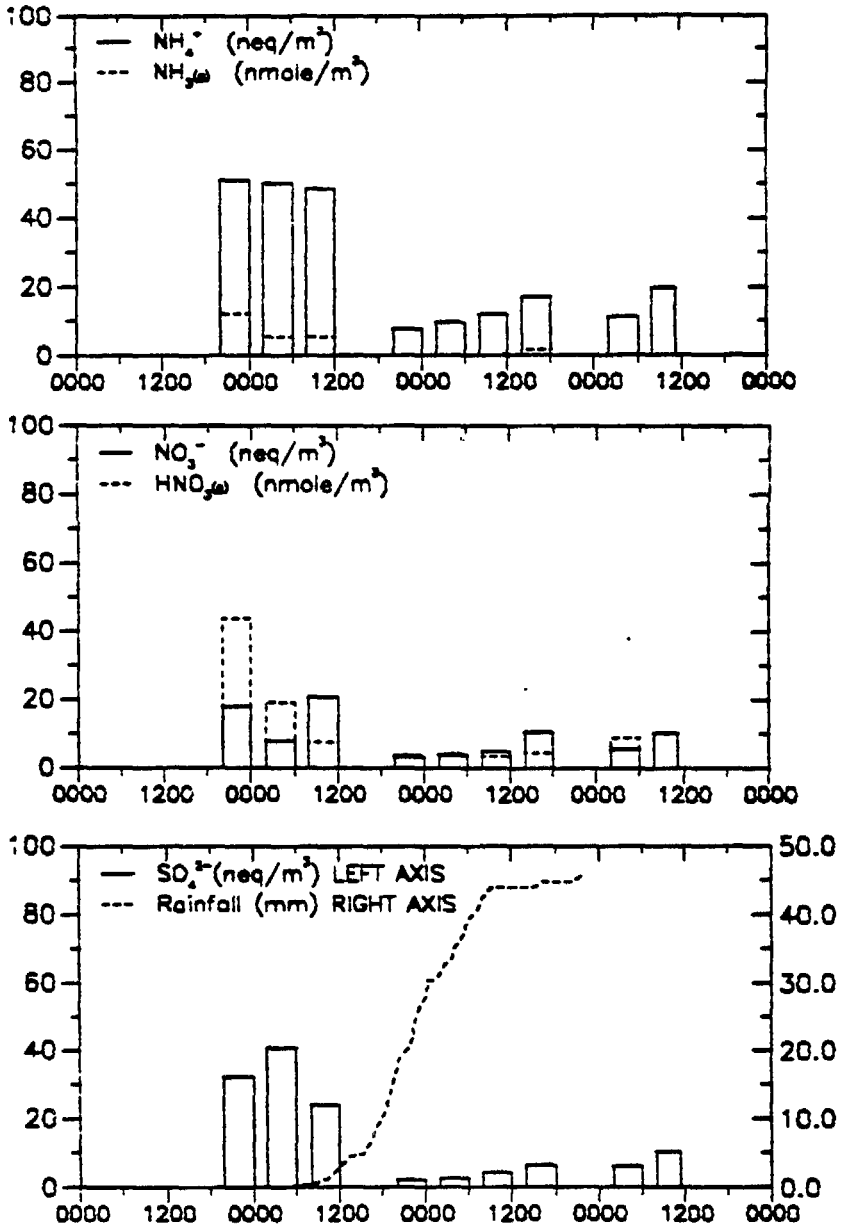

Figure 23. Concentrations of selected aerosol and gas phase species measured at Mt. Wilson from March 4 through March 7, 1987. Also shown is the cumulative rainfall measured at the same site during this period.

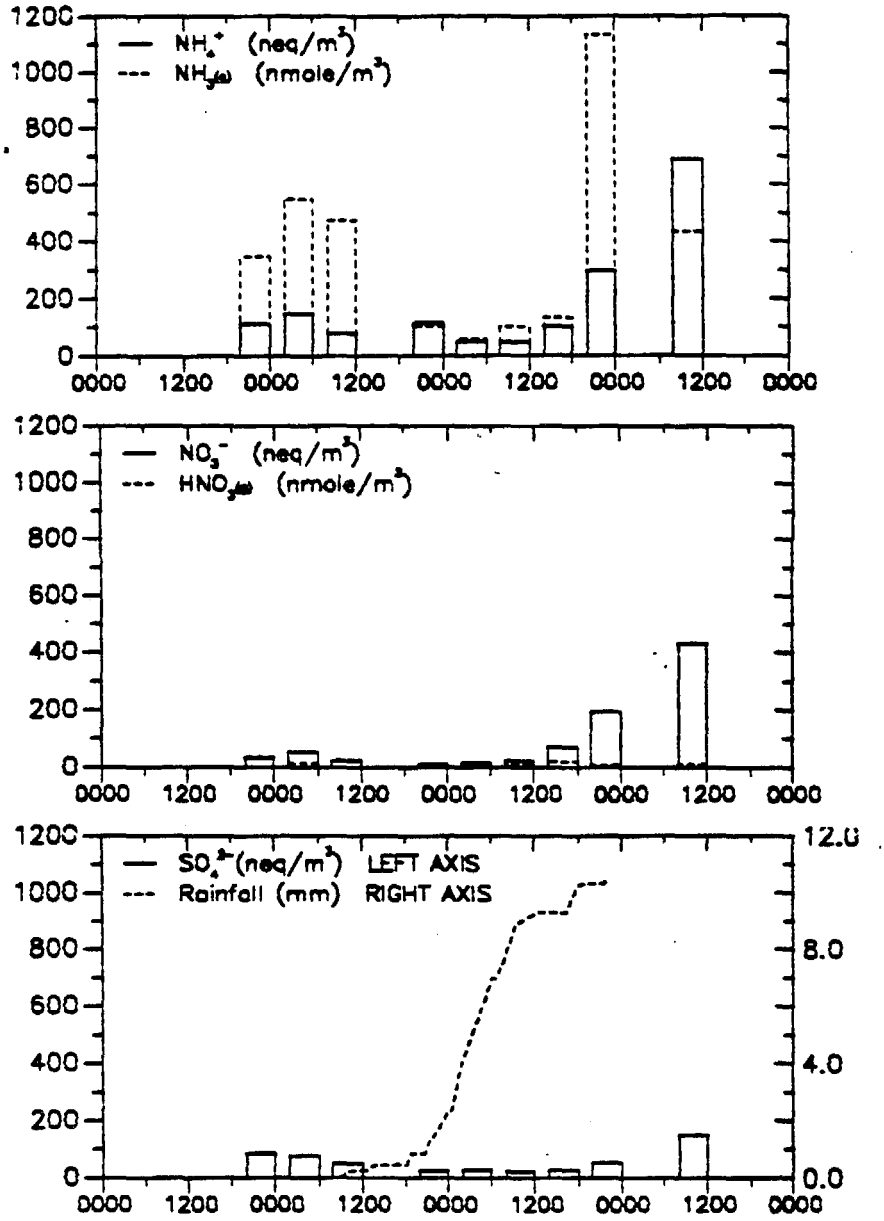

Figure 24. Concentrations of selected aerosol and gas phase species measured at Riverside from March 4 through March 7, 1987. Also shown is the cumulative rainfall measured at the same site during this period.

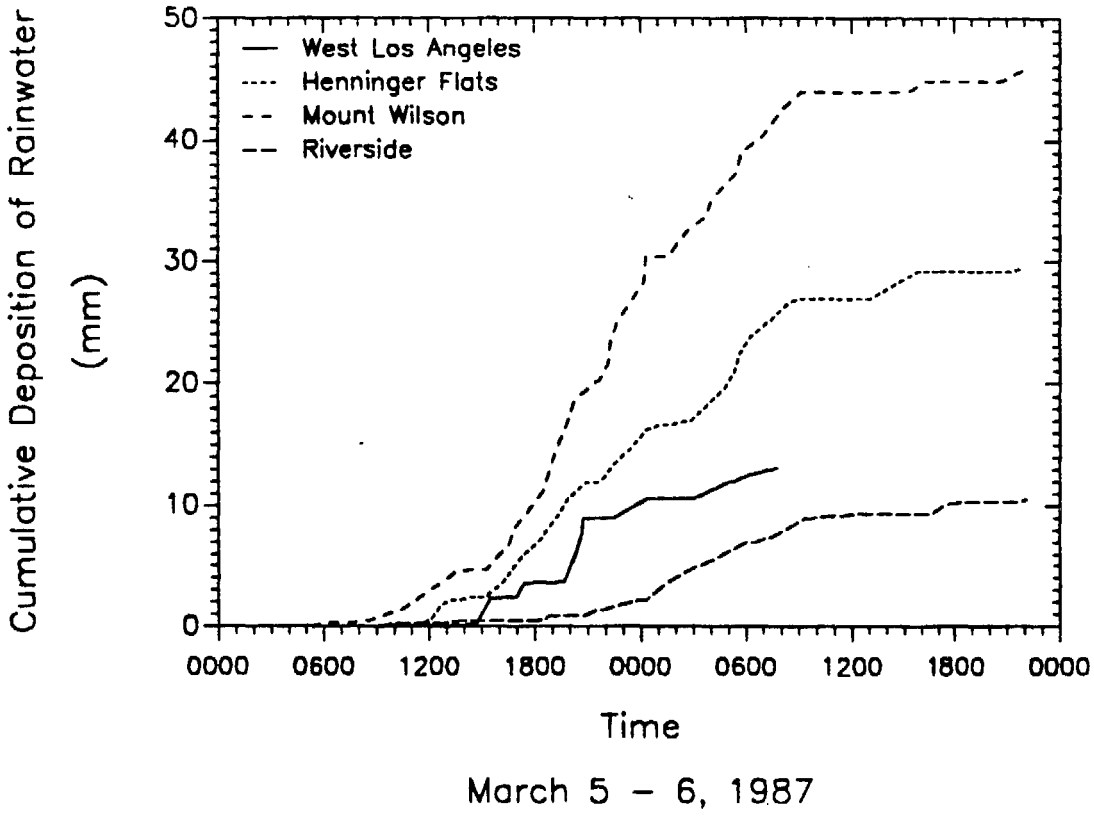

Figure 25. Cumulative rainfall measured at West Los Angeles, Henninger Flats, Mt. Wilson, and Riverside on March 5 and 6, 1987.

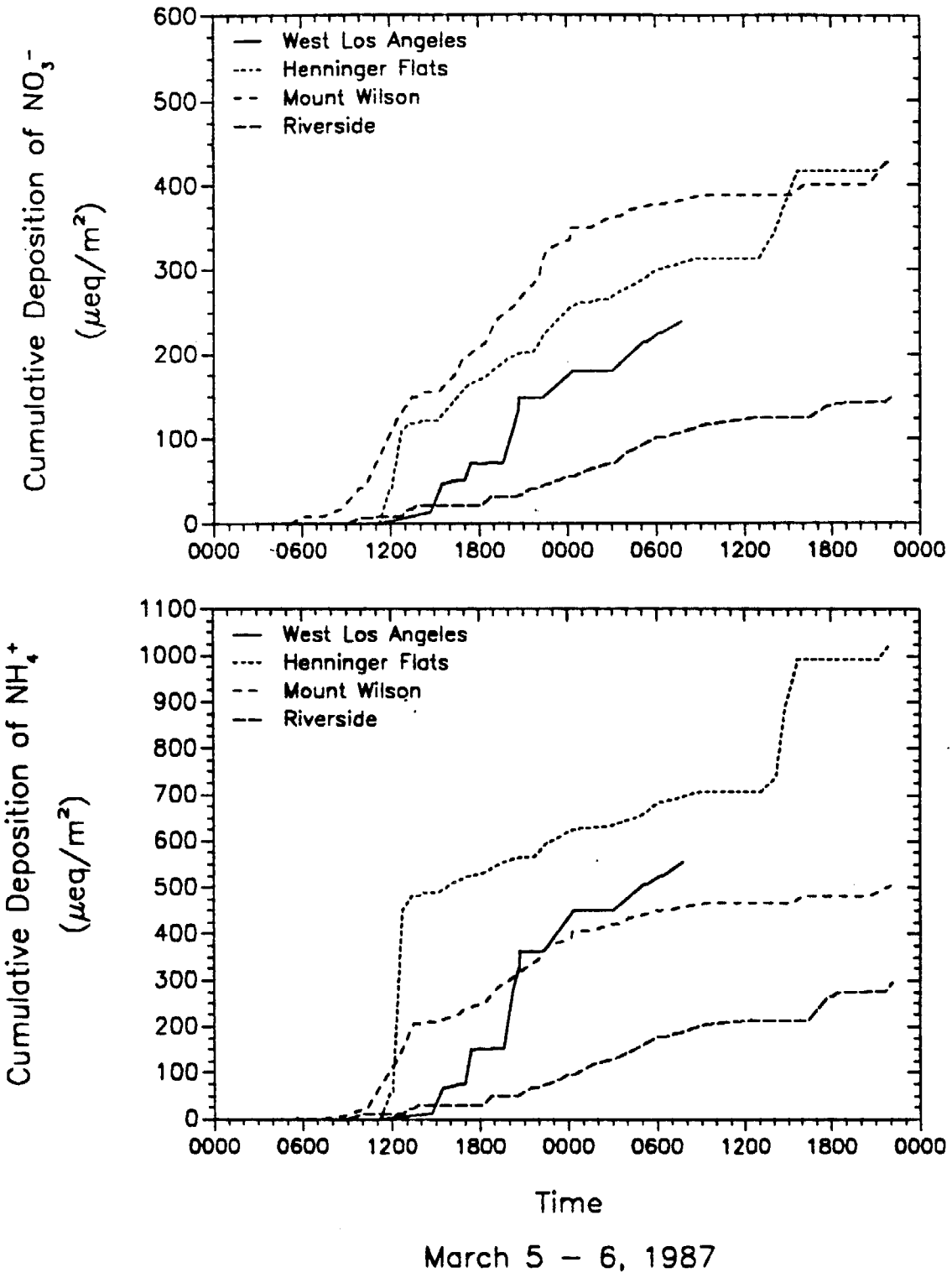

Figure 26. Cumulative deposition of NO_3^- and NH_4^+ measured at West Los Angeles, Henninger Flats, Mt. Wilson, and Riverside on March 5 and 6, 1987.

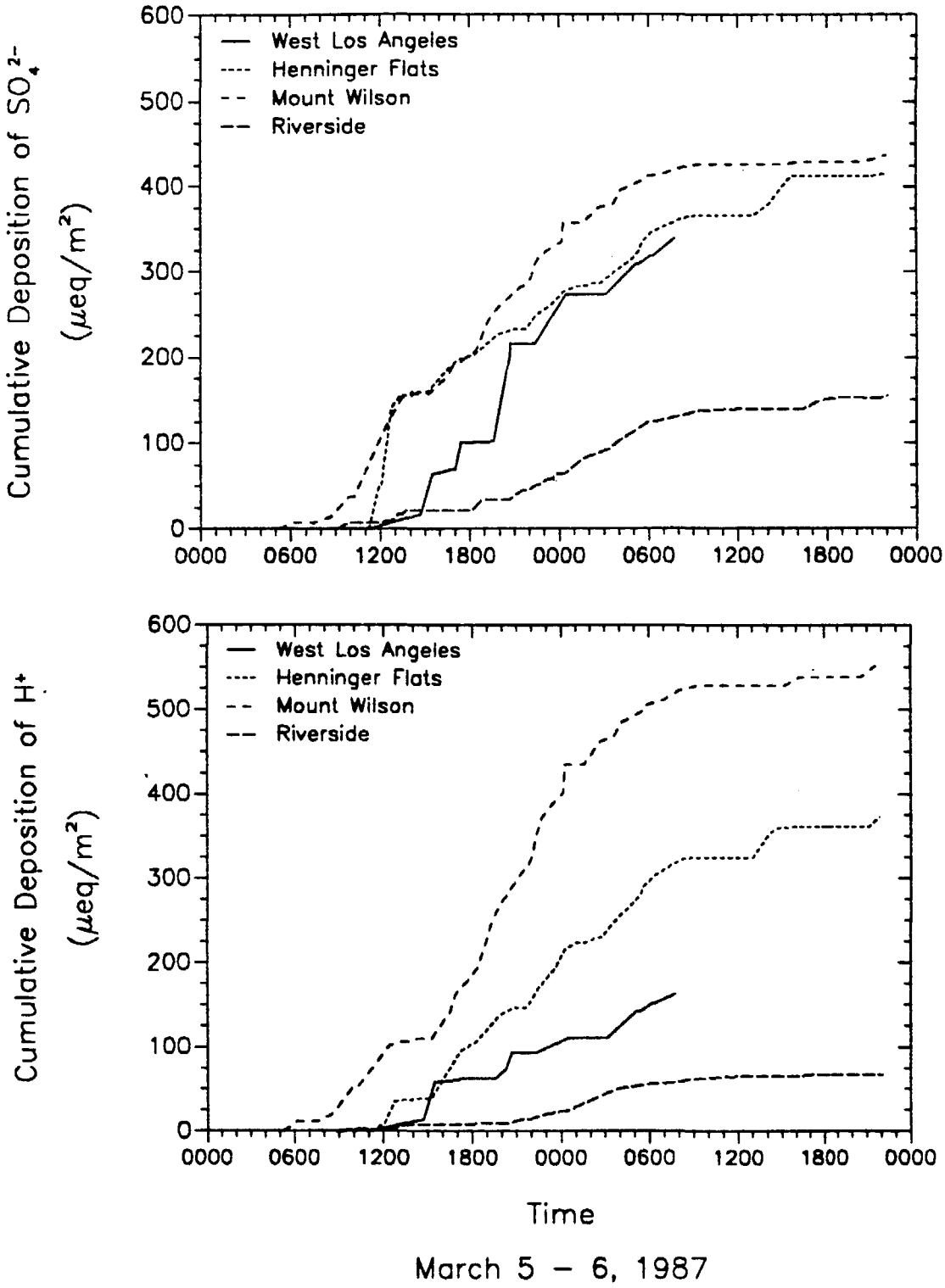

Figure 27. Cumulative deposition of SO_4^{2-} and H^+ measured at West Los Angeles, Henninger Flats, Mt. Wilson, and Riverside on March 5 and 6, 1987.

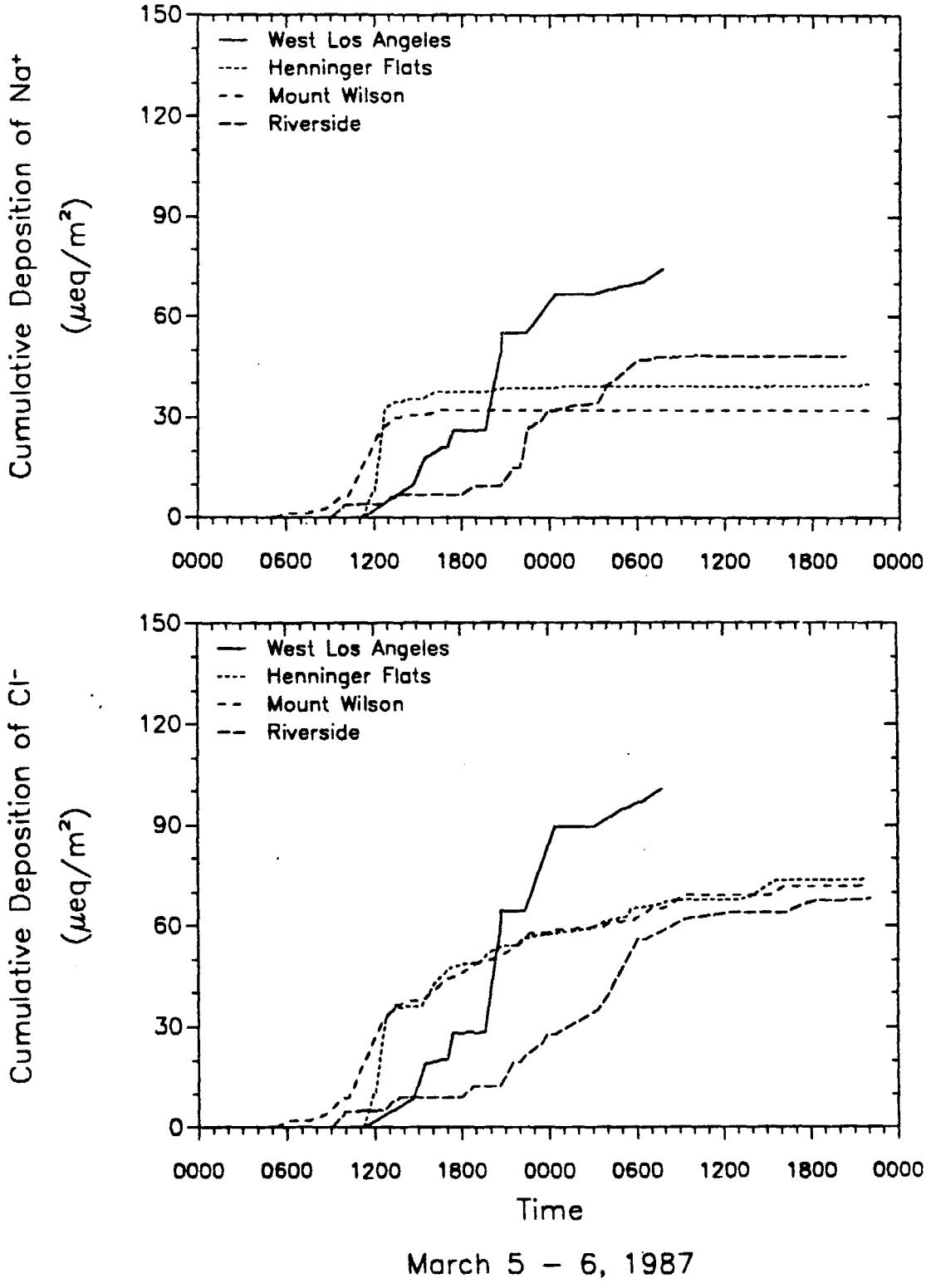

Figure 28. Cumulative deposition of Na^+ and Cl^- measured at West Los Angeles, Henninger Flats, Mt. Wilson, and Riverside on March 5 and 6, 1987.

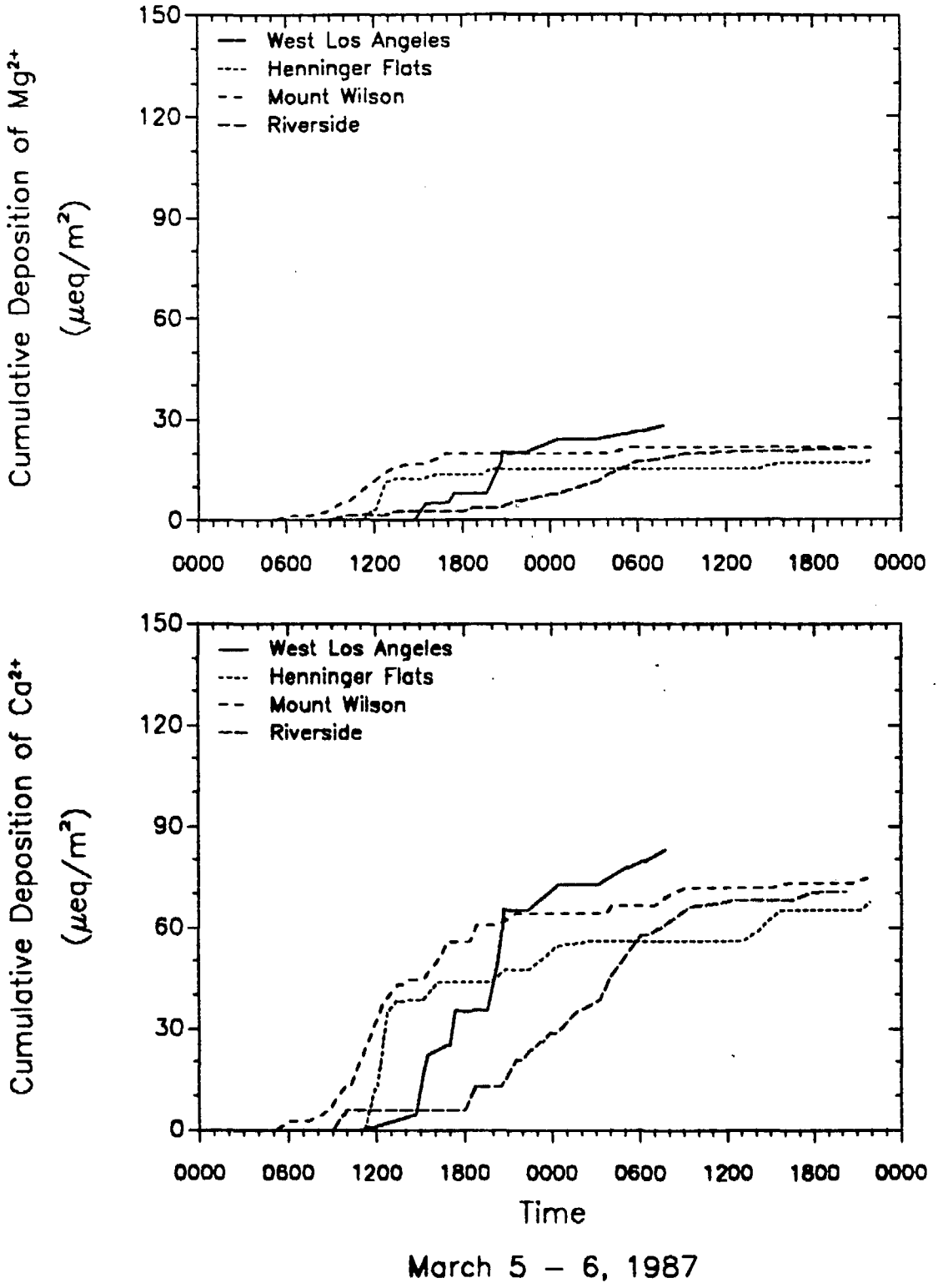

Figure 29. Cumulative deposition of Mg^{2+} and Ca^{2+} measured at West Los Angeles, Henninger Flats, Mt. Wilson, and Riverside on March 5 and 6, 1987.

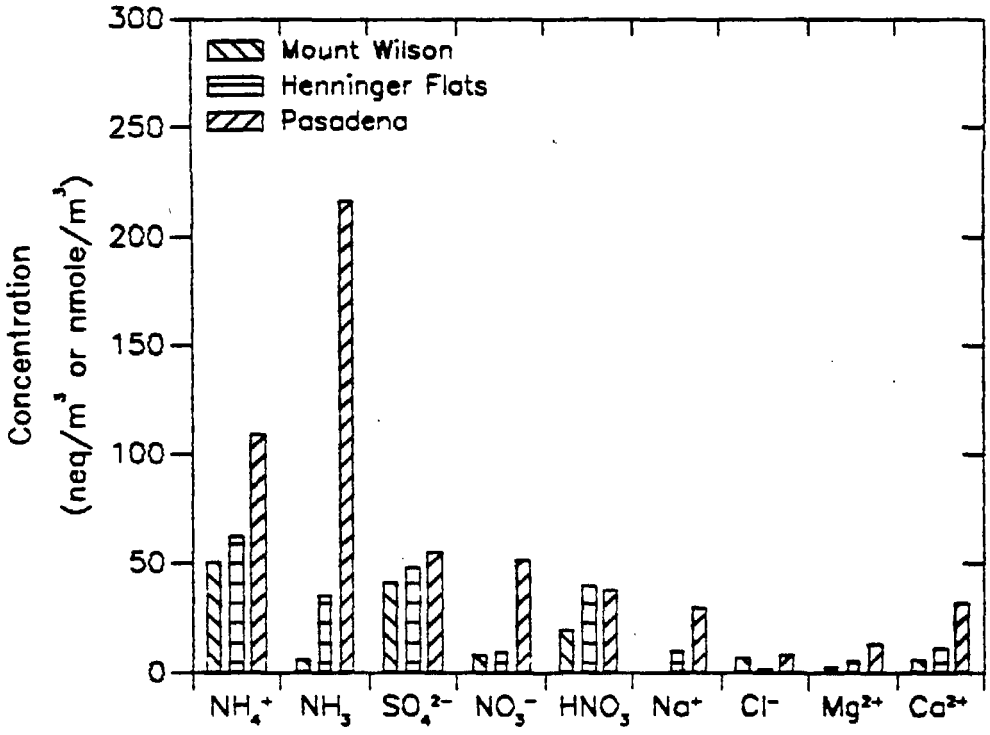

Figure 30. Concentrations of selected aerosol and gas phase species measured at Pasadena, Henninger Flats, and Mt. Wilson on the morning of March 5, 1987. Samples were collected from 0200 to 0600 PST.